Heat Transfer in Packed Bed Reactors: Heating versus Cooling

A comparative Study

A Major Qualifying Project Report

Submitted to the Faculty of the
WORCESTER POLYTECHNIC INSTITUTE

in partial fulfillment of the requirements for the
Degree of Bachelor of Science
In Chemical Engineering

Todd Alexander _____

Brianna Ledwith _____

Meghan Linskey _____

April 2011

Approved:

_____
Anthony G. Dixon

Abstract

This study aimed to explain why previous packed bed reactor heat transfer performance heating and cooling experiments did not agree within engineering error. In order to explain the disagreement, cooling experiments were performed in a 4 inch column and compared to previous cooling experiments in order to validate data collection methods. The experiments were then performed in a 2 inch column to compare data from this study, a previous Major Qualifying Project, and a heating experiment from literature. The data in this study was comparable to heating data, which was a result of adding a correction factor and using modified data collection methods.

Executive Summary

Packed beds are used in many chemical processing applications including absorption, stripping, distillation, and catalytic reactors. Understanding and optimizing the heat transfer through packed beds is important in order to decrease the cost of running the equipment. Due to the fact that this is so important to the chemical processing industry, researchers have been running experiments to develop theoretical heat transfer models which can be used to optimize column design. In particular there have been discrepancies among heat transfer parameters between heating and cooling experiments despite the fact that these parameters should theoretically be the same.

In order to determine why the heating and cooling experiments do not agree within engineering error, this study performed cooling experiments and compared our results to previous cooling experiments as well as previous heating experiments. In these experiments, air was heated to an average of 95^{o}C and sent through a brass column with a cooling jacket. The base of the column was packed with 4 inches of ¼ inch steel spheres which was used as the calming section. The calming section was used to evenly disperse the air throughout the column and to ensure fully developed fluid flow before the air stream entered the test section filled with packing. All of the experiments in this study used ½ inch ceramic raschig rings as the packing material. The bed was packed to four different heights at 4, 6, 8, and 10 inches per Reynolds number. The experiments were run at five different Reynolds numbers in the 4 inch column and six different Reynolds numbers in the 2 inch column.

Using a thermocouple cross, various radial temperatures were collected once the column had reached steady state at a specific bed height. The thermocouple cross was rotated 45^{o} at each bed height in order to get a more representative temperature profile. The temperature data was averaged and analyzed using the GIPPF Fortran program, which calculated the heat transfer parameters at each Reynolds number. The heat transfer parameters allowed our group to compare this study's data to previous heating and cooling experimental data. This study found that altering the experimental procedure for the cooling data would yield higher heat transfer parameter values, making it closer to the heating experiments. This study also found that our data was slightly higher than the heating data due to the moisture in the inlet air-line.

Table of Contents

Table of Figures

Table of Tables

Introduction

For many years experiments have been done to study heat transfer in fixed bed reactors. At Worcester Polytechnic Institute (WPI), these experiments were performed mainly for analysis of steam reformer performance. Most of the experiments have been performed by flowing room temperature air into a tube with steam heated walls. More recently, experiments have been performed where the air is heated and then passed through a tube with water cooled walls. These two experiments should reveal the same heat transfer parameters through the packed beds. However, recent studies performed at WPI and in other graduate work (Ashman et al., 2009; Borkink et al., 1993) have shown trends of less heat transfer through the cooled packed bed reactors than through the heated packed beds.

This study aimed to explain the differences seen in heat transfer trends between heating and cooling experiments. This study also aimed to establish a standard data collection method that would ensure consistent results within engineering error. In order to determine the causes of discrepancies between heating and cooling data, experiments were performed to eliminate possible sources of error. The columns used to perform experiments were constructed of a brass cooling jacket that was set on top of a nylon calming section filled with ¼ inch steel spheres. The calming section created fully developed fluid flow in the test air stream. This study performed a temperature analysis of the cooling jacket to ensure that cooling water was evenly distributed across the entire inner wall surface. This study also analyzed the possibility of heat loss through the calming section which would change the inlet temperature of the air in the test section, decreasing the heat transfer driving force. The air used in the experiments displayed varying degrees of humidity and often formed condensation on the inner wall of the brass cooling jacket. As heat transfer is affected by moisture content, this study analyzed the magnitude of humidity effects in regards to heat transfer coefficients.

From these experiments this study determined the following:

- There was uniform temperature distribution across the inner cooling wall surface as the entire cooling jacket filled with the cooling water.
- There was significant heat loss through the calming section; however this study determined that this heat loss was taken into account in the GIPPF Fortran program.
- Humidity does have a slight effect on heat transfer coefficients and should be taken into account when analyzing heat transfer data from cooling experiments.

- Data methods should be modified to collect data for one Reynolds number at all bed heights per day.

Background

Packed beds have many applications in the chemical processing industry. For example, packed beds are used in reactors, separators, dryers, filters, and heat exchangers. The heat transfer throughout a packed bed can have a significant effect on the performance of the equipment. Therefore, it is important to better understand the heat transfer through packed beds which has led researchers to have an increased interest in the subject area.

Researchers have been running experiments on heat transfer through packed beds for many years in order to develop various correlations for the data obtained. Experiments have been conducted using both heating and cooling methods. In the majority of heating experiments, a fluid is sent through a column whose walls are heated whereas in a cooling experiment, the fluid is heated to a certain temperature before it is sent through a cool-jacketed column. The rate of heat transfer for both the heating experiments and cooling experiments should be identical. This is because heat transfer is calculated using the specific properties of each material involved (air, water, etc.) along with the measured temperature difference caused by the transfer of heat. The same magnitude of heat should be transferred into or out of a material because its ability to transfer heat will remain constant regardless of heating or cooling. Unfortunately, the experimentation at WPI has given the appearance that the rate of heat transfer is much higher for the heating experiments than for the cooling experiments (Ashman et al., 2009). Researchers have been trying to determine through experimentation and computer modeling why the heating and cooling experiments do not reveal similar results.

Ratio of Tube to Particle Diameter

Reactors with small tube to particle diameter ratios are often used in very exothermic catalytic reactions. The ratio of tube to particle diameter (N) can have an effect on the heat transfer parameter correlations. It is very important to figure out how N has an effect on the data correlations and what causes that effect. Researchers have found that when N is low, it can be difficult to obtain consistent correlations. However, other researchers argue that there is little effect of the tube to particle ratio on data correlations.

Researchers, such as Dixon et al. (1997) and Chu and Ng (1989) believe that the ratio of the tube to particle diameter has a large effect on the data obtained. They believe that it is due to the fact that the wall effects are more prominent in tubes with a low particle to tube diameter ratio. Dixon et al. (1997) found that the effects of the ratio of tube to particle diameter is negligible, except when N is less than 4 for spheres and when N is less than 2 for non-spheres (Dixon, 1997). For this study the N values for the both the 2 inch column and the 4 inch column were greater than 4 so the wall effects were negligible. Chu and Ng (1989) focused on the flow

of fluid near the wall region, which can have an effect on both the wall heat transfer coefficient and the flow distribution in the column, even at high ratios. Cohen and Metzner (1981) and Nield (1983) argued that the tube walls restrict the fluid flow. As the ratio of tube to particle diameter decreases, the permeability also decreases. Through Chu and Ng's (1989) research, they concluded that higher porosity in the wall region can help fluid flow near the walls while higher surface area per unit would hinder the flow. There are two different scenarios; if porosity is the dominant factor then permeability increases in larger tubes, but if surface area is the dominant factor then the opposite is true. Chu stressed the importance of having computer models that would account for the interaction of the solid particle matrix and the fluid phase (Chu and Ng, 1989). Another factor to consider is the effect of the Reynolds number on the fluid flow. At low Reynolds numbers, the drag caused by wall friction reduces the flow rate. At high Reynolds numbers, the fluid flow increases due to channeling at the wall caused by the unique geometry in that region. For this study, the model needed to take into account the drag due to the wall created at low Reynolds numbers.

Borkink and Westerterp (1992) also researched the effects of the ratio of tube to particle diameter on heat transport coefficients. From their research, they concluded that the ratio of the tube to particle diameter did not have any noticeable effect on the heat transport coefficients when using the pseudo-homogeneous 2-dimensional model. They found that the size of the particle diameter may influence the effective radial heat conductivity, although not enough experiments were run to conclude that. The effective radial heat conductivity is affected by the shape of the packing, whereas the wall heat transfer coefficient was less influenced by the shape of the packing. Borkink and Westerterp (1992) believe that the variations in the effective radial heat conductivity and the wall heat transfer coefficient are not influenced by the ratio of tube to particle diameter, but rather mixing on a particle scale (Borkink and Westerterp, 1992).

Length Effect and Axial Dispersion

Researchers have been studying the axial dispersion of heat in packed beds and its effect on various tube lengths for years. Young and Finlayson (1970) concluded that including axial dispersion in a mathematical model can significantly affect the results. They came up with a set of rules that showed when axial dispersion should be included in the mathematical model and when it should be left out. Young and Finlayson concluded that axial dispersion was independent of tube length. Other researchers argue that the effect of axial dispersion decreases with increasing tube length. Still others, such as Borkink et al. (1993), concluded that axial dispersion of heat can be neglected for both heating and cooling experiments without reactions (Borkink et al., 1993).

Throughout his heating experiments, Dixon (1985) found several other factors that are responsible for the length effects. One factor that contributed to the length effects was the conduction of the thermocouple cross. Thermocouple crosses constructed of conductive material would conduct heat and influence the temperature readings. As a result of this factor, Dixon (1985) concluded that low thermal conductivity materials should be used for the thermocouple cross and the calming section. The second factor was that the heat is conducted through the column walls into the calming section. This would lead to an increase in the inlet air temperature, which would be higher than the temperature that the PF model had assumed. The temperature difference is greater as the bed depths increase (Dixon, 1985).

Researchers have given many reasons for why there may be a length effect. Some of these reasons include: the radial velocity and temperature profiles have to develop over certain bed lengths, the presence of a radial velocity profile, the device holding the thermocouple conducts heat which flattens the radial temperature profiles, the gas is preheated because heat is conducted through the walls of the calming section, and the axial dispersion of heat is neglected in computer models. Borkink et al. (1993) found that depth dependence had an effect on the calculated temperature profiles when the nominal inlet temperature was used. In order to eliminate the depth dependence, Borkink et al. (1993) modified the model to fit the data to the first bed depth temperature profile.

Heat Transfer Models

Thermal energy transfer can be described by three defined modes of transportation: conduction, convection and radiation. For the purpose of this study, heat transfer effects from radiation were ignored because the temperatures used are relatively low and thus heat transfer due to radiation is negligible. Typical models approach the problem of heat and mass transfer using Fourier's and Fick's Laws respectively (Dixon, 2001). In the model of heat transfer, lumped sums are used to take into account the major modes of heat transfer. Axial convection of heat is assumed to be a result of the velocity profile. The velocity profile is assumed to be unidirectional and constant. The other modes of heat transfer are combined into two lumped parameters k_r and k_f , which are effective thermal conductivities. The thermal conductivity, k_f is the molecular thermal conductivity of the fluid. The effective radial thermal conductivity, k_r represents all modes of heat transfer in the center of the bed that are unaffected by wall affects. Heat transfer at the wall is lumped into a term h_w , the wall heat transfer coefficient. h_w represents the increased heat transfer resistance near the wall due to film resistance. These parameters are used in the Generalized Inlet Profile Plug Flow (GIPPF) program.

The physical system is extremely complex and very hard to mathematically model due to the bed geometry and flow fields, therefore assumptions and simplifications need to be made.

In order for the pseudo-homogeneous plug-flow model to be applicable, the assumptions are as follows:

- the system is at steady state
- pseudo-continuum- the particles are not explicitly represented
- the system is pseudo-homogeneous ($T_f = T_s$)
- no reaction takes place
- no axial heat dispersion
- no free convection of heat
- no radiation
- constant pressure in the packed bed
- constant wall temperature
- physical properties of the gas and solid are independent of temperature
- No radial variation of the superficial gas velocity (velocity unidirectional and constant)

The model used to analyze the temperature data acquired in this study was the GIPPF Fortran program. This program uses the first measured bed depth temperature profile as the inlet profile which is used to compute the subsequent profiles at other bed depths. The first bed depth is used as the inlet temperature profile because there is a significant amount of heat loss from the calming section and is it impossible with the current apparatus set up to determine the inlet temperature profile at z=0.

The GIPPF model is obtained from the following energy balance:

$$v\rho c_p \frac{dT}{dz} = k_r \left(\frac{\partial^2 T}{\partial r^2} + \frac{1}{r}\frac{\partial T}{\partial r}\right)$$

The boundary conditions are as follows:

$$\frac{\partial T}{\partial r} = 0 \; at \; r = 0$$

$$T(r, z_o) = T_{zo}(r) \; at \; z = 0$$

$$-k_r \frac{\partial T}{\partial r} = h_w (T - T_w) \; at \; r = R$$

The energy balance is made dimensionless through the following definitions:

$$y = \frac{r}{R}$$

$$x = \frac{z}{R}$$

$$\theta = \frac{(T - T_W)}{(T_o - T_W)}$$

Thus:

$$\frac{d\theta}{dx} = \frac{k_r}{v\rho c_p R}\left(\frac{d^2\theta}{dy^2} + \frac{1}{y}\frac{d\theta}{dy}\right)$$

Radial Peclet number:

$$Pe_r = \frac{v\rho c_p d_p}{k_r}$$

Dimensionless boundary conditions:

$$\frac{\partial\theta}{\partial y} = 0 \ at \ y = \mathbf{0}$$

$$\frac{\partial\theta}{\partial y} + \frac{h_w R}{k_r}\theta = 0 \ at \ y = \mathbf{1}$$

Wall Biot number:

$$Bi_w = \frac{h_w R}{k_r}$$

Thus, boundary conditions become:

$$\frac{\partial\theta}{\partial y} = 0 \ at \ y = \mathbf{0}$$

$$\frac{\partial\theta}{\partial y} + Bi_w\theta = 0 \ at \ y = \mathbf{1}$$

Further definitions:

$$\theta(y, x_o) = \theta_o(y)$$

Where:

$$x_o = \frac{z_o}{R}$$

$$\theta_o = \frac{(T_{so} - T_W)}{(T_o - T_W)}$$

The solution to the differential equation can be solved by separation of variables.

Define:

$$\theta(y,x) = Y(y)X(x)$$

Substituting into the differential equation:

$$YX' = \frac{1}{Pe_r(\frac{R}{d_p})}(Y'' + \frac{1}{y}Y')$$

Divide by XY and rearrange:

$$Pe_r\left(\frac{R}{d_p}\right)\frac{X'}{X} = \left(\frac{Y''}{Y} + \frac{1}{y}\frac{Y'}{Y}\right)$$

Setting equal to a constant k:

$$\left(Y'' + \frac{1}{y}Y'\right) = kY$$

Boundary Conditions:

$$XY' = 0 \; at \; y = 0$$

$$XY'(1) + Bi_w XY(1) = 0$$

Thus:

$$Y'(0) = 0$$

$$Y'(1) + Bi_w Y'(1) = 0$$

Only possible solution is when $k < 0$. K is set to $k = -\lambda^2$

Rearranging and multiply $\left(Y'' + \frac{1}{y}Y'\right) = kY$ by y^2 :

$$y^2Y'' + yY' + ky^2Y = 0$$

The above equation is a Bessel function of zero order. This means that there two solutions that are infinite series. These solutions can be denoted $J_o(y)$ and $Y_o(y)$.

Thus:

$$Y(y) = AJ_o(\lambda y) + BY_o(\lambda y)$$

As y approaches zero, $Y_o(\lambda y)$ approaches infinity. This doesn't make physical sense so B is set equal to zero to get rid of that term.

At $y = 1$ the following is obtained:

$$\frac{\partial Y}{\partial y} = A\frac{\partial}{\partial y}\{J_o(\lambda y)\} = \lambda A J_{-1}(\lambda y)$$

$$J_{-1}(\lambda y) = -J_1(\lambda y)$$

The boundary condition is as follows:

$$\lambda J_1(\lambda) - Bi_w J_o(\lambda) = 0$$

λ must satisfy the characteristic equation as well as the boundary condition.

Going back to the separated equation:

$$Pe_r \frac{R}{d_p} X' + \lambda_i^2 X = 0$$

$$X' + \frac{\lambda_i^2}{Pe_r \frac{R}{d_p}} X = 0$$

$$X_i = \exp\left\{\frac{\lambda_i^2 x}{Pe_r \frac{R}{d_p}}\right\}$$

For every eigenvalue λ_i there is an eigenfunction $J_o(\lambda_i y)$; there are an infinite number of eigenfunctions so the solution is:

$$\theta(y, x) = \sum_i^{\infty} A_i J_o(\lambda_i y) \exp\left\{\frac{-\lambda_i^2 x}{Pe_r \frac{R}{d_p}}\right\}$$

Use initial condition to solve for A_i:

$$\theta_o(y) = \sum_i^{\infty} A_i J_o(\lambda_i y) \exp\left\{\frac{-\lambda_i^2 x}{Pe_r \frac{R}{d_p}}\right\}$$

In order to shorten:

$$B_i = A_i \exp\left\{\frac{-\lambda_i^2 x}{Pe_r \frac{R}{d_p}}\right\}$$

Thus:

$$\theta_o(y) = \sum_i^{\infty} B_i J_o(\lambda_i y)$$

Both sides are then multiplied by $yJ_o(\lambda_j y)$ and integrated:

$$\int_0^1 \theta_o(y) J_o(\lambda_j y) y dy = \sum_i^{\infty} B_i \int_0^1 J_o(\lambda_i y) J_o(\lambda_j y) y dy = B_j \int_0^1 \left[[U]_o(\lambda_j y)\right]^2 y dy$$

From the orthogonality property of eigenfunctions and the solution to the well-known Lommel's integrals:

$$\int_0^1 \left[[U]_o(\lambda_j y)\right]^2 y dy = \frac{1}{2\lambda_j^2}\left[[U]_o(\lambda_j)\right]^2 \left(\lambda_j^2 + Bi_w^2\right)$$

Then:

$$B_j = \frac{2\lambda_j^2 \int_0^1 \theta_o(y) J_o(\lambda_j y) y dy}{\left[[U]_o(\lambda_j)\right]^2 \left(\lambda_j^2 + Bi_w^2\right)}$$

And:

$$A_j = \frac{\exp\left\{\frac{\lambda_j^2 x_o}{\frac{Pe_r R}{dp}}\right\}}{\left[[U]_o(\lambda_j)\right]^2 \left(\lambda_j^2 + Bi_w^2\right)} x 2\lambda_j^2 \int_0^1 \theta_o(y) J_o(\lambda_j y) y dy$$

Then:

$$\theta(y,x) = 2\sum_{i=1}^{\infty} \frac{\lambda_i^2 J_o(\lambda_j y)}{[U_o(\lambda_j)]^2(\lambda_j^2 + Bi_w^2)} \exp\left(\frac{-\lambda_i^2(x - x_o)}{Pe_r \frac{R}{d_p}}\right)(x \int_0^1 \theta_o(y) J_o(\lambda_j y) y dy)$$

Note: when $x = x_o$ the infinite series does not converge.

Dimensionless Numbers

The Reynolds number (Re) is a dimensionless parameter that gives a measure of the ratio of inertial forces versus viscous forces. It is directly proportional to the superficial fluid velocity. The Reynolds number for air flowing through a fixed bed reactor is determined by the following equation:

$$Re = \frac{v_s \rho d_p}{\mu}$$

v_s is the superficial velocity of the air in ft/min, ρ is the density of air in lb_m/ft^3, d_p is the equivalent packing diameter in inches, and μ is the dynamic viscosity of air in pound force per foot squared. As the Reynolds number increases in a packed bed, the temperature difference between the particles and the gas also increases. "The increase in the Reynolds number not only increases the particle-gas heat transfer coefficient in the bed, but also increases the amount heat transferred into the bed as wall temperature is constant" (Wen and Ding, 2005).

The radial Peclet number (Pe_r) is defined as:

$$Pe_r = \frac{Re * Pr}{\frac{k_r}{k_f}}$$

If it is assumed that $\frac{k_r}{k_f}$ is linearly related to the Reynolds number and the Prandtl number is assumed to be constant then:

$$Pe_r = \frac{Re * Pr}{m * Re + b}$$

The values for m and b can be obtained from a plot of $\frac{k_r}{k_f}$ versus the Re number. M is the slope of the best fit line obtained and b is the intercept. Based on this equation, the Peclet number should initially increase rapidly when the range of Reynolds number is low but should remain relatively constant with larger Reynolds numbers.

The Biot number (Bi) relates the heat transfer coefficient of the wall to the thermal conductivity of the packing. The Biot number is defined as:

$$Bi_w = \frac{h_w R}{k_r} = Nu_w \frac{\frac{R}{d_p}}{\frac{k_r}{k_f}}$$

The dimensionless number N is the ratio of the tube diameter to particle diameter.

$$N = \frac{2 * R}{d_p}$$

Many studies suggest that in order to obtain accurate data, N should be greater than 3.5 otherwise wall affects will dominate (Smirnov, 2003). Another condition that affects the accuracy of the model is the depth of the bed studied. Many studies suggest that the first bed depth used should be at least 1.5 times the diameter of the column (Borkink & Westerterp, 1993). For the 4 inch column due to a lack of available packing the first bed depth studied was 4 inches which is less than the 6 inch depth that would have been desirable. For the 2 inch column studied the guideline was followed and the starting bed depth was 4 inches. This research was conducted to try to determine why heating and cooling experimental results have not agreed in the past.

An example of such a trend can be seen below in Figure 1 showing a comparison of the Nusselt number between a heating experiment and cooling experiment performed at WPI.

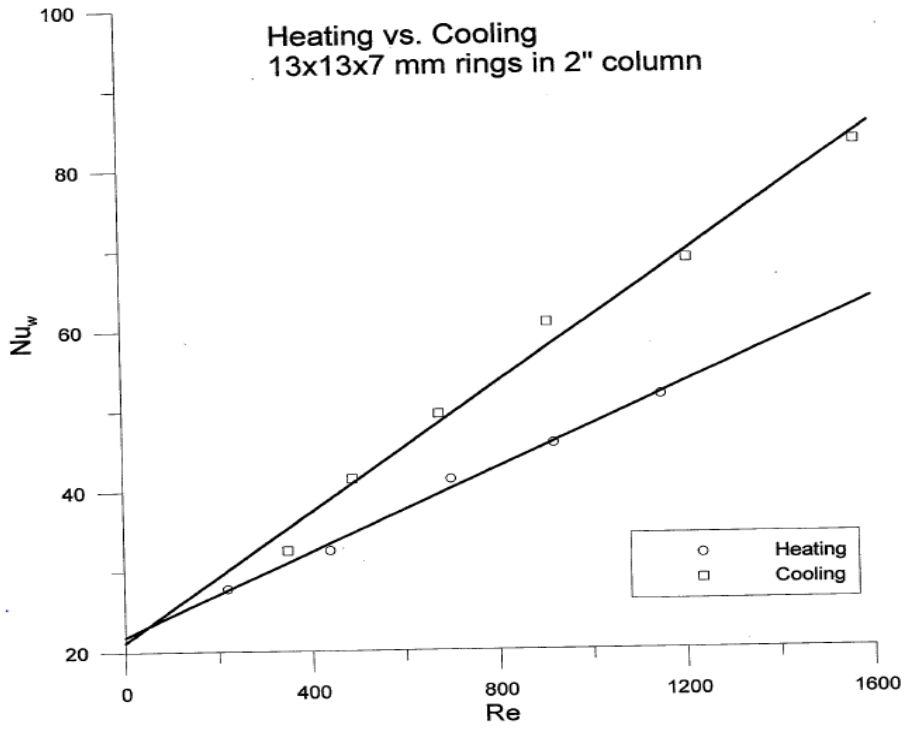

Figure 1: Heating v. Cooling Experiments at WPI

From the graph, it is clear that there is not good agreement between the heating and cooling data. In order to be in good agreement, which should be the case, we would expect the trends

to be both parallel and have similar intercepts. Since these experiments were performed using the same equipment it raises many questions as to why there is such a discrepancy. This trend is not limited to experiments performed at WPI and thus warrants careful study.

Apparatus

The experimental apparatus used in the cooling experiments for this study is shown in Figure 2 below.

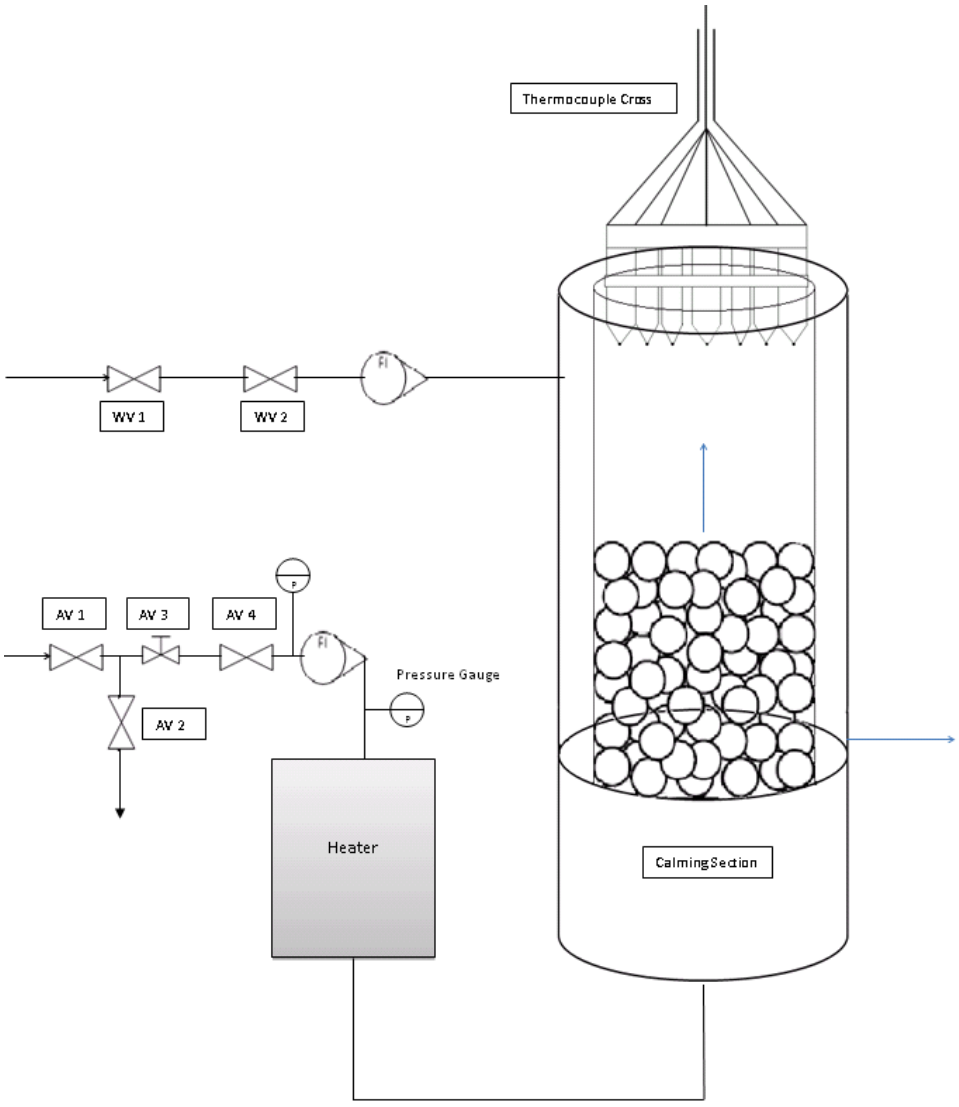

Figure 2: Schematic of Experimental Apparatus

Columns

Two columns were used in this study, one had a 4 inch inner diameter and one had a 2 inch inner diameter. Both columns were constructed of two brass tubes, one inside the other, welded together to form an annular space in which the cooling water flowed. The columns

were attached to a nylon calming section using four screws. The screws used for the four inch column were nylon and the screws used to attach the two inch column were made of steel. The calming sections were filled with ¼" steel spheres and were separated from the packed section of the column by a piece of steel mesh. The calming section was designed to evenly distribute the airflow across the test section of the column and to allow for a fully developed flow.

Air Metering System

Air entering the column was sent through an air drying unit which was designed to condense moisture out of the air to avoid flooding of the rotameter. The rotameter tube used was FP-1/2-50-G-9/55 and contained a GNSVT T60 1/2 48A float. Pressure of the air entering the column was obtained from a pressure gauge just before the Micromega heater.

Reynolds Numbers

Data Sheet to calculate the Reynolds Number

For the 4" Column:

RUN:_____ Packing: _____
Date:_____

Re:_____ (= 95(d_p)(SCFM)*1.2) Bed Depth:_____

Pressure:_____ PSIG

Max Flow:_____CFM

%Reading:_____%

Act Flow:_____SCFM = (%)(MAX)(14.7+PSIG)/14.7

For the 2" Column

RUN:_____ Packing: _____
Date:_____

Re:_____ (= 380(d_p)(SCFM)*1.2) Bed Depth:_____

Pressure:_____ PSIG

Max Flow:_____CFM

%Reading:_____%

Act Flow:_____SCFM = (%)(MAX)(14.7+PSIG)/14.7

The pressure reading was obtained by reading the pressure gauge downstream of the rotameter (the one right next to the heater). The maximum flow rate was determined from a table provided in the laboratory. The table gave the manufacturer's calibration for the different rotameter size and float size combinations at the given pressure.

There was also a constant that took into account the diameter of the column and the viscosity of air. This was provided on the worksheets for calculating Reynolds numbers, located in the lab. The constants were 95 for the four inch column and 380 for the two inch column.

Because the air was heated to approximately 100°C (an average of 95°C was assumed), the Reynolds number needed to be adjusted for the changes in density and viscosity caused by the heat. Hence, the Reynolds number was multiplied by 1.2, which is the correction factor for heating the air. The air is initially metered at 298K and then is heated to 368K before entering the column. The correction factor is determined by dividing the inlet air temperature by the metered air temperature through use of the ideal gas law.

$$\frac{P_1 V_1}{T_1} = \frac{P_2 V_2}{T_2}$$

$$P_1 = P_2$$

$$V_1 = \frac{V_2 T_1}{T_2}$$

The correction factor was determined by using the above equations.

Omega Micromega Heater

The inlet air was heated using a heater controlled by an Omega Micromega CN77000 Series Controller. A more detailed description as well as instructions on how to use the controller can be found at http://www.omega.com/Manuals/manualpdf/M2491.pdf. The heater in this study was used to heat the inlet air to approximately 100^{o}C. The rate at which the air was heated was controlled by the set ramp and soak values. Time required for the system to reach equilibrium was affected by the rate of heating. Although the desired temperature was set to 100^{o}C, it was impossible to maintain this temperature at all times; the temperature oscillated around this value during experimental runs. This was due to the fact that the heater heats the air until it reaches 100^{o}C but does not add heat into the system until the temperature drops below 100^{o}C, thus creating this oscillation. Faster heating of the air caused the inlet temperature to reach the desired temperature of 100^{o}C quicker. However, this rapid heating resulted in larger oscillations. Slower heating of the air led to smaller oscillations in the inlet temperature, but it took more time for the inlet air to reach 100^{o}C. Typically the inlet temperature averaged 95^{o}C.

Procedure

Startup

1. Carefully unscrew and remove the top (brass) section of the tower.
2. Remove the steel mesh support and fill the calming section with desired packing. (In this study ¼" steel spheres). Place steel mesh support back onto the top of the calming section.
3. Re-attach the top section of the tower. Make sure to line up the screw holes as evenly as possible before screwing it back into the calming section. This will allow for easier removal later if necessary.
4. Measure inner height of the empty column and record this value.
5. Add packing until the desired bed depth is reached. The bed depth is determined by the following equation: bed depth = height of empty tower – height of empty space left
    a. Packing should be added in small increments and gently compacted after the addition of new catalyst particles. This helps assure that the particles are evenly distributed and that there is no change in packing orientation with time.
6. The thermocouple cross should be set up such that the thermocouple tips are within 3-6 mm of the packing (however they should not touch the packing). This can be achieved by taking the measurement of the empty space left in the tower obtained in step 5 and subtracting 3-6 mm from the measurement. Take this new measurement and measure from the tip of the thermocouple and adjust the crossbar such that the bottom of the crossbar matches the depth attained in the above calculation. Next check to make sure all the thermocouple tips are straight and centered in the plastic guide tubes.

7. The thermocouple cross is then carefully lowered into the column. If the thermocouple tips hit the top of the packing, remove the thermocouple cross from the column. All the thermocouple tips should be straightened and the crossbar height should be readjusted to ensure that the thermocouple tips do not hit the top of the packing.
8. Slowly open WV 1.
9. Slowly open WV 2 until the rotameter reads a flow of 95%.
10. Slowly open AV 1. Make sure that AV 3 and AV 4 are fully closed.
11. Slowly open AV 2. This valve will allow for condensed water to drain from the line to reduce moisture flowing into the system. This valve should be opened for 5 minutes or until there is no visible sign of water in the air. When this valve is fully opened, an extremely loud noise is produced so ear plugs or other forms of ear protection may be desirable.
12. Close AV2. Open AV4
13. Slowly open AV 3. AV3 is used to adjust the Re value.
    a. Make sure that the rotameter never reaches 100% flow or above.
    b. The pressure gauge used to calculate the Reynolds numbers is the one just above the heater (downstream from the rotameter).
14. Once the air flow is adjusted such that the desired air flow is achieved open ExceLINX. Instructions on how to set up ExceLINX can be found in the section labeled ExceLINX.
15. Turn on the heater by plugging in the power cord into the power strip or outlet. If the Omega Micromega heating control is not properly set up, make sure to take the time to set it up now.
16. Start recording the data using the ExceLINX previously set up.
17. Record data until steady state is reached. Steady state is obtained when the temperature oscillations are within 0.05 of the next reading within the same thermocouple channel. The time it takes to reach steady state depends on a number of factors including Reynolds number, bed height, and whether or not it is the first run of the day. The time it takes to reach steady state varies between 45 minutes to 3 hours depending upon these factors.
18. Once steady state is achieved, carefully rotate the thermocouple cross 45 degrees. Markings at the top of the column indicate positions of 0 and 45 degrees.
19. Continue recording data in ExceLINX. Make sure the data is being recorded in a different Excel sheet than the previous data set.
    a. It should only take 15 to 30 minutes for steady state to be obtained after the thermocouple is rotated.
20. Once the system has reached steady state, stop recording data and remove the thermal couple cross.

21. Add additional packing to the column following step 5 until the new desired bed depth is reached.
22. Repeat steps 6 and 7 when placing the thermocouple cross back into the column.
23. Repeat steps 16 through 22 until data for desired bed depths is obtained.
24. Shut down the system in the reverse order in which it was started, leaving air flowing through the heater to ensure that it does not overheat.
25. After waiting 15 minutes with just the air flowing through the column, close AV1 and then AV4, making sure AV3 is fully closed.

Safety

One should avoid touching the surface of the heater because the temperature could reach as high as 150^{o}C and could cause burns. Any objects that may fall on top of the heater for any reason, for example during the packing of the column, should be removed using pliers to avoid contact with the heater.

In the winter, the steam line may become hot due to the production of steam. So even though the line is not in use, it may be hot and can cause burns so contact should be avoided at all times.

The catalyst particles used in this study (ceramic raschig rings) are inert and pose no major health risk. Dust from the particle can cause lung irritation, however, there was no visible dust emitted from the packed bed.

Thermocouple

A thermocouple cross was used to record the temperature of the air exiting the top of the column. A diagram of the thermocouple cross used is shown in Figure 3 below.

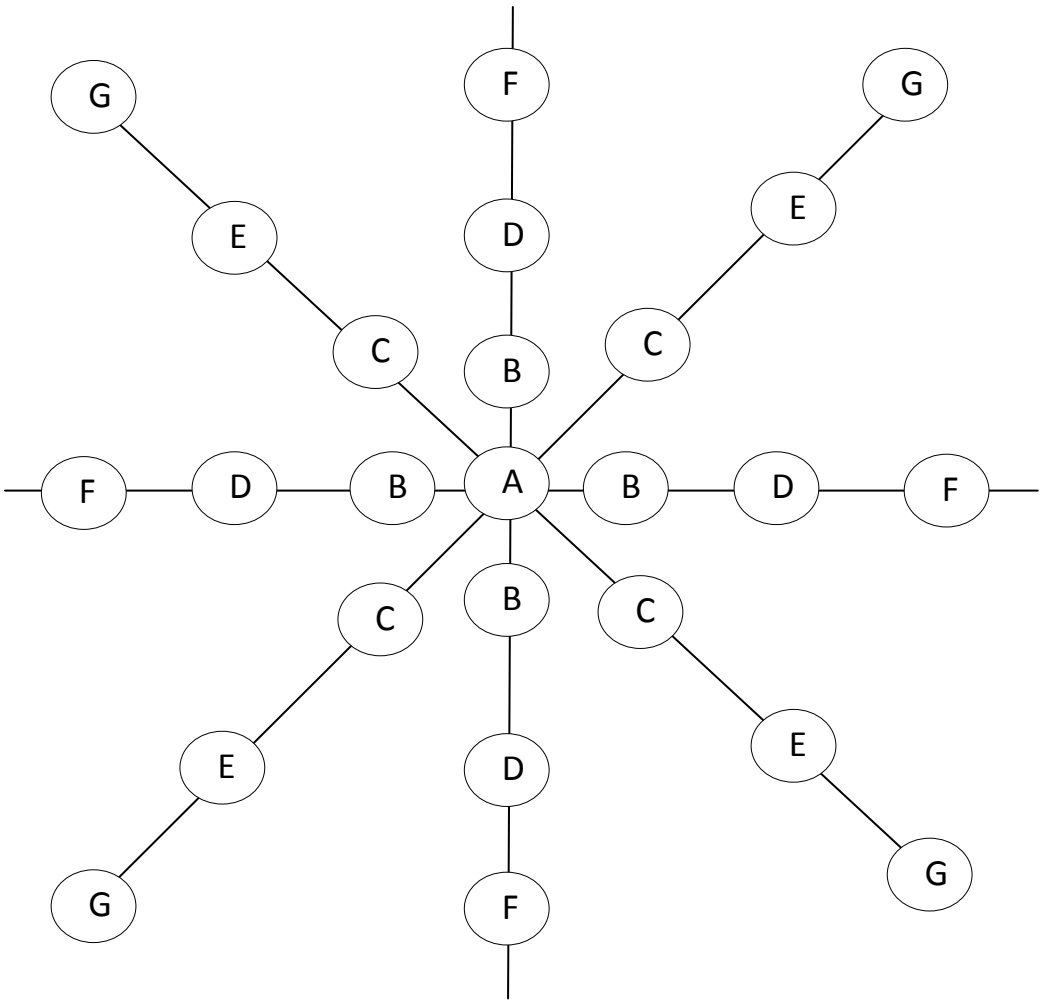

Figure 3: Thermocouple Cross

The thermocouple cross was made out of nylon. It consisted of 8 arms, with each arm 45^{o} apart from one another. Each arm had three thermocouples attached to it at different radial positions. Arms adjacent to one another had three thermocouples that totaled six radial positions, as shown in Figure 3 above. The radii of each of the six different radial positions are shown in Table 1 below.

Table 1: Radial Position of Each Radial Position on the Thermocouple Cross for the 2" and 4" Columns

Thermocouple	2 inch column (mm)	2 inch column (dimensionless)	4 inch column (mm)	4 inch column (dimensionless)
A	0	0	0	0
B	8.5	0.33	9.5	0.19
C	12	0.47	19	0.37
D	15	0.59	28	0.55
E	18	0.71	41	0.81
F	21.5	0.85	44	0.87
G	24	0.94	48	0.94

Additionally, there was a thermocouple that measured the inlet air temperature entering the column as well as three thermocouples that were inserted into the wall of the column. The tips of these thermocouples lay right against the wall and were at heights of 7.5, 24.5, and 37.5 mm from the bottom of the column. The thermocouple cross was able to record twenty-four different temperatures at six different radial positions as well as one additional temperature at the center of the bed.

Before beginning any of the experiments, it was important to figure out which thermocouple corresponded to which number in the computer program. In order to determine this, one member held their finger against one of tips on the thermocouple cross. The computer program, ExceLinx, was run to collect one set of data. The data was then looked at to see which number thermocouple did not read room temperature. This procedure was continued until all of the thermocouples were matched up with the numbers that were output in the computer program.

Throughout this research, data was collected at various bed heights. At each bed height, data was collected two times, once at a 0^{o} angle and then again at a 45^{o} angle. This is because changing the angular position of the thermocouple cross, allows for the radial temperature profiles to be averaged which provides a better representation of the entire bed. Dixon (1997) concluded that a 45^{o} rotation of the thermocouple cross would produce approximately the same results as the previously used 15^{o} rotation (Dixon, 1997). This rotation allowed for the thermocouple cross to record two different radial temperature profiles, making the data collected more representative of the entire bed. Therefore, data was collected at one position and then again at a 45^{o} rotation at each bed height.

For one of the experiments conducted, a probe had to be made in order to measure the temperature of the inner wall at different heights up the column. The probe was made by attaching a thermocouple tip, held in place by thin plastic tubing, to a ruler. The thermocouple

tip was attached to the ruler to allow for an accurate measurement of the height up the column where the temperature was being read at. The thermocouple was plugged into one of the empty plugs on the control board that was used to collect data.

Data Collection:

The temperature data was collected using a Keithley Series 2700 Datalogger along with Excelinx (an add-in designed for Microsoft Excel.) The Datalogger can collect data for up to 200 channels at a time but only 34 channels were used for this experiment.

To install the Excelinx add-in the program ExeLINX.xla must be added into the Microsoft Excel Add-Ins folder. Once in Excel, go to Tools→ Add In and click on ExceLINX.xla from the menu. Once installed, Excelinx will be available from the menu at the top of Excel. It is recommended that the security settings be chosen such that macros are always accepted, otherwise every time a new sheet is opened with Excelinx a new menu will be added to the top bar in Excel.

In order to configure the Keithley instrument, the ExceLinx file needed to be set up to read all of the channels and create an output in the correct units.

From the ExceLinx add-in menu select “Create→ DMM Config” in order to open a sheet in Excel to configure the Kiethley instrument for proper data collection. The DMM Config sheet can be seen in Figure 4 below.

ExceLINX

ExceLINX KEITHLEY A Greater Measure of Confidence

Task: Configure Scanning DMM Channels

Task	Name	DMM Config
	Description	
	Created By	mlinskey
	Company	Worcester Polytechnic Institute
	Date Created	2/15/2011
	Date Modified	2/15/2011
	Status/Cmds	Start
Instrument	Device	KE2700_COM1
	Password	
	Slot 1 Module	MM7700
	Slot 2 Module	MM7700
	Slot 3 Module	
	Slot 4 Module	
	Slot 5 Module	
	Front Panel Lockout	Off
Setup	Line Sync	Off
	Autozero	On
	Display Digits	6½
	DCV Input Divider	Off
	Open TC Detection	Off
	Temp Scale	°C
Limits	Digital Outputs	Off
	Pulse Output	Off
	Polarity	High
	Duration	60 sec
	Master Latch	Off

Channel Scan List

Channel			Measurement		Scaling					Alarm Limits						Rep Filter		Sampling		Options			
Enb	List	Tag	Function	Range	Rel	Math	mxref	b	U	En1	Hi1	Lo1	En2	Hi2	Lo2	Enb	Count	Rate	ACBW	Opt 1	Opt 2	Opt 3	Opt 4
On	101-120,201-214		TEMP	K	Off	None				Off			Off			Off		SLOW		INT			

Figure 4: DMM Config Worksheet

The following selections should be made in the worksheet for the configuration of the Keithley instrument:

In the dropdown menu for “Device,” Ke2700_COM1 should be selected. For “Slot 1 Module” and “Slot 2 Module,” select MM7700. For the “Front Panel Lockout” option select “off.” All of the other dropdown menu options should be left as the default option.

For the channel Scan list set the channels to “101-120,201-214” this will ensure that all of the channels are recognized by the instrument. The input “101-120” corresponds to the channels labeled 101-120 on the thermocouple faceplate and the input “201-214” corresponds to the channels that read “121-134” on the channel face plate. The function should be set to “TEMP” from the dropdown menu. If this option is not chosen the data collected will not be useable. The range should be set to “K” so that the correct degree interval will be measured and under “Options”, “INT” should be chosen for option 1.

Once all of the correct options have been chosen from each dropdown menu the option “start” should be selected from the status/commands menu and the Enter key should be used to start the configuration of the instrument.

Once the DMM Config worksheet is filled out and the instrument is configured select a new tab and click “ExceLinx→ Create→ DMM Scan.” As long as a new blank tab is selected new scan worksheets can be opened for each run within the same Excel workbook. The DMM Scan worksheet can be seen below in Figure 5.

ExceLINX KEITHLEY A Greater Measure of Confidence

Task: Scan DMM Channels			
Task	Name	DMM Scan	
	Description		
	Created By	mlinskey	
	Company	Worcester Polytechnic Institute	
	Date Created	2/15/2011	
	Date Modified	2/15/2011	
	Status/Cmds	Stop	
Configuration	Worksheet	CMM Config	
Trigger	Model	Scan	
	Source	Immediate	
	Delay	Auto	sec
	Reading Count	INF	
	Timer	0.1	sec
	Monitor	None	
	Monitor Limits	None	
Data Location	Worksheet	CMM Scan	
	Starting Col	A	
	Starting Row	37	
	Organize By	Rows	
	Autoincrement	Use one table	
	Auto Wrap	On	
	Log File		
	Format	Delimited text (comma)	
Data Display	Add Channel Tags	Yes	
	Add Channels	Yes	
	Add Units	No	
	Scrol Display	No	
	Limits	None	
	Timestamp	None	
	Update Interval	100	msec
Task Data			

Figure 5: DMM Scan worksheet

Within the scan worksheet the following options need to be selected:

For reading count, “INF” should be selected when doing an entire run to ensure that data will be collected until the column reaches steady state. For the menus “Add Channel Tags” and

"Add Channels" the option "yes" should be selected. Update Interval should be set to 100msec. All other menus should be left as the default option.

Once the column is running and the heater is plugged in, "Start" should be selected from the Status/Commands menu and the enter key should be hit to begin data collection.

Data Analysis

The following format in Figure 6 was used for the input files that were entered into the GIPPF program in Fortran. These files were typed as a text document and saved with the extension .cdat.

# of Profiles	# of Radial Positions	# Wall readings	# of Angles		
Column Diameter	Particle Diameter				
Raduis 1	Radius 2	Radius 3	Radius 4	Radius 5	Radius 6
Revnolds Number	Bed Depth	Angle of rotation			
Inlet Temperature					
Radius 1 Thermocouple 1	Radius 1 Thermocouple 2	Radius 1 Thermocouple 3	Radius 1 Thermocouple 4		
Radius 2 Thermocouple 1	Radius 2 Thermocouple 2	Radius 2 Thermocouple 3	Radius 2 Thermocouple 4		
Radius 3 Thermocouple 1	Radius 3 Thermocouple 2	Radius 3 Thermocouple 3	Radius 3 Thermocouple 4		
Radius 4 Thermocouple 1	Radius 4 Thermocouple 2	Radius 4 Thermocouple 3	Radius 4 Thermocouple 4		
Radius 5 Thermocouple 1	Radius 5 Thermocouple 2	Radius 5 Thermocouple 3	Radius 5 Thermocouple 4		
Radius 6 Thermocouple 1	Radius 6 Thermocouple 2	Radius 6 Thermocouple 1	Radius 6 Thermocouple 4		
Wall Thermocouple 1	Wall Thermocouple 2	Wall Thermocouple 3			

Figure 6: Input file format for GIPPF program

All length units were in millimeters and the temperatures in degrees Celsius were reported to two decimal places. In order for the GIPPF program to analyze the data, at least 3 bed heights are needed because the first bed height is used as a reference for the other data input into the program.

In order to run the GIPPF Fortran program, the following steps should be followed.

1. Double click on the Microsoft Developer Studio Icon to open the program.
2. Open the existing workspace named "GIPPF_FIT.for" this will open the code for the GIPPF model.
3. Click on Build→ Rebuild All
4. Click on Build→ Execute GIPPF_FIT.exe.
    a. The following Screen will appear (Figure 7):

Figure 7: GIPPF Program .exe Window

5. Input the name of the input file including the extension and hit enter.
6. Enter in the range of Reynolds numbers you want to analyze. Only one Reynolds number should be analyzed at a time and the model requires a symmetric input where the actual value is between the two extremes. (eg. Min=48, Max=52, actual Re=50)
7. Enter the bed depths to be analyzed. To analyze all bed depths input 0.0 for the minimum and 1000.0 for the maximum values.
8. Enter a guess for the Peclet number (Pe_r) and the Biot Number (Bi). Generally starting guesses of 5.0 and 10.0 respectively yields results.
9. Name the output file with the extension .res.
10. Run the analysis.
11. Once the analysis is complete the .res file can be opened and the dimensionless temperature profile and model results can be viewed.

Fitting the Collected Data with the GIPPF Model

When the GIPPF program is executed in order to obtain a solution to the data provided, a number of iterations are performed to minimize the sum of squares. The function that is minimized is provided below:

$$\min(Pe_r, Bi)\, S = \sum (T_{calc} - T_{measured})^2$$

The measured temperatures are those taken at each radial and angular position for the provided bed depths. Temperature is made dimensionless by using the following:

$$\vartheta = \frac{(T - T_w)}{(T_o - T_w)}$$

From this, the GIPPF program iteratively solves the partial differential equation in order to minimize the sum of squares, which is a function of the input parameters. When the file is executed, the GIPPF program will require an input for initial guesses of Pe_r and Bi numbers. The program then solves the partial differential equation, solves for the value of S, and if S is not at a minimum the program then guesses a new value for the Pe_r and Bi numbers. This process is then continued until S is at a minimum.

Initial values for the Pe_r and Bi numbers were usually guessed to be 5 and 10, respectively. In a few tests performed, it was proven that as long as this initial guess was within the right range it did not matter what was input as an initial guess as the program would converge upon the same values. The end point of the iterations is ended based on the desired accuracy selected by the user.

F-Test

Data collected for the same flow rate and radial and axial positions, but different angular positions are "replicates". For each bed depth, there are eight replicate sets of six measurements. The preliminary test to determine model accuracy is to perform an F-test. The pure error sum of squares is determined by the following:

$$SSPE = \sum_{1}^{N}\left(\sum_{1}^{6}\sum_{1}^{8}(T_{observed} - T_{average})^2\right)$$

N is the number of bed depths. The mean square pure error can be calculated by:

$$MSPE = \frac{SSPE}{n_2}$$

$$n_2 = m - (number\ of\ averages\ found)$$

The mean lack-of-fit sum of squares can be determined by:

$$MSLF = \frac{S - SSPE}{n_1}$$

$$n_1 = mnumber\ of\ parameters\ estimated - n_2$$

If the model is linear in the parameters than the MLSF is an independent estimate of error variance. If the model is non-linear than the test of model accuracy is as follows:

$$F_c = \frac{MLSF}{MSPE} < F_{0.05}(n_1, n_2)$$

If F_c is greater than $F_{0.05}$ the model is a poor fit or there is low variability in the data. If F_c is less than $F_{0.05}$, the model is a good fit.

Results

The objective of this study was to determine why there had been discrepancies in the effective radial heat transfer data between heating and cooling experiments. In order to verify our data collection method, cooling experiments were performed using ½" raschig rings in the 4 inch column to compare to previous cooling experiments such as those performed by Ashman et al. (2009). Once our data collection methods were verified, cooling experiments were continued with ½" raschig rings in a 2 inch column in order to compare this study's data to available heating data obtained by Dixon (1997).

Heat Transfer Parameters

In this analysis, the k_r/k_f, Nu_w, Pe_r, and Bi vary with different Reynolds numbers. With each Reynolds number, these heat transfer parameters were estimated using the GIPPF program. Each run had four different bed heights at 4, 6, 8, and 10 inches. The first bed height was used as the inlet temperature profile which the other three bed heights were related to in order to calculate the heat transfer parameters. These values were recorded for each Reynolds number that was run. After all experiments were run for a specific column size, the k_r/k_f, and Nu_w were each plotted against the respective Reynolds numbers. Once these parameters were plotted on a graph, it was important to see if the heat transfer parameters followed a linear trend. The effective thermal conductivities and the wall heat transfer coefficient both increase with an increase in Reynolds number. The graphs of k_r/k_f, and Nu_w versus Reynolds number are shown in Appendix C.

Dimensionless Temperature Profiles

After running the data through the GIPPF Fortran program, the results had to be analyzed to determine if the experiment produced expected temperature profile results. In a cooling experiment, the air is cooled by the walls of the column and so the temperature of the air decreases the farther up the column it travels. Therefore, the dimensionless profile for a cooling experiment is expected to have lower temperatures at higher bed depths. Also, the temperature difference between bed depths decreases as the height of the bed depth increases. Since the air is cooled as it goes up the column, the temperature of the air becomes closer to the wall temperature, which leads to a decrease in the driving force for heat transfer. In a dimensionless profile, the temperature should also decrease as it moves away from the center of the column and towards the cooled wall. Theta (dimensionless temperature) values should never exceed 1 in these dimensionless profiles because 1 is the dimensionless starting temperature of the air. The air temperature should be the highest right before it enters the column and decrease as it moves through the column. An example of an expected dimensionless temperature profile is shown in Figure 8 below.

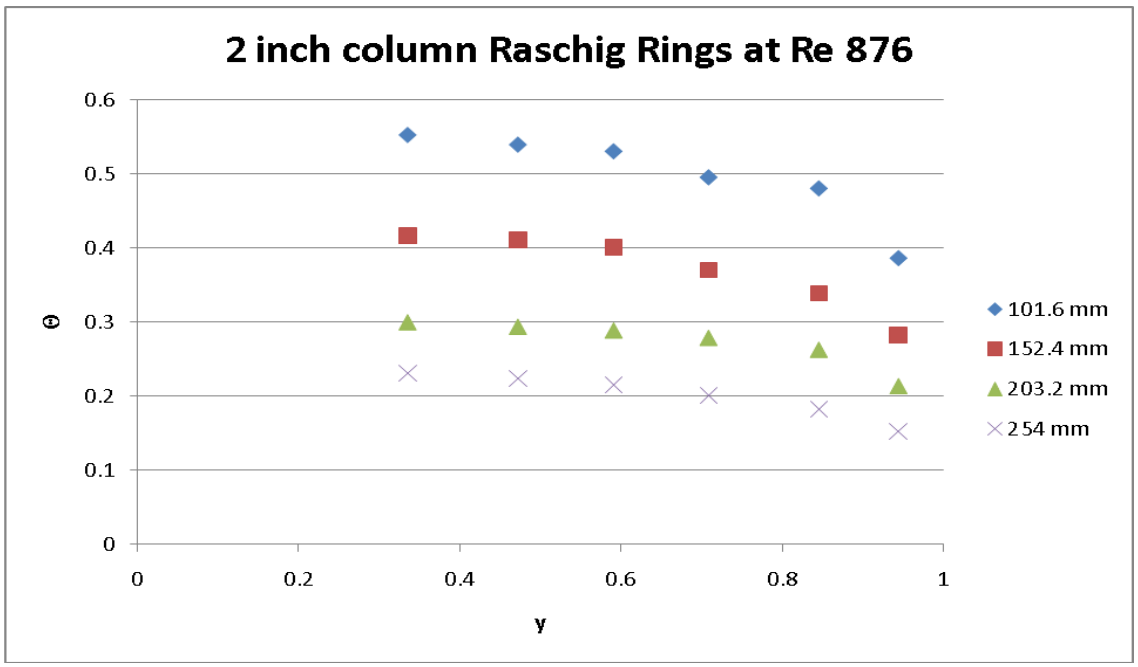

Figure 8: Dimensionless Temperature Profile for Raschig Rings in the 2 inch column at a Reynolds Number of 876

Figure 8 shows the dimensionless bed depth profile for raschig rings in the 2 inch column at a Reynolds number of 876. The temperature decreases as the air moves away from the center of the column (as y increases) and as the profile moves up the column. Table 2 below shows the numerical data that corresponds to the figure above.

Table 2: Dimensionless Temperature Data Re 876

	Dimensionless Radial Position (y)					
	0.335	**0.472**	**0.591**	**0.709**	**0.846**	**0.945**
Bed Depth (z/R)	Dimensionless Temperature Θ					
4	0.552	0.539	0.53	0.495	0.48	0.386
6	0.417	0.411	0.401	0.37	0.339	0.282
8	0.3	0.294	0.289	0.279	0.263	0.214
10	0.231	0.224	0.215	0.201	0.182	0.152

From Table 2, the trends described above can be seen. The dimensionless temperature decreases as y increases as well as when the bed depth increases. Additionally, the temperature difference between bed depths decreases as the bed depths increase. This means that there will be a greater temperature difference between the 4 inch and 6 inch bed depths than between the 8 inch and 10 inch bed depths. This is because as the air moves up the

column, it loses heat, so there is less available heat to be transferred to the column walls at higher bed depths.

Some of our initial dimensionless temperature profiles deviated from the expected trends. Figure 9 below shows the temperature profiles for one of our first experimental runs.

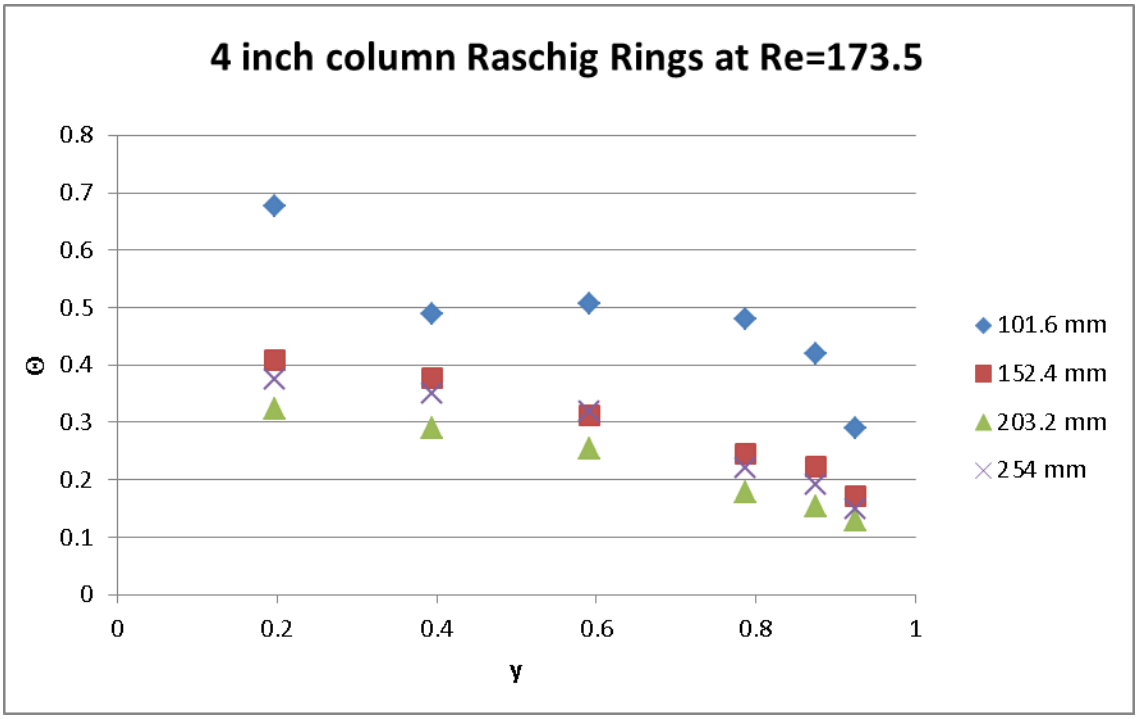

Figure 9: Dimensionless Temperature Profile in the 4 inch column for Raschig Rings at Re=173.5

The dimensionless temperature profile shown in Figure 9 above for this experimental run does not reveal expected results. As the air moves up the column, the temperature of the air should decrease. However, in this run, the temperature of the air at the ten inch bed depth is greater than the temperature of the air at the eight inch bed depth. The temperature should decrease as the thermocouple positions become closer to the wall of the column (as y increases). At the 4 inch packing, the temperature of the column decreases and then increases as the thermocouples move from the center towards the wall of the column. This dimensionless profile is clearly incorrect which means that the experimental data collected does not follow the expected trends. As a result, the heat transfer parameters that the GIPPF Fortran program calculates will not be accurate. The first few experimental runs that were performed in the 4 inch column produced unexpected dimensionless temperature profiles. The poor temperature profile results from many experimental runs revealed that something was fundamentally wrong with the way that the data was being collected.

Potential Causes of Error

Initial data collected in this study yielded temperature profiles that were vastly incorrect and showed trends that were physically impossible. In order to eliminate potential sources of error, multiple diagnostic experiments were performed on the column to ensure it was functioning properly. The potential sources of error analyzed were:

1. Heat loss through the calming section
2. Uniform cooling wall temperature
    a. co-current cooling water flow
    b. counter-current cooling water flow
3. Data collection methods
4. Air humidity

Heat Loss in Calming Section

The first reason for the unexpected results that this study investigated was potential heat loss through the calming section. Experiments were performed to determine if heat loss in the calming section of the experimental column apparatus had an effect on the results. In order to collect data for this analysis, the column was emptied of any packing and the thermocouple cross adjusted so it read the temperature profile of the air a few millimeters above the exit of the calming section. Two different types of calming section packing were used: ¼" steel spheres and ¼" nylon spheres. Data was then compared using graphical analysis.

The experimental data collected showed that there was a significant amount of heat loss in the calming section. This result was more obvious at low flow rates of air than at higher flow rates where temperature loss is masked by the larger flow. This is due to a larger amount of heat entering the calming section while the heat loss remains approximately constant due to the limits of heat transfer. The maximum temperature difference for all flows and packing types was at the wall, proving that heat must be exiting at the wall and bottom of the calming section. This trend can be seen below in Figure 10 and Figure 11, respectively. A nominal radial position of one is the inner most radial position and a nominal radial position of 6 is the outer most radial position, closest to the wall. The maximum temperature difference between entrance temperature and exit temperature for the calming section filled with ¼" steel spheres was 76.5 degrees Celsius and the minimum temperature difference was 10.56 degrees Celsius. The maximum temperature difference between entrance temperature and exit temperature for the calming section filled with ¼" nylon spheres was 66.65 degrees Celsius and the minimum temperature difference was 8.81 degrees Celsius. Based on these numbers and the graphs

presented below, it can be seen that there is a significant heat loss through the calming section of the experimental equipment.

The percentages on the labels for the graphs below represent percentage of air flow through the rotameter used in the study. It was not important to convert these values to Reynolds numbers as a direct comparison could still be made.

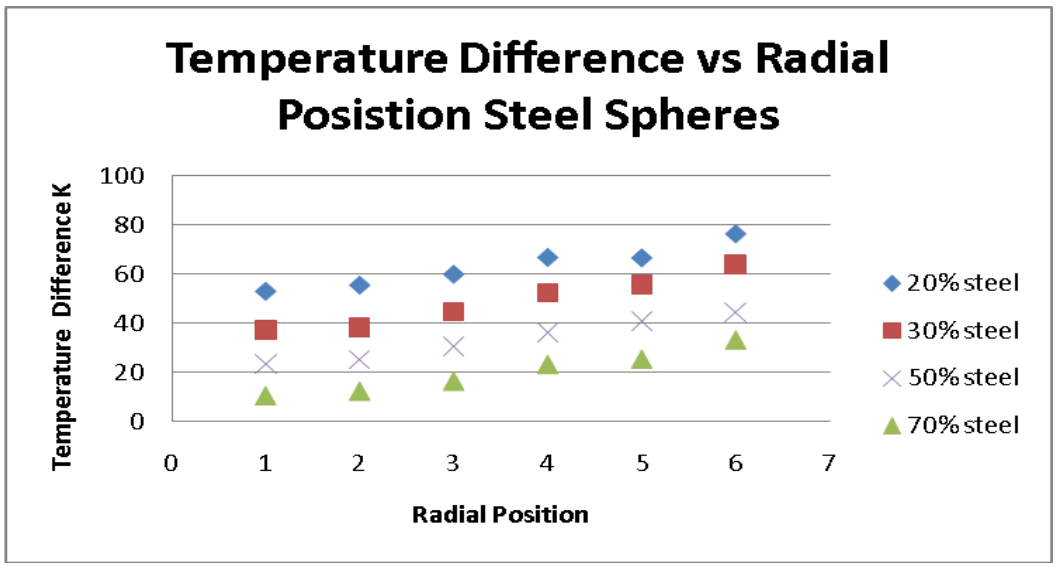

Figure 10 Temperature Difference vs. Radial Position Steel Spheres

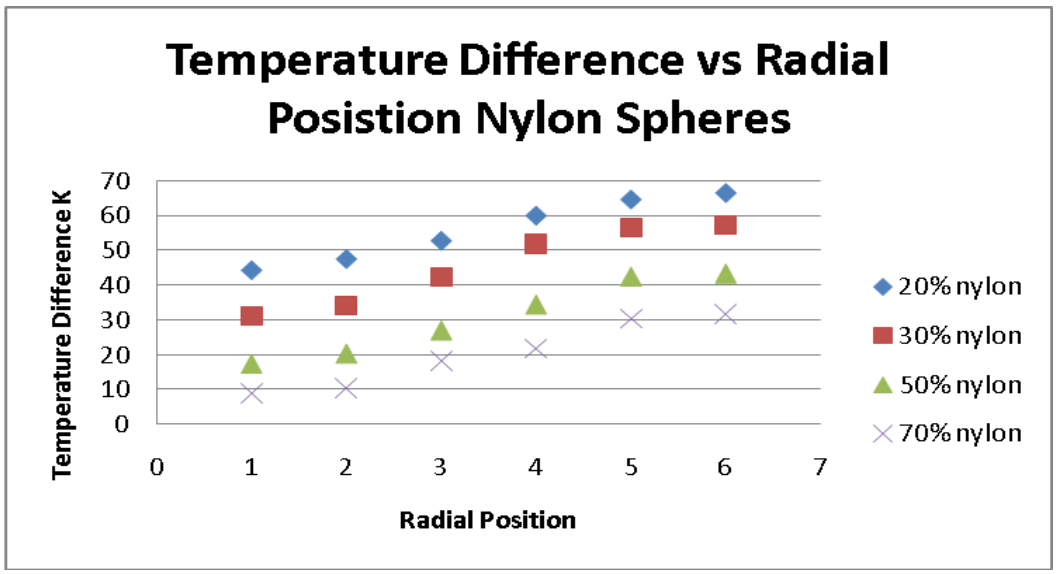

Figure 11 Temperature Difference vs. Radial Position Nylon Spheres

Heat loss was compared between the steel and nylon spheres to see if there was a difference between the two at varying flow rates. Both the steel and nylon spheres follow similar trends however based on the data there is slightly less heat loss when nylon spheres are used. This can be seen in the trends seen in Figure 12 and Figure 13 below. Graphs at other flow rates can be seen in Appendix D: Calming Section Tests (4 inch column with Raschig Rings). This could be due to the fact that steel has a higher thermal conductivity than nylon and therefore more readily transfers heat from the center of the calming section packing to the wall and bottom of the calming section where heat is lost.

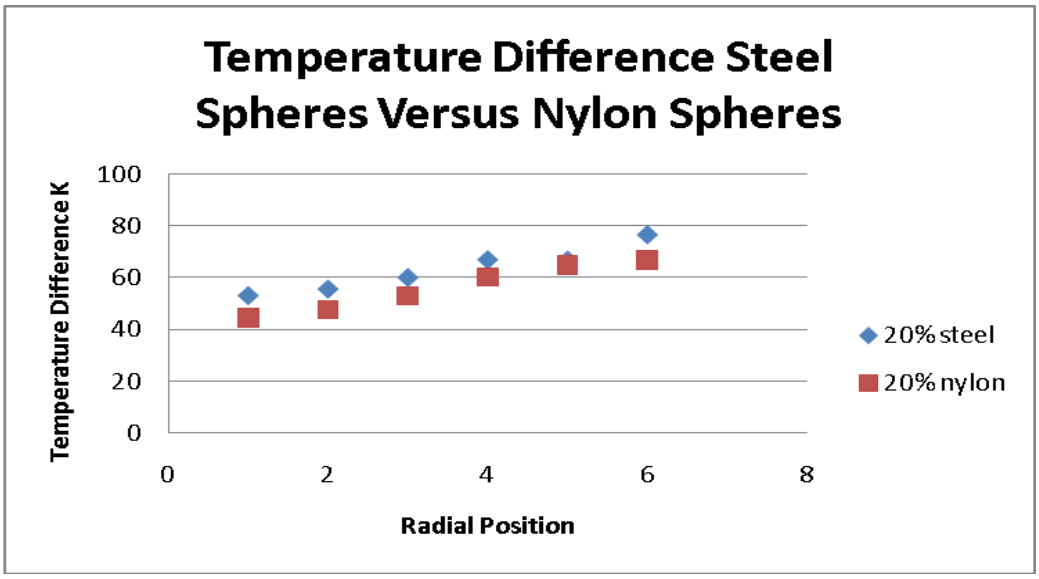

Figure 12 Temperature Difference Steel Spheres vs. Nylon Spheres Low Flow

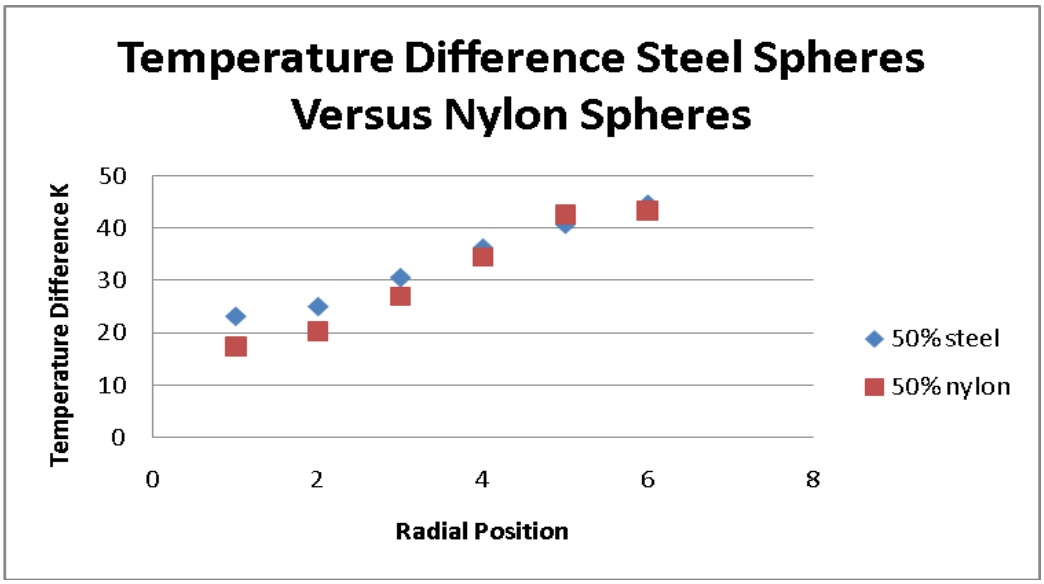

Figure 13 Temperature Difference Steel Spheres vs. Nylon Spheres High Flow

Based on these results, this study recommends that nylon spheres be used in the calming section in place of steel spheres to reduce heat loss in the calming section. A thermocouple or multiple thermocouples could be added to the calming section to get a more accurate inlet temperature reading of air entering the column. Alternatively the column could be suspended using a vertical support and the wall and bottom of the calming section could be insulated to significantly reduce heat loss.

While there was significant heat loss through the calming section, this factor was eliminated as a source of error since the GIPPF program uses the first bed height as the inlet data for comparison to the higher bed heights (6 inches-10 inches). As the inlet is measured at the first bed height, the heat loss through the calming section will not change the results as it is not taken into account for the dimensionless temperature profile calculations. This heat loss could cause a discrepancy between the results obtained for previous heating and cooling experiments by reducing the driving force in the test section of the column, and may lead to less accurate cooling results.

Wall Cooling Tests

Since heat loss through the calming section was not the reason for the inaccurate data, diagnostic tests were run on the cooling wall to determine if this was a main source of error. Temperature profiles of the inner annular wall were obtained in order to determine whether a uniform temperature was maintained. This is important as this is one of the assumptions used in the modeling of the system. This test was also performed to see if there were any blockages in the annular space which would affect the temperature profile and thus the results obtained.

In order to run this experiment, a thermocouple was fastened to the end of a ruler which was then pressed against the inner wall of the tube and the temperature was recorded. Temperatures were recorded at one inch intervals starting just above the calming section and at four radial positions for each height (90 degrees apart). The temperature profiles were then plotted for each depth and compared. It is important to note that hot air was flowing through the column at the time the test was performed so temperature readings near the calming section of the column were expected to be higher than those readings obtained from the top of the column. The water flow direction was changed so that data could be obtained for both countercurrent and co-current flows. This allowed us to see if the one of the flow directions of water gave a more uniform temperature profile than the other.

For countercurrent flow, it was found (except for the lower bed depths) that the wall temperatures were within two degrees Celsius of one another (between 14 degrees and 16 degrees Celsius). For co-current flow it was found (except for the lower bed depths) that the wall temperatures were within two degrees Celsius of one another (between 10.5 degrees and

12.5 degrees Celsius). This test was performed after the test for countercurrent flow and thus the temperatures on average are lower. This profile is reasonably uniform and variation may be due to the fact that steady state was still not achieved.

It was determined that there were no blockages in the annular space between the column walls. There was little difference in the uniformity of the temperature profiles for co-current and countercurrent flows and thus water flow direction did not matter. These graphs show that any discrepancy between the heating and cooling data is not due to a difference in the uniformity of the wall temperature or any sort of blockage in the annular space. The graphs can be seen in Appendix D: Wall Cooling Tests.

Data Collection Method

After ruling out that the calming section and cooling wall temperature had an effect on our results, this study decided to try to develop a new method for gathering data, believing that it may yield more consistent and accurate results than the methods used in previous cooling experiments at WPI. While collecting data, it was noticed that the air quality would change drastically from day to day. The drastic changes in initial conditions from day to day led this study to believe that the method that had been previously used may need to be altered in order to obtain consistent results.

The previous data collection method entailed packing the column to a single bed height and then acquiring data for all potential Reynolds numbers at that particular bed height. This meant that each separate bed height had differing initial conditions, which could cause unexpected temperature trends relating to bed height changes similar to the trends that were observed in our early data collection (Figure 9). This study changed the method so that data was collected for one Reynolds number at every bed height in a given day. This meant that in the morning the column was packed to 4 inches, the initial bed height, and the air flow was started. Throughout the day packing was added to the column at 2 inch intervals and the data was collected for each change. This method took more time because repacking had to be done throughout the day rather than just in the morning. However, this study found that the new method provided consistent physically feasible data, which the old method did not. Once the methods were changed the temperature profiles obtained made physical sense.

4 Inch Results

Once the new data collection method was determined to provide expected dimensionless temperature profiles, this study's experimental data could be compared to other cooling experiments. This study ran several Reynolds numbers in the 4 inch column with ½" raschig ring packing. The 4 inch column was used so that it could be compared to Borkink (1991) and

Ashman et al. (2009). This study's data was compared to previously run cooling experiments in order to confirm the repeatability of the results and to eliminate human error as a major source of discrepancy. It is important to note that the Peclet number used in this comparison is not the radial Peclet number described above. The Peclet number used is determined by the following equation: Pe = Re * Pr. In this study and in Ashman et al.(2009), the Prandtl number for air is assumed to be constant at 0.71.

As discussed briefly in the methodology, the Reynolds numbers from this study and Ashman et al. (2009) were multiplied by a factor of 1.2 to account for the fact that the air was metered before being heated. The correction factor comes from the fact that the air is metered at 298K but is heated and enters the column at 368K. The equation PV=nRT can be rearranged to the following:

$$\frac{368K * V_1}{298K} = V_2$$

Which when rounded leads to a correction factor of 1.2. The Reynolds number in Ashman et al. (2009) was determined in the same manner as this study so the correction factor could be applied. It was not applied to the Reynolds numbers obtained in Borkink (1991) because the flow rate in that study was measured downstream of the heater, taking into account the volume change.

The data from Borkink (1991) was obtained from a column with an inner diameter of 49.9mm and ½" raschig rings with an equivalent spherical diameter of 6.2 (N=8). Both this study and Ashman et al. (2009) used ½" raschig rings in a column with an inner diameter of 4 inches (N=7).

The data was plotted for all three studies and best fit lines were added. The comparison of the data can be seen in Figure 14. The slope of the best fit line for this study and Borkink (1991) are nearly identical. The slope of the best fit line from the Ashman et al. (2009) was not as close to the slope of the best fit lines for this study and Borkink (1991) The discrepancy between the data for this study and that of Ashman et al. (2009) can be attributed to the data collection method used in the Ashman et al. (2009) study. In the Ashman et al. (2009) study, data was collected using the previous method of collecting several Reynolds numbers at one bed depth per day. Therefore, the results in Ashman et al. (2009) would be affected by the changing initial conditions from day to day. The new procedure of collecting one Reynolds number for each bed depth in a day provided more accurate results that proved to be consistent with other literature studies, including Borkink (1991). The comparable data showed that there was not an issue with this new experimental procedure and that the results were repeatable. This allowed for confidence for continuing the study using the same procedure for the two inch column.

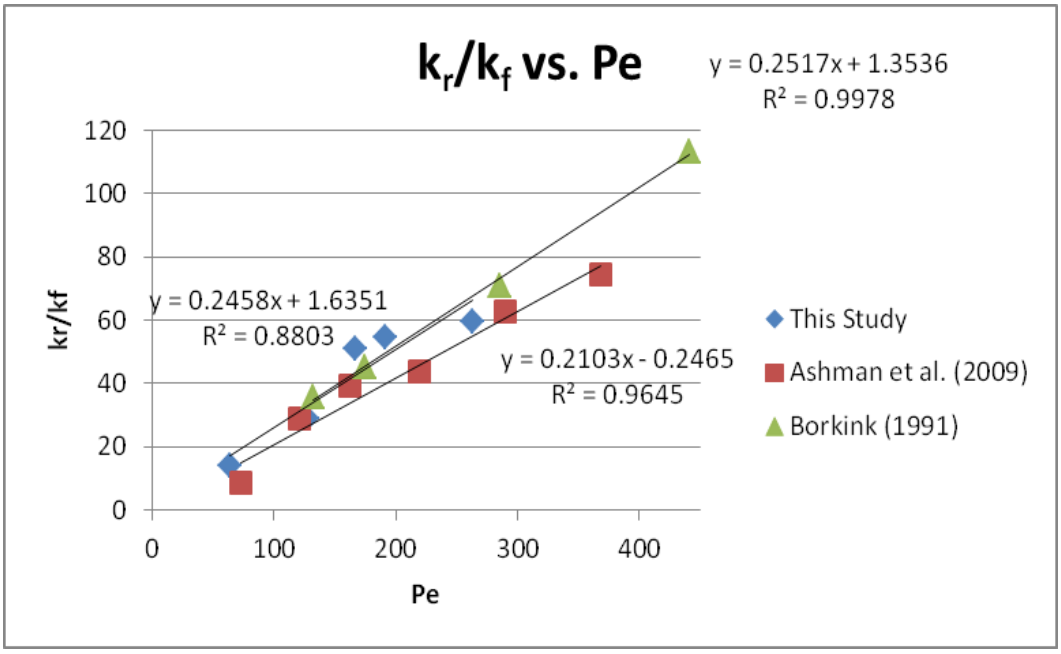

Figure 14: Comparison of Radial Heat Transfer between Cooling Experiments

Data for the Nusselt number (Nu_w) and the effective radial thermal conductivity were compared for this study and that obtained in Ashman et al. (2009) as compared to the Reynolds number. The results can be seen below in Figure 15. The data from this study and the data from the Ashman et al. (2009) study are in good agreement when comparing the Nusselt number verses the Peclet number. This is to be expected as the equipment used in this study and in Ashman et al. are identical. The Nusselt number (Nu_w) is the ratio of convective to conductive heat transfer across the wall. Since the equipment used is the same it would be expected that the Nu_w should be the same or similar, which was the case. The Nusselt numbers for this study and the Borkink (1991) study are not in good agreement. This could be explained by the experimental setup used in the Borkink (1991) study. In that study, the nearest wall thermocouple was at dimensionless radial position of 0.875 whereas in this study the closest dimensionless radial position to the wall was 0.94. This would affect the results obtain for the Nusselt number in Borkink (1991).

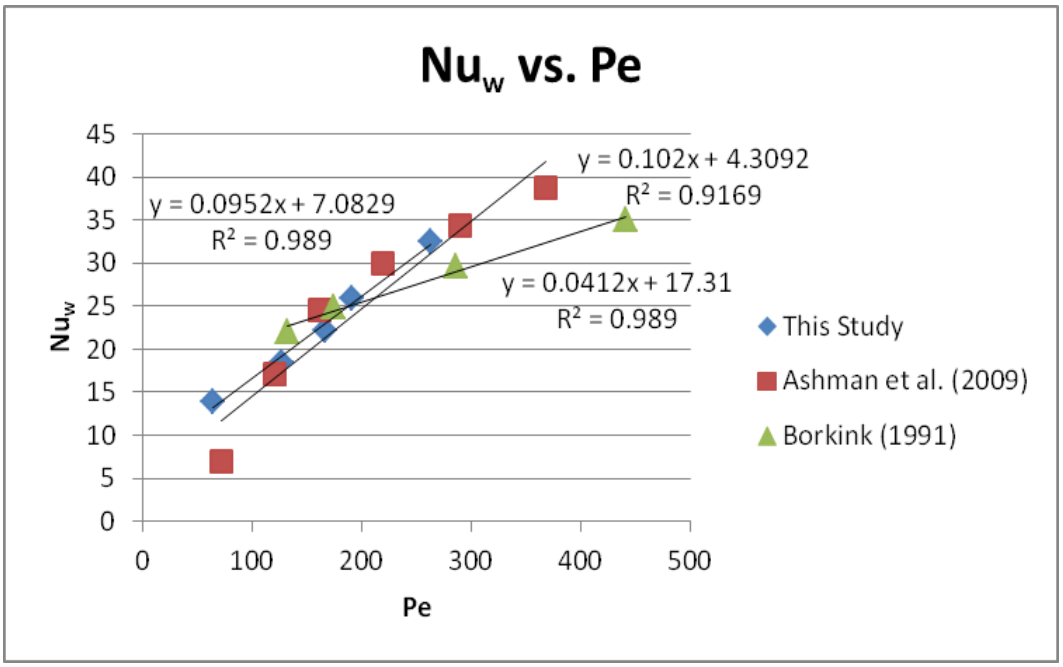

Figure 15: Nusselt Number versus Reynolds Number

This study's four inch column data is comparable and within engineering error with both Ashman et al. (2009) and Borkink (1991). This proved that our data collection method and results were valid and similar to other cooling experiments.

Two Inch Results

The main focus of this study was to determine why there were discrepancies between results obtained in heating experiments to those obtained in cooling experiments. Data from this study and Ashman et al. (2009) (both cooling studies) was compared to previous heating data obtained by Dixon (1997). The data from all three studies can be directly compared as the same set up and equipment was used. The data comparison can be seen in Figure 16 and Figure 17 below. The slope of the best fit lines from both this study and the heating experiment were nearly identical when the effective radial thermal conductivity versus Reynolds number was plotted. The graph shows that in this study there was slightly higher radial thermal conductivity than there was in Dixon (1997) and in Ashman et al. (2009). A contributing factor to why the data from this study was slightly different from the heating data is humidity which will be described below (Air Humidity). The data for the Nusselt number versus Reynolds number for this study and the heating study are also in good agreement. There is discrepancy in the data for this study and the Ashman et al. (2009) study however due to the large amount of scatter in the data no conclusions can be made. Theoretically the effective radial thermal conductivity should be very similar if not the same. See Figure 16 and Figure 17 below:

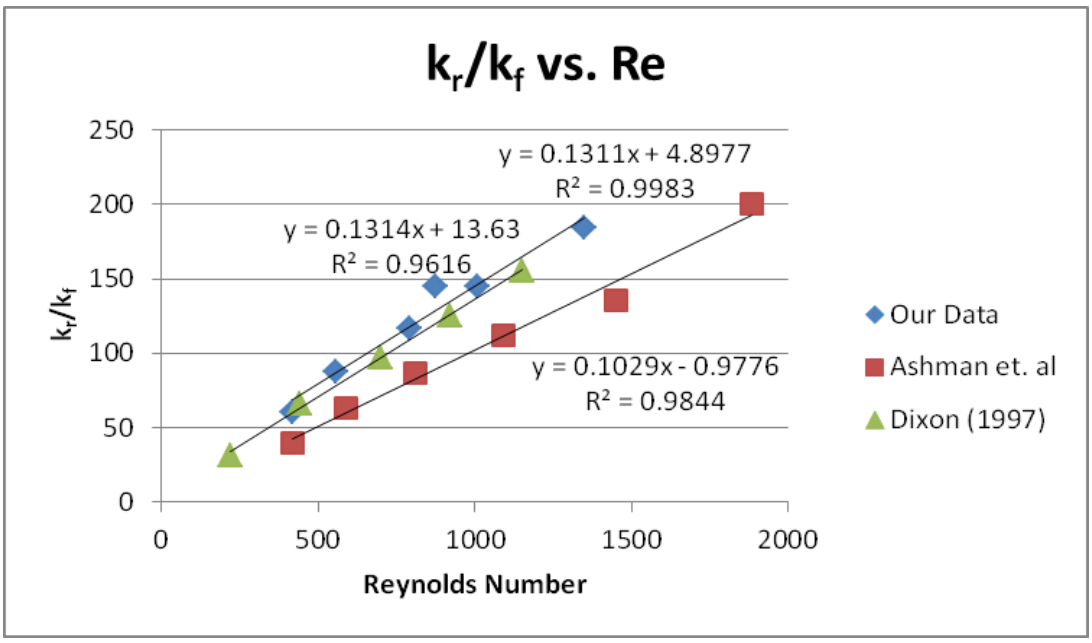

Figure 16: Comparison of Effective Radial Thermal Conductivity between Heating and Cooling Experiments

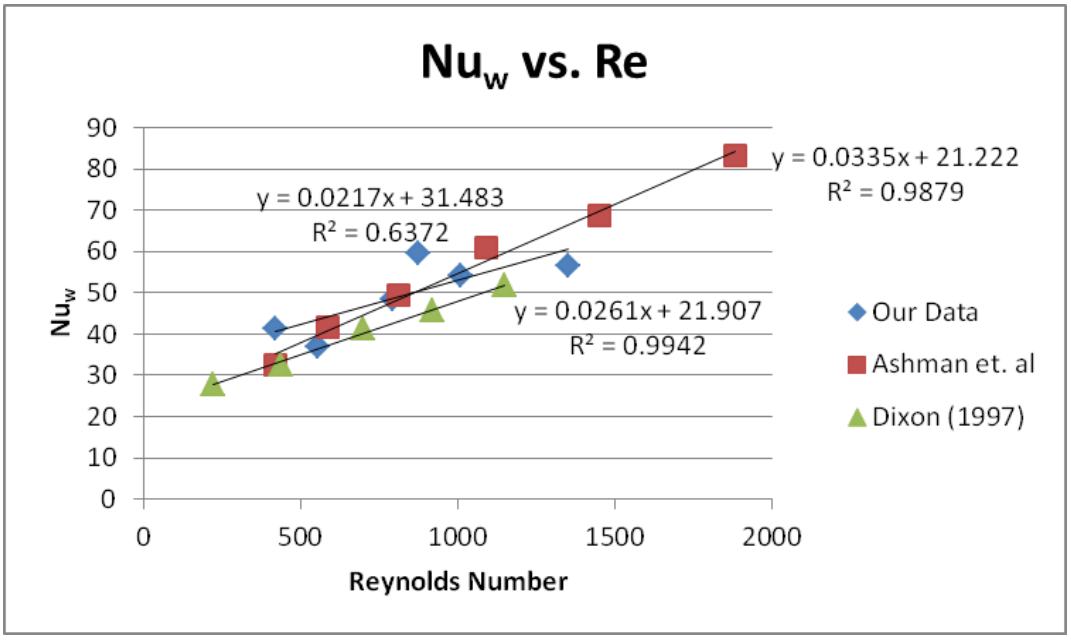

Figure 17: Comparison of Nusselt Number Cooling versus Heating Experiments

Air Humidity

One of the factors that contributed to the difference seen between this study and the heating experiment was the supply air humidity. The supply air to the column varied in humidity on a daily basis. This humidity usually caused condensation to form on the inner wall of the column.

This condensation explains why this study's data appears to have a higher radial thermal conductivity than the heating experiment data. Humid air has a much higher heat capacity than dry air so the Prandtl Number would change:

$$Pr = \frac{\rho c_p}{\mu}$$

When the water vapor from the air condenses on the inner wall of the tube, it releases the energy more rapidly than can be released by dry air alone. This release of energy from the water explains the appearance of higher heat transfer for this study. Condensation was found on the inner wall of the column during many of the experiments. While there may have been humid air in the supply for the heating experiment, the air would not have condensed and thus the energy contained in the water vapor would not have been released as the stream passed through the column. The mode of heat transfer in the heating experiment deals with the increase in internal energy (increase in temperature) of the air and water vapor molecules after hitting the heated wall from which the particles gained energy. In the cooling experiment, gaseous phase particles lose internal energy after hitting the cooled walls similar to the heating experiment. In the cooling experiment, there was an additional mode of heat transfer which was the transfer of energy from the water vapor as it condensed on the wall of the column. This additional mode of heat transfer makes it such that the rate of effective radial heat transfer is slightly higher in the cooling experiment performed in this study. Figure 18 below depicts Q (heat flow) versus the mass percent of water in a humid air mixture. The trend is shown for values of humidity ranging from 0-10 mass percent water to represent the possible ranges of humidity throughout the experimental process. An exact value could not be obtained because a new air dryer was installed in the building air supply before full humidity tests could be performed.

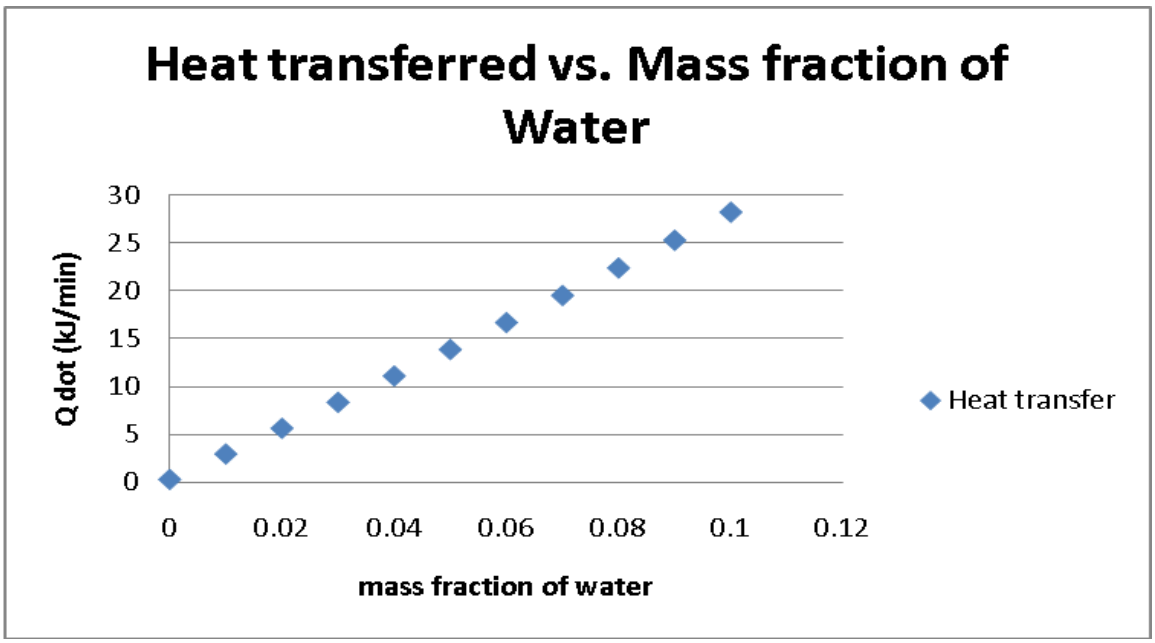

Figure 18: Qdot versus Mass Fraction water

These results show that the heat transfer will increase with the mass fraction of water. However, this will only change the results very slightly. So while this would shift this study's data closer to the heating data, it would not create a significant change in results. Air humidity should still be monitored and taken into account but will not greatly affect results unless there is an excessive amount of moisture in the supply air stream.

Conclusion

After performing multiple experiments and analyzing the gathered data in comparison to literature data, this study determined that the main factor affecting the discrepancies was the method of experimentation. Humidity was determined to have a minor effect on the results but should still be taken into account. Other factors that could have contributed to the error were eliminated through experimentation, including uniform wall cooling and heat loss through the calming section.

Previous cooling experiments collected data by running a series of experiments as follows: one bed height for a series of Reynolds numbers per day. This method of data collection skewed the temperature profile results because it meant that different bed height data for each Reynolds number, which should have been comparable, had different initial conditions. This difference in conditions caused unexpected trends in the data profiles especially in the temperature changes between different bed heights. This study changed the method to run experiments so that one Reynolds number is run per day at 4 bed heights in order to ensure consistent conditions for the data collection and to yield more reliable results.

The data collected in this study showed slightly higher radial heat transfer than previous cooling and heating experiments. This was found to be caused mainly by humidity in the air being passed through the column. The water vapor in the air condensing on the inner wall of the column released heat more rapidly than could be released by just air molecules. This rapid heat loss through condensation explains the apparent increase in radial heat transfer in this study from the literature heating data (Dixon, 1997).

Nomenclature

$Bi_w = wall\ Biot\ number = \frac{h_w R}{k_r}$

$c_p = heat\ capacity$

$d_p = particle\ diameter$

$h_w = wall\ heat\ ransfer\ coefficeint$

$k_r = effective\ radial\ thermal\ conductivity$

$k_f = thermal\ conductivity\ of\ the\ fluid$

$N = tube\ to\ particle\ diameter\ ratio = \frac{2 * R}{d_p}$

$Nu_w = Nusselt\ Number = \frac{h_w d_p}{k_f}$

$Pe_r = radial\ Peclet\ number = \frac{v \rho c_p d_p}{k_r}$

$r = radial\ position$

$R = radius\ of\ the\ tube$

$Re = Reynolds\ Number = \frac{v_s \rho d_p}{\mu}$

$T = temperature$

$T_w = wall\ temperature$

$T_{zo} = center\ temperature\ of\ the\ first\ bed\ depth$

$v = superficial\ velocity$

$x = dimensionless\ bed\ depth = \frac{z}{R}$

$y = dimensionless\ radial\ position = \frac{r}{R}$

$z = bed\ depth$

$\rho = density$

$\theta = dimensionless\ temperature = \frac{(T - T_w)}{(T_o - T_w)}$

$\mu = viscosity$

References

Ashman, Michael, Dmitriy Rybak and William Skene. Heat Transfer Parameters of Cylindrical Catalyst Particles with Internal Voids in Fixed Bed Reactor Tubes. Major Qualifying Project. Worcester, MA, 2009.

Borkink, J.G.H. and K.R. Westerterp. "Influence of Tube and Particle Diameter on Heat Transport in Packed Beds." AIChE Journal 38.5 (1992): 703-715.

Borkink, J.G.H. Heat Transport in Wall-Cooled Packed Beds of Low Tube-To-Particle Diameter Ratio. PhD Thesis. University of Twente. Enschede, 1991.

Borkink, J.G.H., P.C. Borman and K.R. Westerterp. "Modeling of Radial Heat Transport in Wall-Cooled Packed Beds." Chemical Engineering Communications 121 (1993): 135-155.

Chu, C.F. and K.M. Ng. "Flow in packed tubes with a small tube to particle diameter ratio." AIChE Journal 35.1 (1989): 148-158.

Demirel, Y., R.N. Sharma and H.H. Al-Ali. "On the effective heat transfer parameters in a packed bed." International Journal of Heat and Mass Transfer 43 (2000): 327-332.

Dixon, Anthony G. "An Improved Equation for the Fixed Bed Tubular Reactor Overall Heat Transfer Coefficient." Chemical Engineering Process 35.5 (1996): 323-331.

Dixon, Anthony G. "Heat Transfer in Fixed Beds at Very Low (<4) Tube-to-Particle Diameter Ratio." Industrial & Engineering Chemistry Research 36.8 (1997): 3053-3064.

Dixon, Anthony G. "The length effect on packed bed effective heat transfer parameters." The Chemical Engineering Journal 31.3 (1985): 163-173.

Felder, Richard M. and Ronald W. Rousseau. Elementary Principles of Chemical Processes. 3rd. United States: John Wiley & Sons, Inc., 2005. p 373, 635-637.

Lerou, Jan J. and Gilbert F. Froment. "Estimation of heat transfer parameters in packed beds from radial temperature profiles." The Chemical Engineering Journal 15.2 (1978): 233-237.

Nijemeisland, Michiel and Anthony G. Dixon. "CFD study of fluid flow and wall heat transfer in a fixed bed of spheres." AIChE Journal 50.5 (2004): 906-921.

Smirnov, E.I., et al. "Radial Heat Transfer in Packed Beds of Spheres, Cylinders, and Raschig Rings." Chemical Engineering Journal (2003): 91, 243-248.

Tariku, F., M.K. Kumaran and P. Fazio. "Transient model for coupled heat, air and moisture transfer through multilayered porous media." International Journal of Heat and Mass Transfer 53.15-16 (2010): 3035-3044.

Van Dongeren, J.H. "Influence of Tube and Particle Diameter at Fixed Ratios on Heat Transport in Packed Beds." Final Year Project Report. University of Twente, 1994.

Wen, Dongshen and Yulong Ding. "Heat Transfer of gas flow through a packed bed." Chemical Engineering Science 61.11 (2006): 3532-3542.

Appendices

Appendix A: Sample Fortran Input Text File (2 inch column Raschig Rings)

```
     4         6          3          2
  50.8       10.49
   8.5        12.0       15.0      18.0     21.5     24
792.0      101.6         .0
  94.75
  51.13       51.79       50.27       52.90
  49.13       50.58       51.04       51.72
  45.58       50.79       47.05       52.82
  44.59       42.32       44.83       45.17
  47.16       41.11       49.00       39.26
  29.83       32.87       48.69       24.10
  7.59        9.28        8.32
792.0       101.6       45.0
  94.92
  52.62       51.65       52.15       52.93
  49.70       52.43       49.31       54.44
  52.32       48.46       48.04       50.97
  43.25       51.24       46.31       51.24
  39.54       36.94       43.43       38.01
  30.81       37.67       37.31       39.56
  8.18        9.76        8.91
792.0       152.4       .0
  94.83
  37.16       40.00       40.04       44.73
  37.16       38.65       41.71       44.58
  41.61       39.16       37.60       45.15
  35.67       33.23       37.22       37.07
  35.28       35.37       37.22       37.07
  27.42       30.21       30.95       27.93
  9.83        11.15       10.57
792.0       152.4       45.0
  94.78
  44.33       40.57       40.64       44.82
  37.12       39.33       39.85       45.58
  43.85       38.77       37.57       43.21
  35.51       34.30       38.01       38.56
  32.59       32.65       32.09       40.56
  27.88       27.38       35.74       29.13
  9.66        10.85       10.42
792.0       203.2       .0
  94.52
  33.86       35.43       32.88       32.83
  34.87       34.36       31.50       33.17
  32.48       35.99       32.56       32.51
  32.90       32.43       28.19       31.64
  33.20       30.81       30.65       28.89
  24.67       29.48       25.86       23.63
  10.33       11.58       11.18
792.0       203.2       45.0
```

```
  94.70
  33.54      35.51      35.71      33.28
  34.39      36.36      33.62      33.82
  33.93      35.67      33.55      30.90
  31.38      36.66      32.43      31.85
  31.56      32.84      27.90      31.40
  28.44      32.59      29.21      29.11
  11.48      12.67      12.28
792.0      254.0      .0
  94.58
  31.66      31.30      30.74      30.59
  32.44      30.76      31.02      34.08
  29.65      32.50      30.39      29.20
  32.79      30.72      30.91      32.84
  30.65      27.37      28.88      29.68
  28.48      28.95      29.44      25.29
  14.22      15.39      14.95
792.0      254.0      45.0
  94.71
  33.34      33.58      31.40      32.01
  31.32      33.01      30.97      30.81
  33.64      34.26      31.86      32.40
  31.80      33.61      29.47      30.45
  32.66      30.77      31.23      29.92
  28.11      28.31      27.62      28.50
  15.58      16.54      16.27
     -1.0       -1.0       -1.0
```

Appendix B: Θ vs. y by Reynolds Number

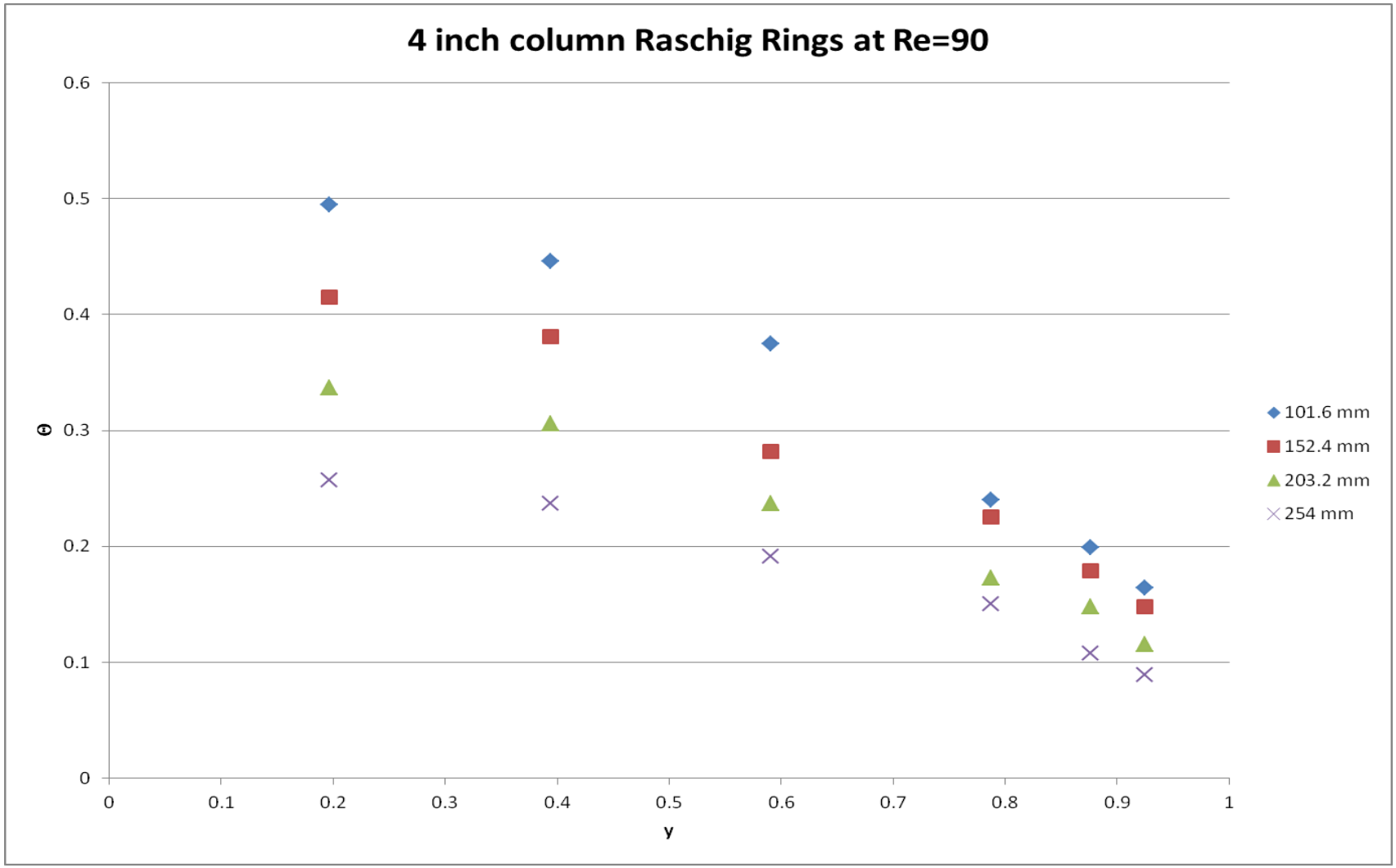
4 inch column Raschig Rings at Re=90
0.6
0.5
0.4
0.3
0.2
0.1
0
Θ
0
0.1
0.2
0.3
0.4
0.5
0.6
0.7
0.8
0.9
1
y
101.6 mm
152.4 mm
203.2 mm
254 mm

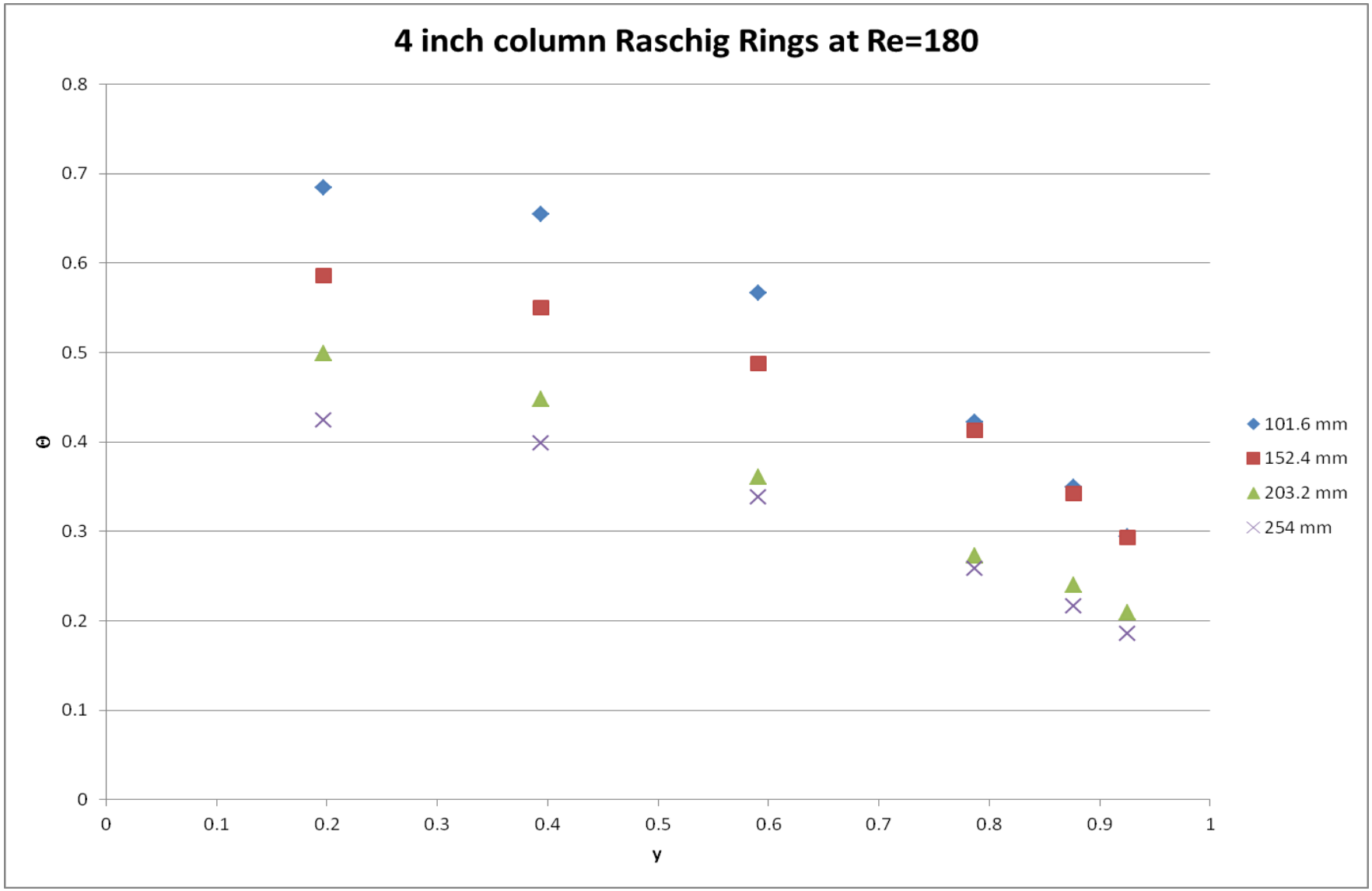
4 inch column Raschig Rings at Re=180
θ
y
0
0.1
0.2
0.3
0.4
0.5
0.6
0.7
0.8
0
0.1
0.2
0.3
0.4
0.5
0.6
0.7
0.8
0.9
1
101.6 mm
152.4 mm
203.2 mm
254 mm

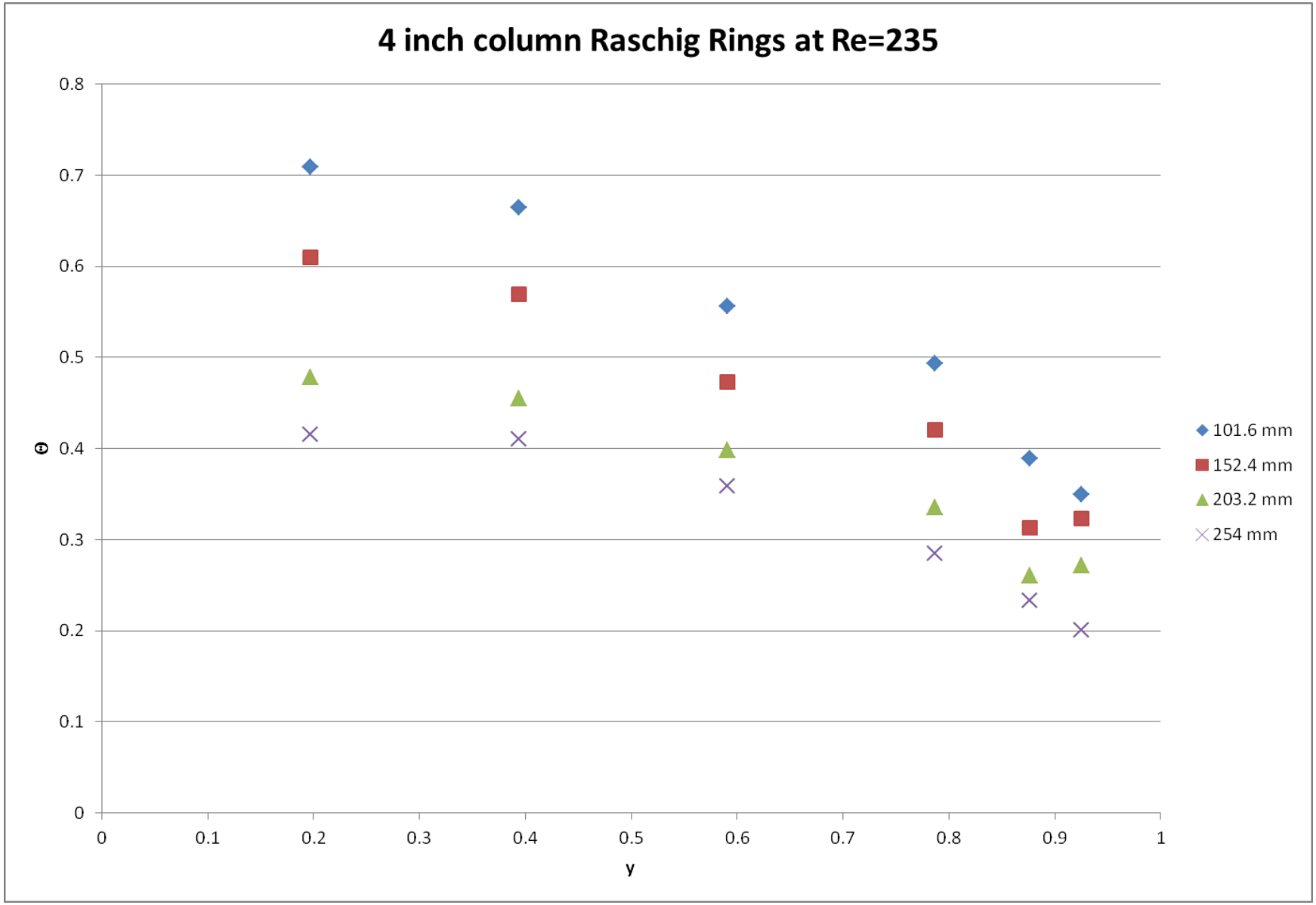
4 inch column Raschig Rings at Re=235
0.8
0.7
0.6
0.5
0.4
0.3
0.2
0.1
0
Θ
0
0.1
0.2
0.3
0.4
0.5
0.6
0.7
0.8
0.9
1
y
101.6 mm
152.4 mm
203.2 mm
254 mm

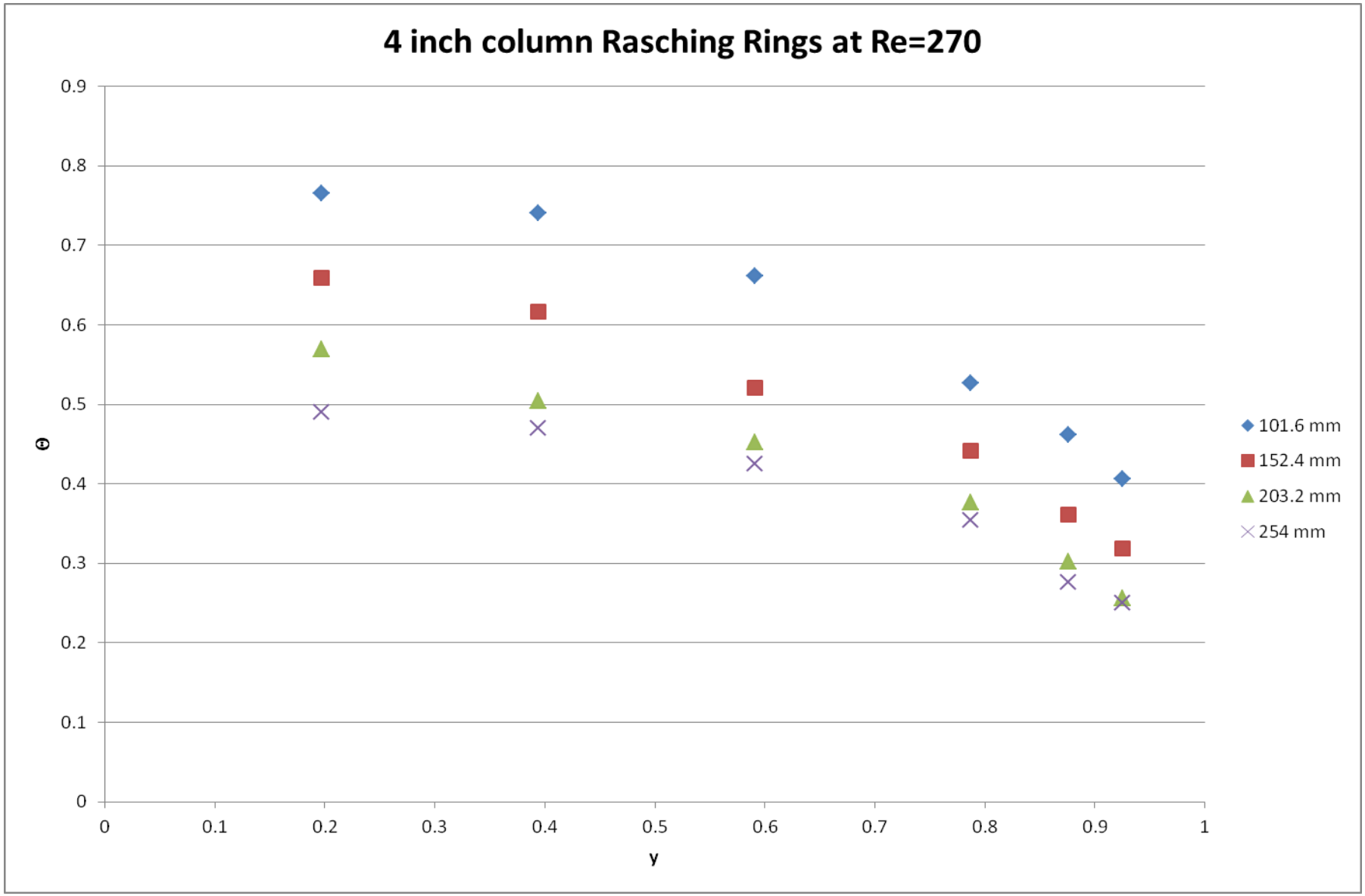
4 inch column Rasching Rings at Re=270
Θ
y
0
0.1
0.2
0.3
0.4
0.5
0.6
0.7
0.8
0.9
1
101.6 mm
152.4 mm
203.2 mm
254 mm

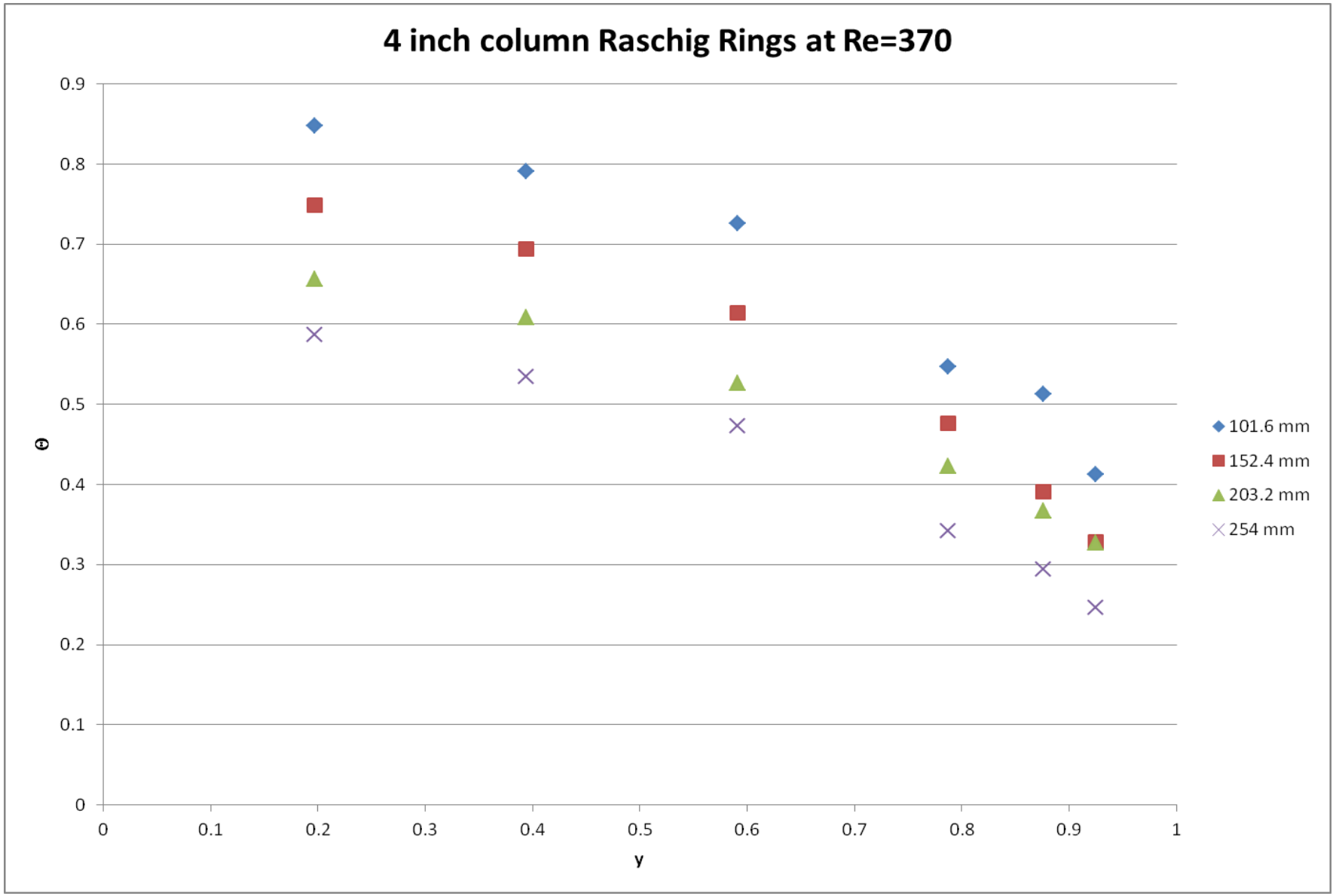
4 inch column Raschig Rings at Re=370
Θ
y
0
0.1
0.2
0.3
0.4
0.5
0.6
0.7
0.8
0.9
1
101.6 mm
152.4 mm
203.2 mm
254 mm

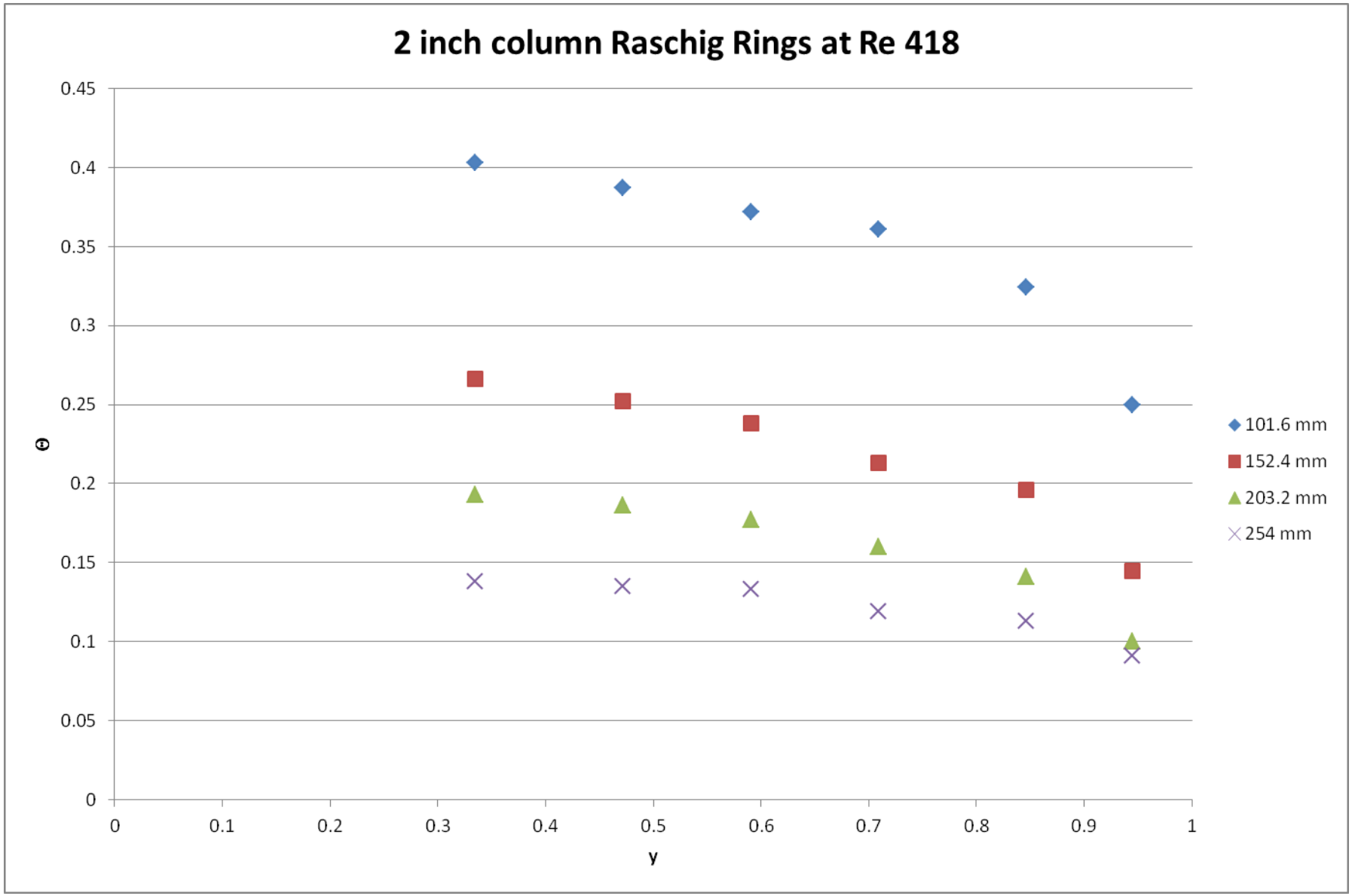
2 inch column Raschig Rings at Re 418
0.45
0.4
0.35
0.3
0.25
0.2
0.15
0.1
0.05
0
Θ
0
0.1
0.2
0.3
0.4
0.5
0.6
0.7
0.8
0.9
1
y
101.6 mm
152.4 mm
203.2 mm
254 mm

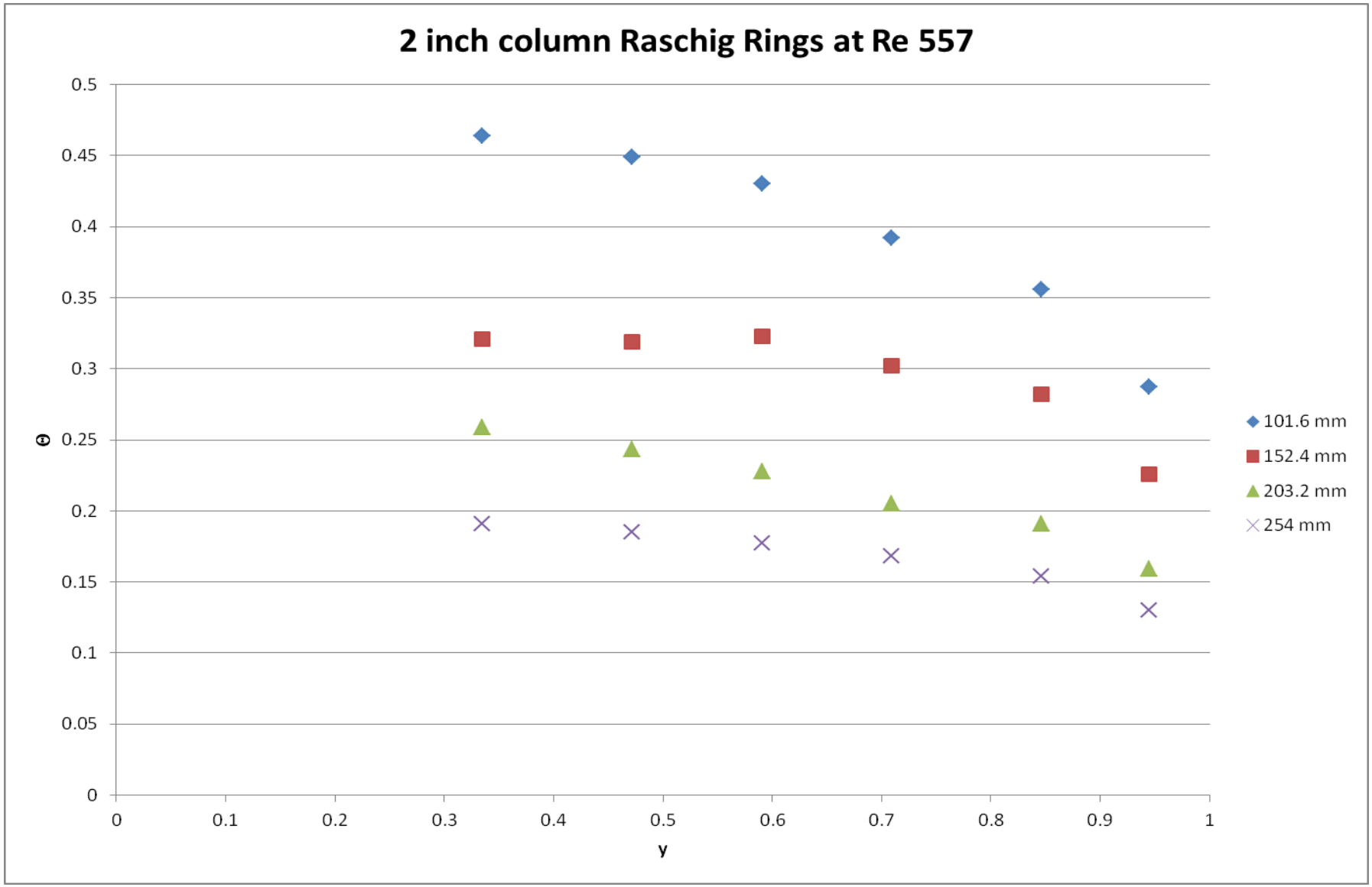
2 inch column Raschig Rings at Re 557
0.5
0.45
0.4
0.35
0.3
0.25
0.2
0.15
0.1
0.05
0
Θ
0
0.1
0.2
0.3
0.4
0.5
0.6
0.7
0.8
0.9
1
y
101.6 mm
152.4 mm
203.2 mm
254 mm

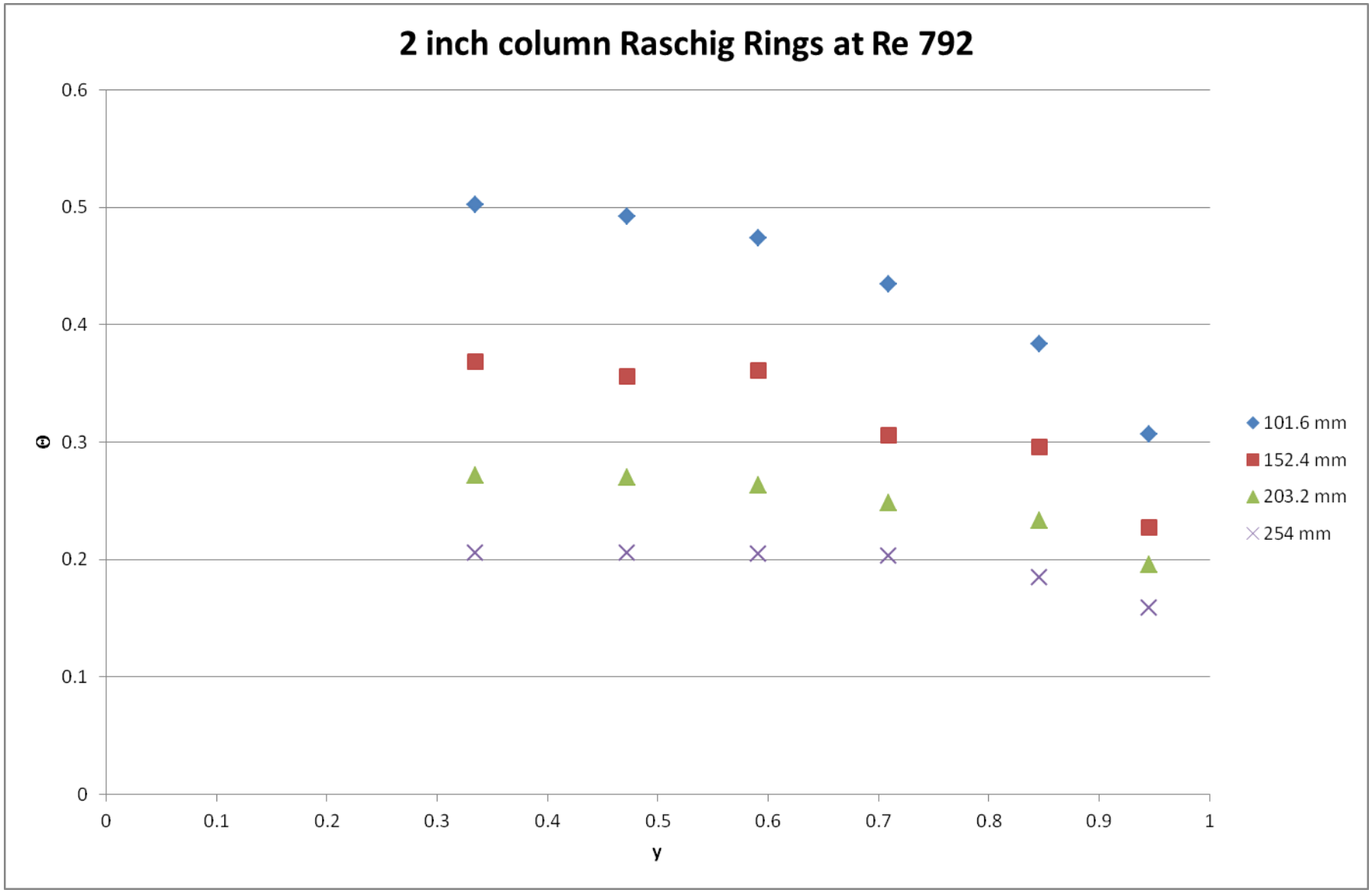
2 inch column Raschig Rings at Re 792
0.6
0.5
0.4
0.3
0.2
0.1
0
Θ
0
0.1
0.2
0.3
0.4
0.5
0.6
0.7
0.8
0.9
1
y
101.6 mm
152.4 mm
203.2 mm
254 mm

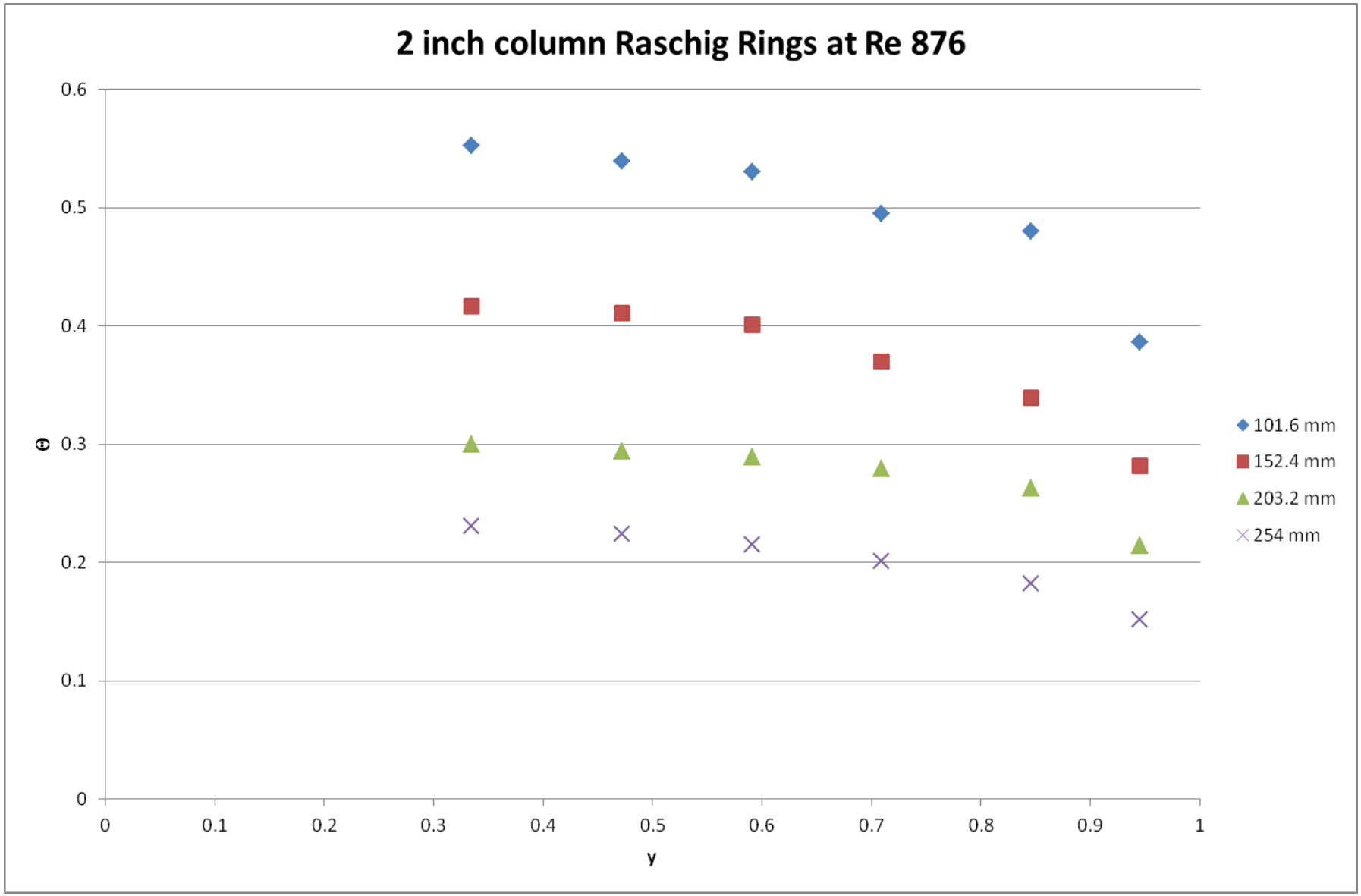
2 inch column Raschig Rings at Re 876
0.6
0.5
0.4
0.3
0.2
0.1
0
Θ
0
0.1
0.2
0.3
0.4
0.5
0.6
0.7
0.8
0.9
1
y
101.6 mm
152.4 mm
203.2 mm
254 mm

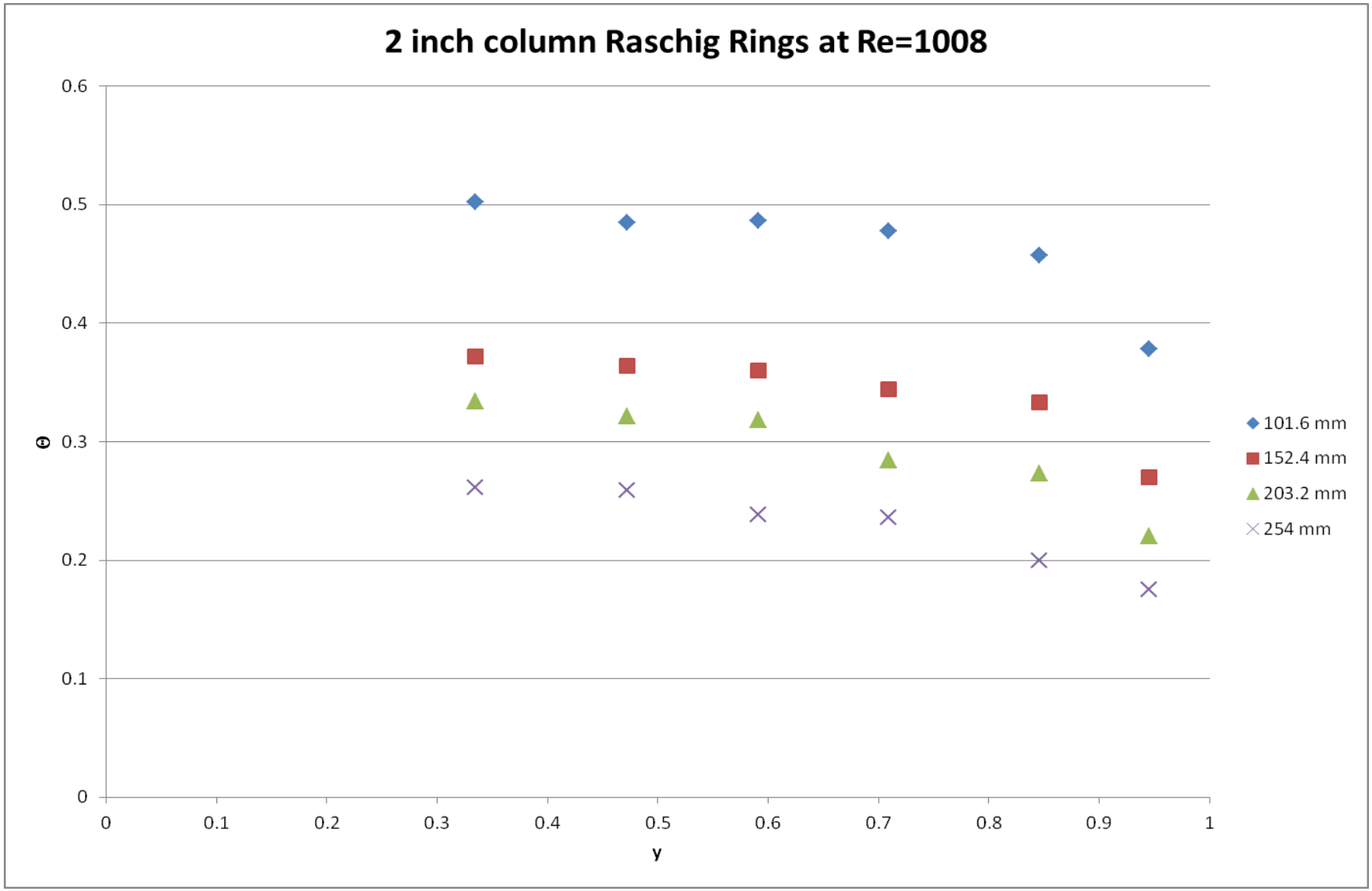
2 inch column Raschig Rings at Re=1008
0.6
0.5
0.4
0.3
0.2
0.1
0
Θ
0
0.1
0.2
0.3
0.4
0.5
0.6
0.7
0.8
0.9
1
y
101.6 mm
152.4 mm
203.2 mm
254 mm

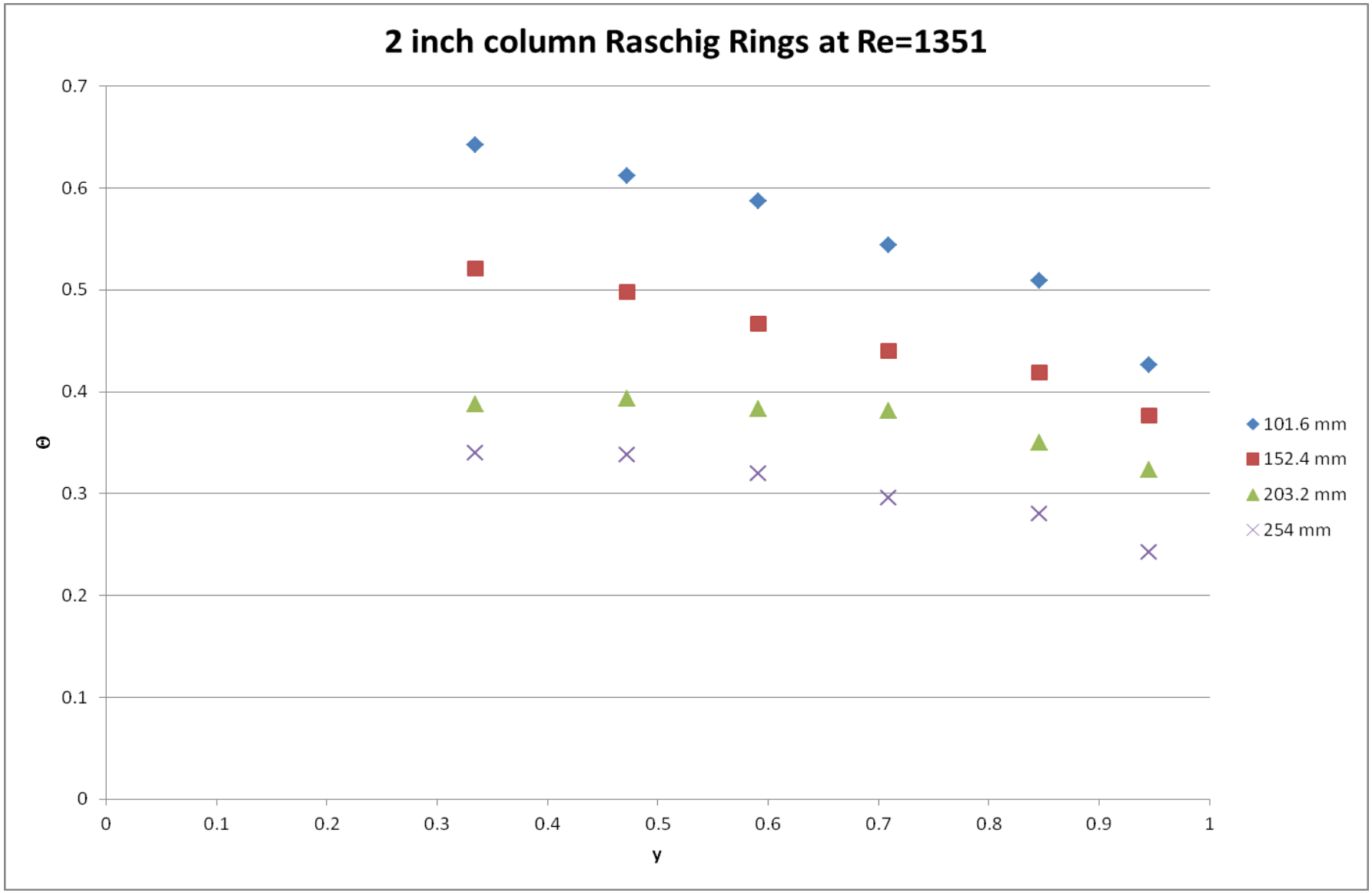
2 inch column Raschig Rings at Re=1351
0.7
0.6
0.5
0.4
0.3
0.2
0.1
0
Θ
0
0.1
0.2
0.3
0.4
0.5
0.6
0.7
0.8
0.9
1
y
101.6 mm
152.4 mm
203.2 mm
254 mm

Appendix C: k_r/k_f, Nu_w, Bi, and Pe_r for all Packings and Columns

4 inch column Raschig Rings

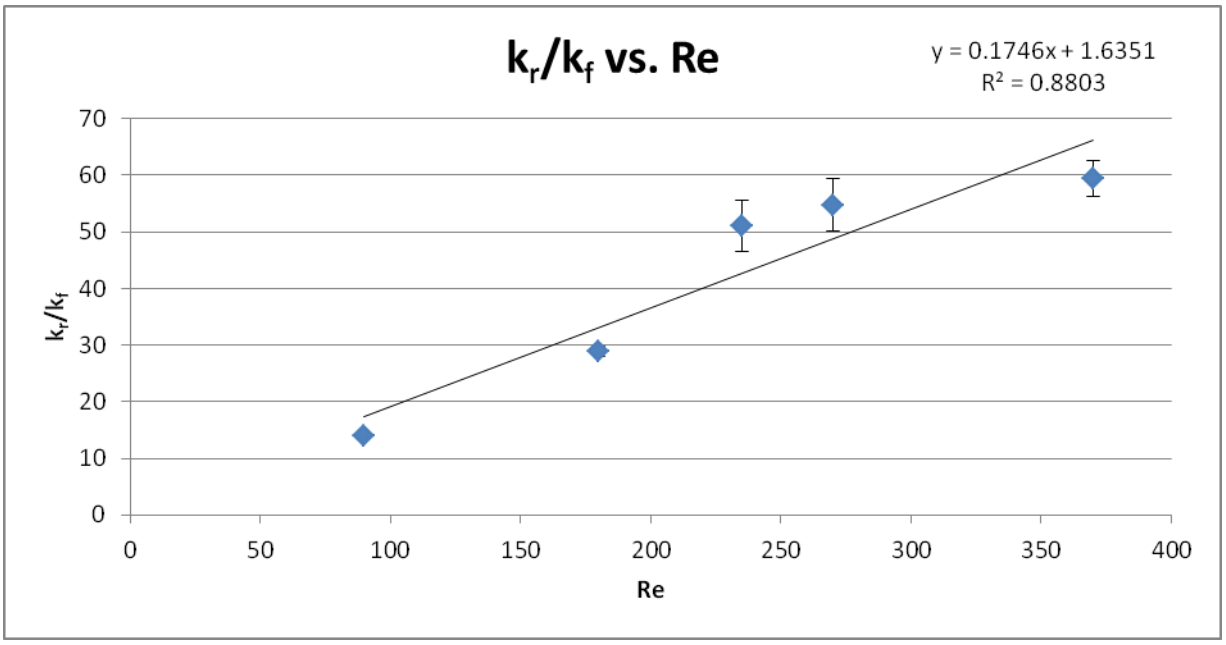

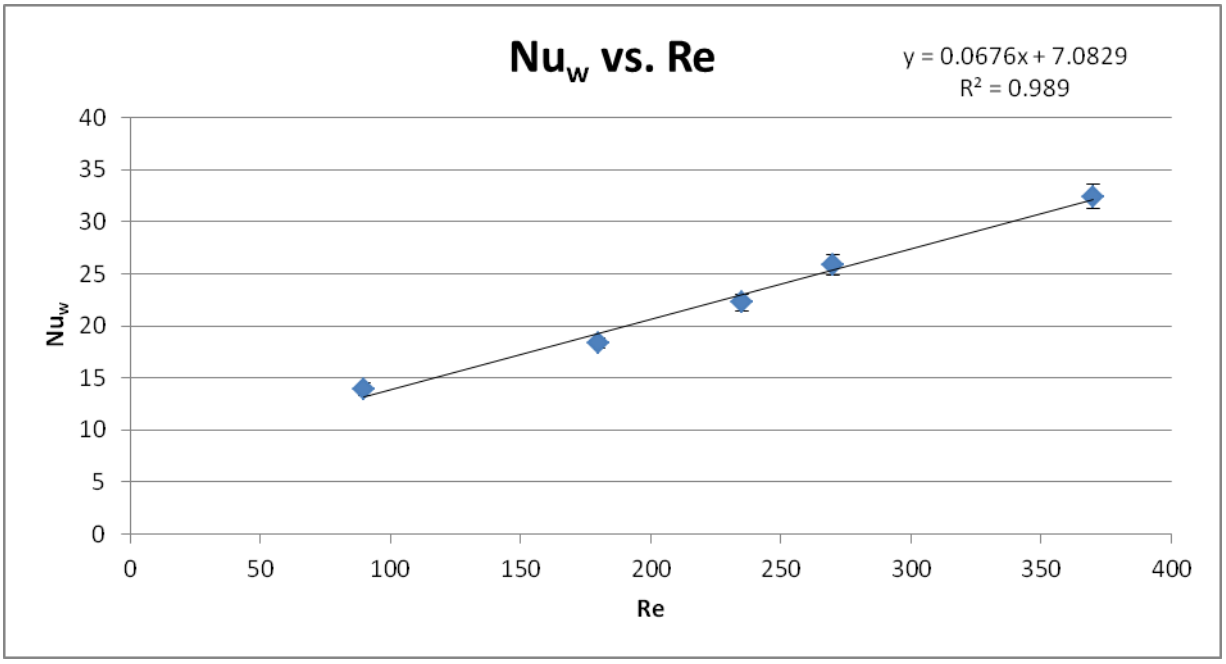

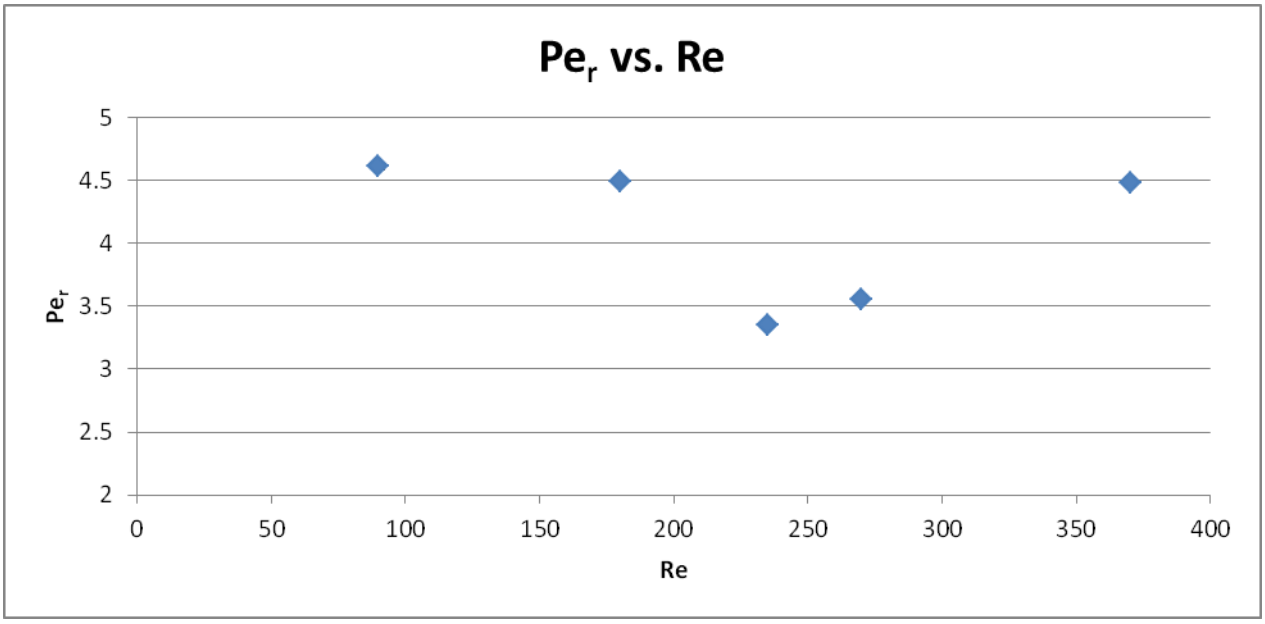
Per vs. Re
5
4.5
4
3.5
3
2.5
2
Per
0
50
100
150
200
250
300
350
400
Re

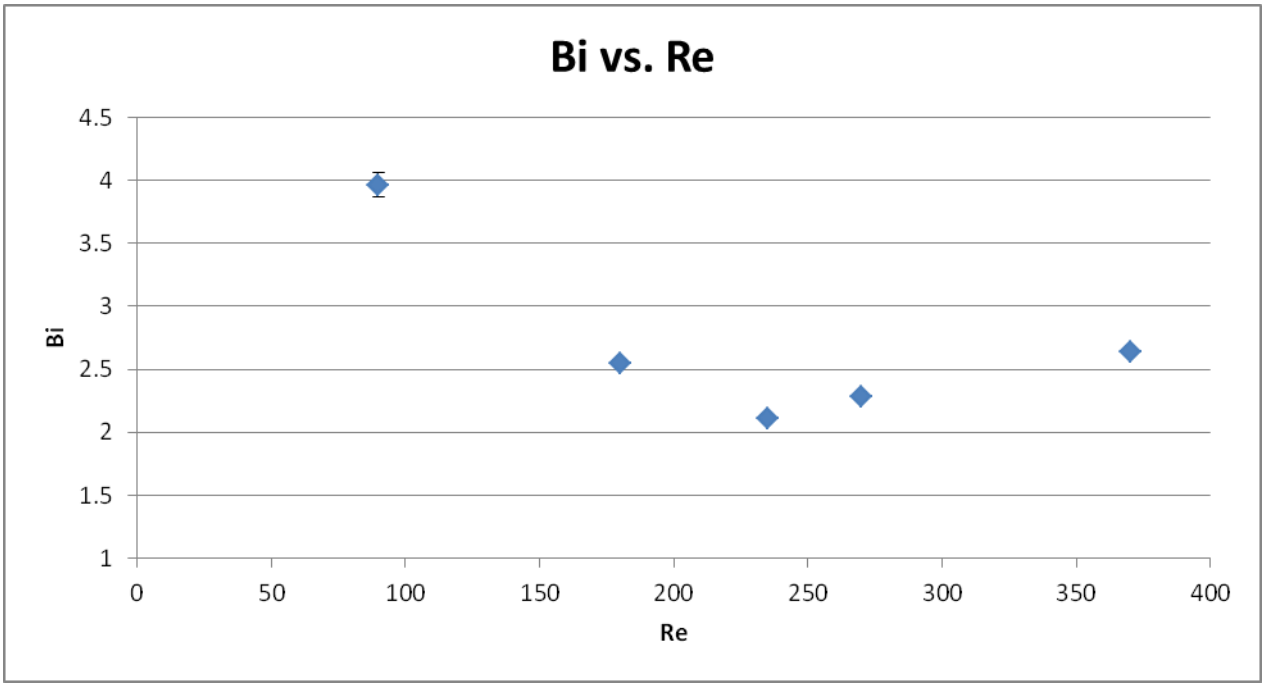
Bi vs. Re
4.5
4
3.5
3
2.5
2
1.5
1
Bi
0
50
100
150
200
250
300
350
400
Re

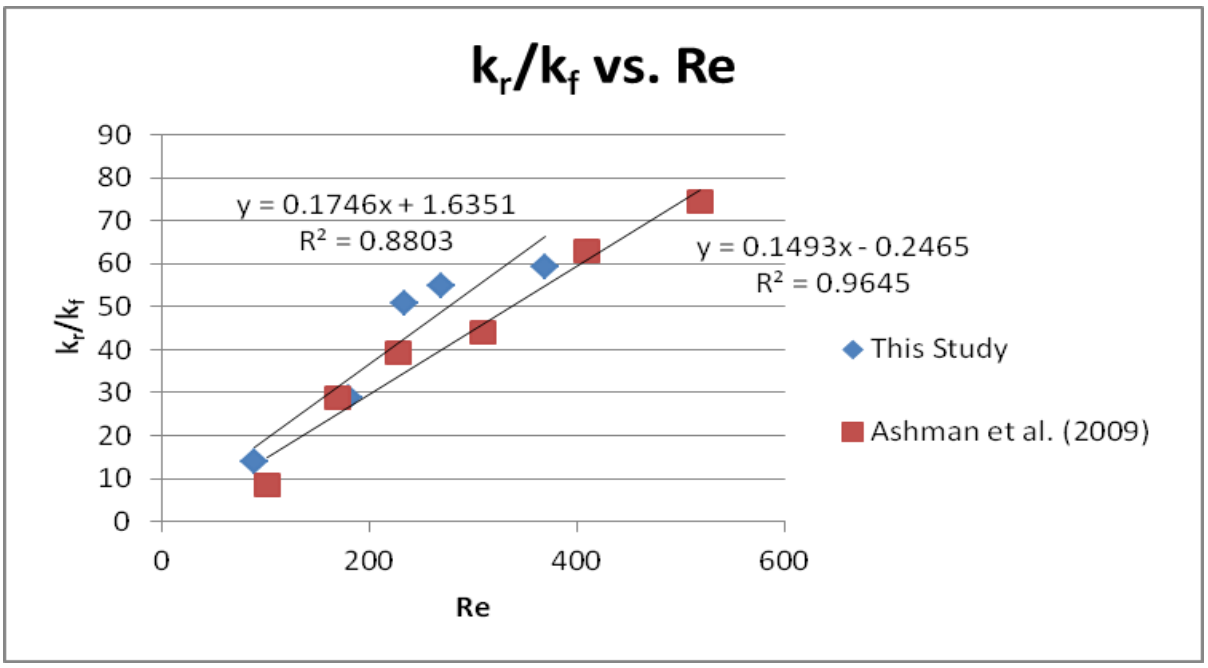
k_r/k_f vs. Re
90
80
70
60
50
40
30
20
10
0
0
200
400
600
Re
k_r/k_f
y = 0.1746x + 1.6351
R² = 0.8803
y = 0.1493x - 0.2465
R² = 0.9645
This Study
Ashman et al. (2009)

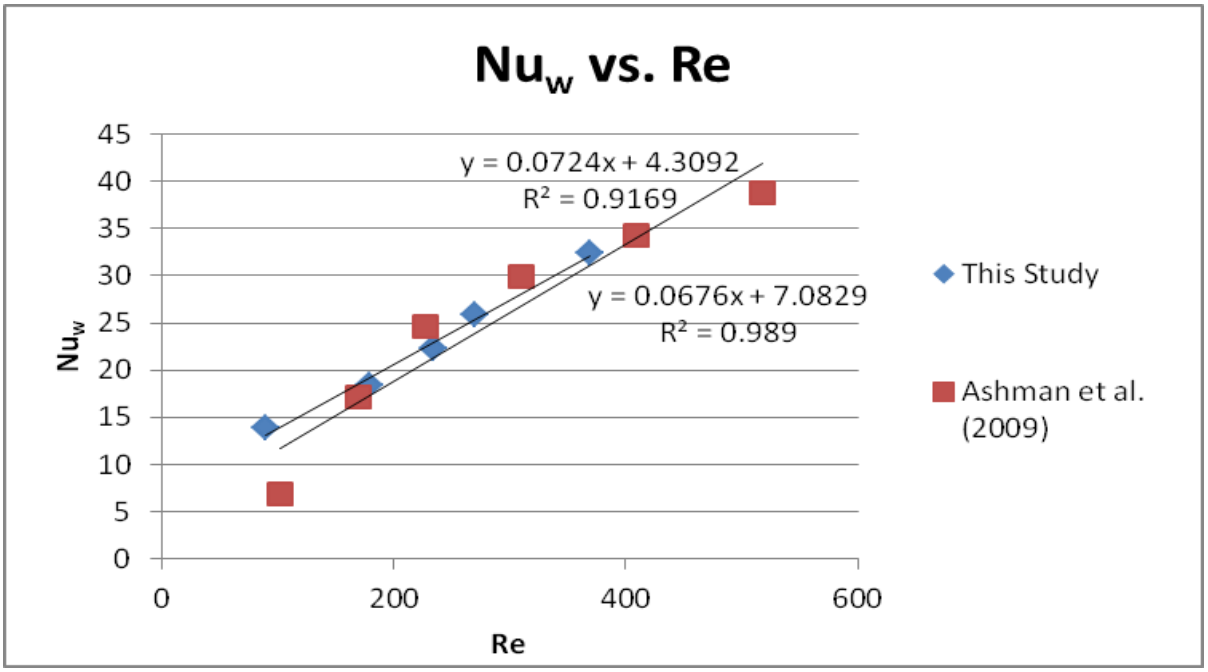
Nu_w vs. Re
45
40
35
30
25
20
15
10
5
0
0
200
400
600
Re
Nu_w
y = 0.0724x + 4.3092
R² = 0.9169
y = 0.0676x + 7.0829
R² = 0.989
This Study
Ashman et al. (2009)

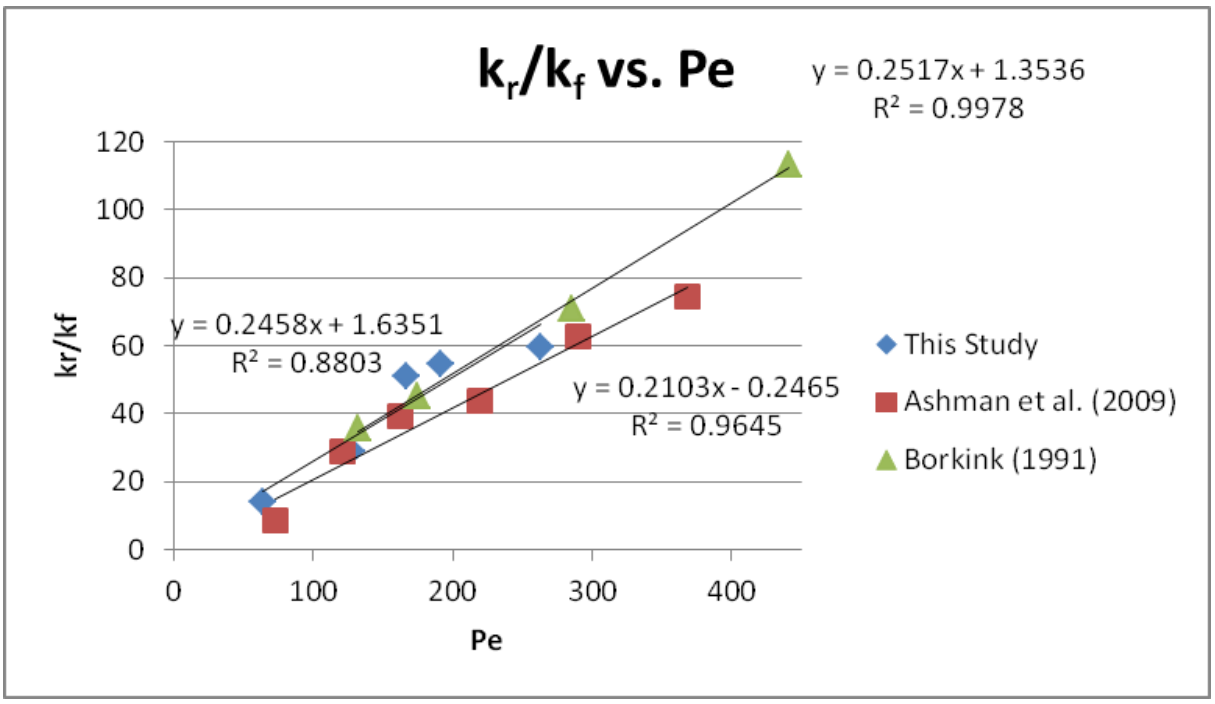
k_r/k_f vs. Pe
y = 0.2517x + 1.3536
R² = 0.9978
y = 0.2458x + 1.6351
R² = 0.8803
y = 0.2103x - 0.2465
R² = 0.9645
kr/kf
Pe
This Study
Ashman et al. (2009)
Borkink (1991)

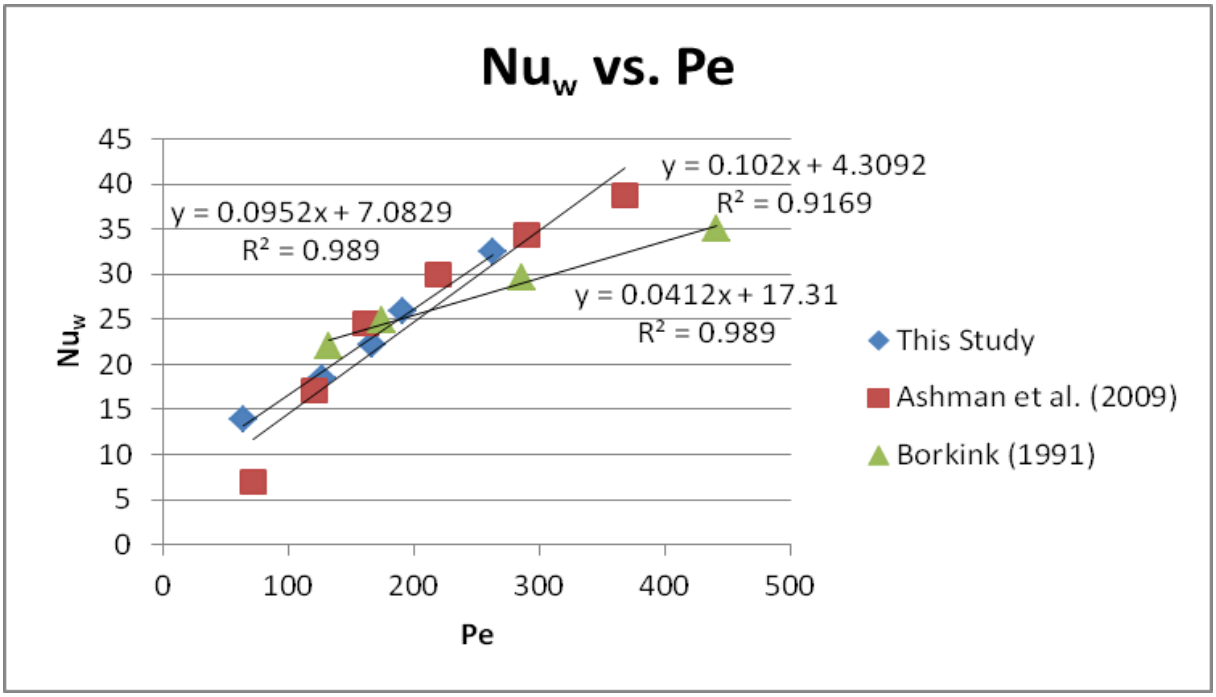
Nu_w vs. Pe
y = 0.102x + 4.3092
R² = 0.9169
y = 0.0952x + 7.0829
R² = 0.989
y = 0.0412x + 17.31
R² = 0.989
Nu_w
Pe
This Study
Ashman et al. (2009)
Borkink (1991)

2 inch column Raschig Rings

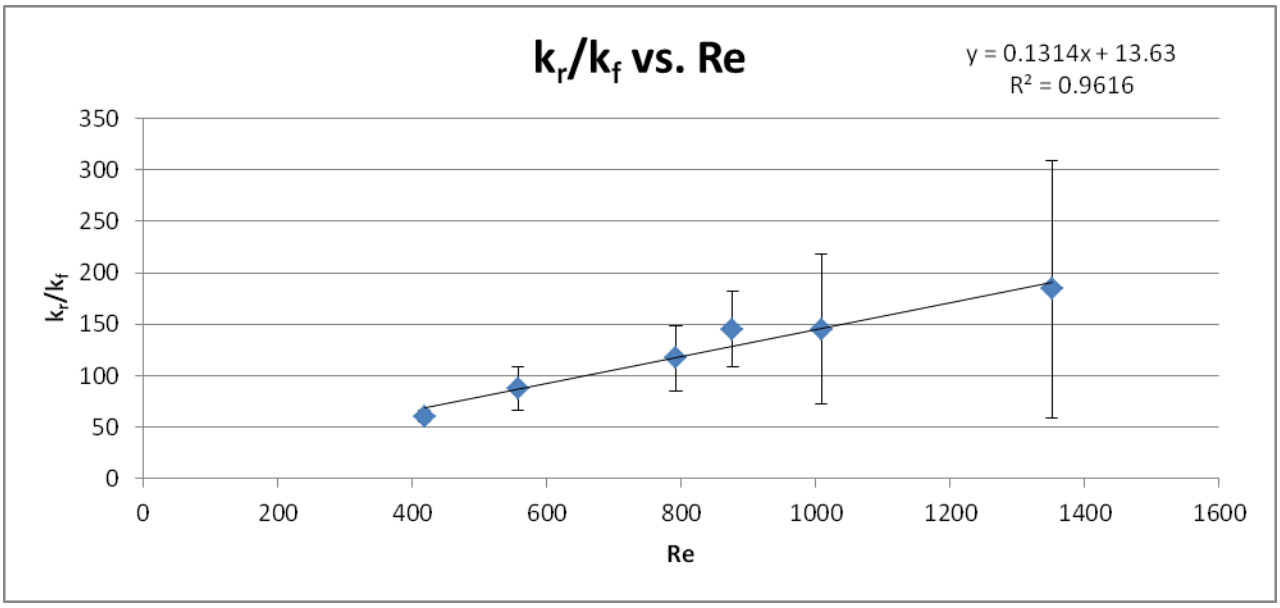

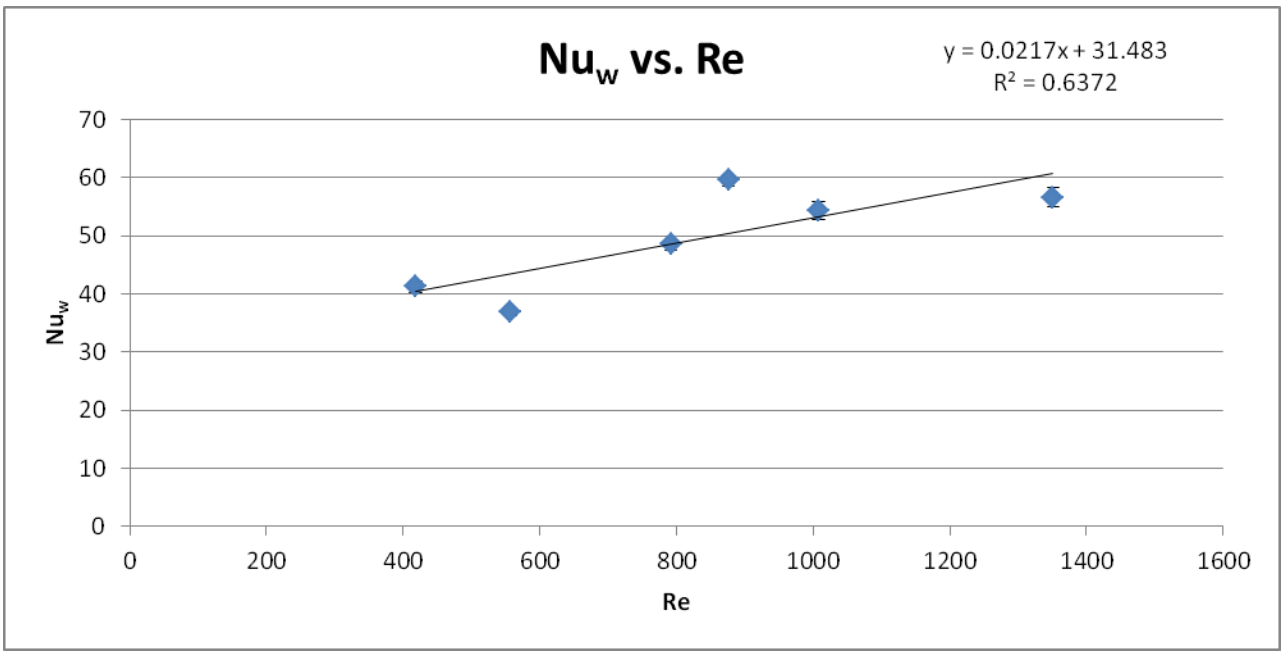

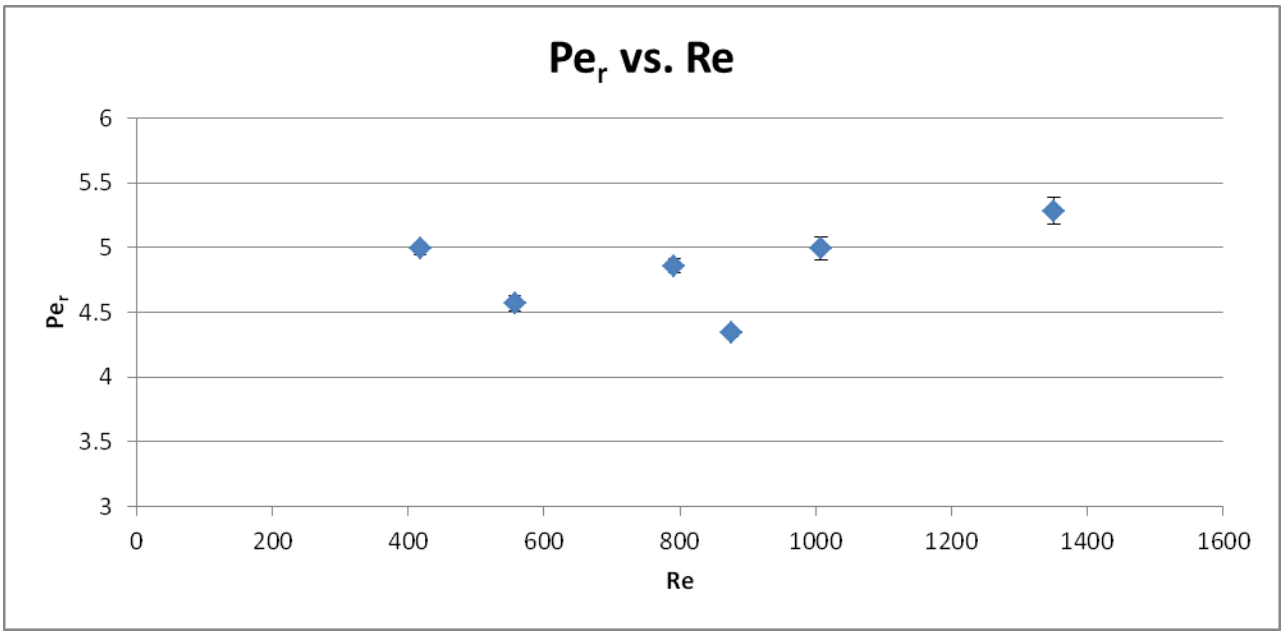
Per vs. Re
6
5.5
5
4.5
4
3.5
3
Per
0
200
400
600
800
1000
1200
1400
1600
Re

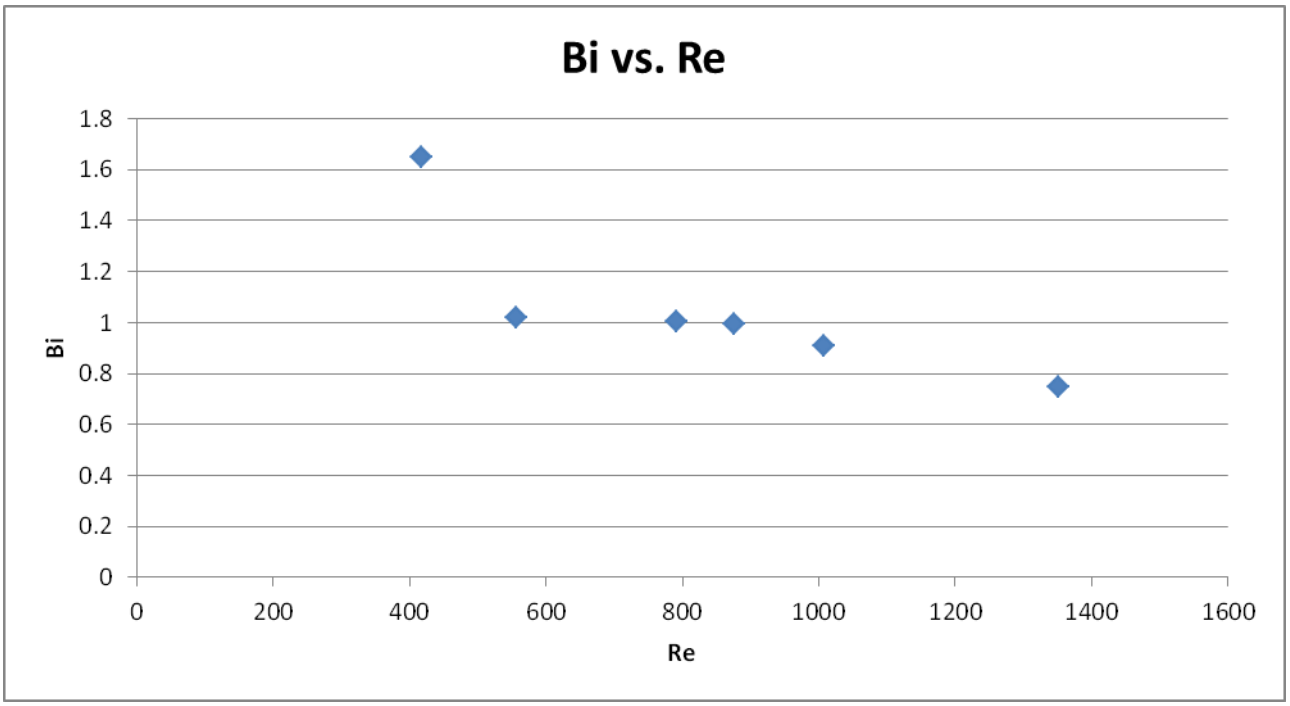
Bi vs. Re
1.8
1.6
1.4
1.2
1
0.8
0.6
0.4
0.2
0
Bi
0
200
400
600
800
1000
1200
1400
1600
Re

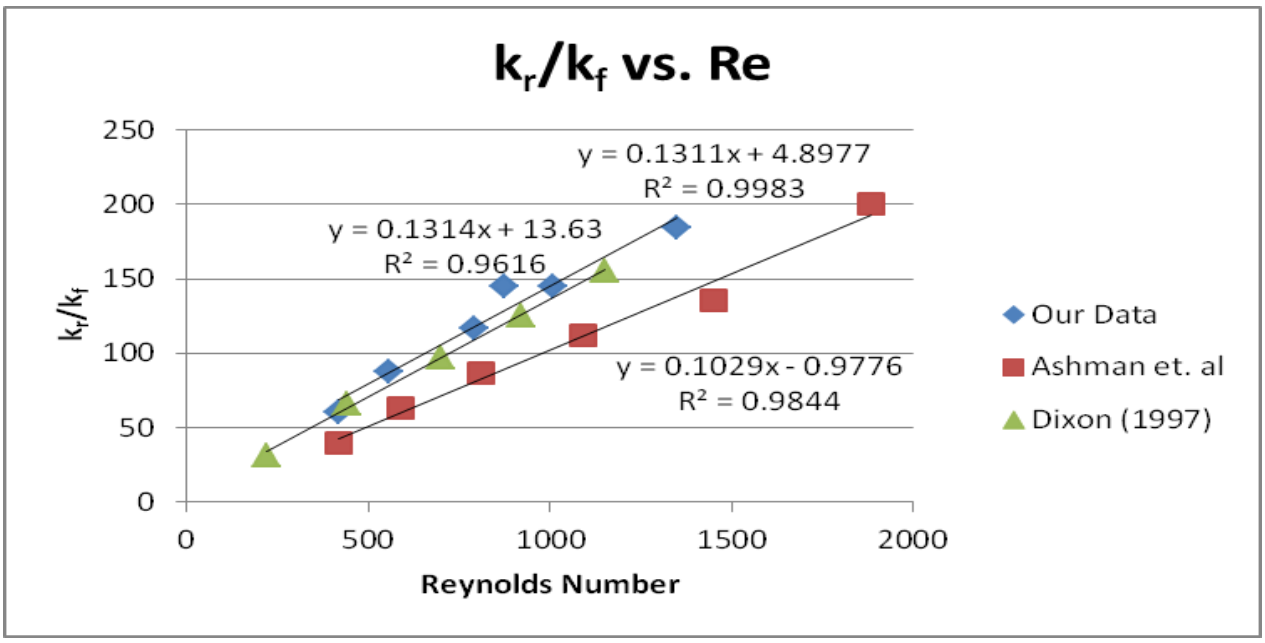
k_r/k_f vs. Re
250
200
150
100
50
0
k_r/k_f
0
500
1000
1500
2000
Reynolds Number
y = 0.1311x + 4.8977
R² = 0.9983
y = 0.1314x + 13.63
R² = 0.9616
y = 0.1029x - 0.9776
R² = 0.9844
Our Data
Ashman et. al
Dixon (1997)

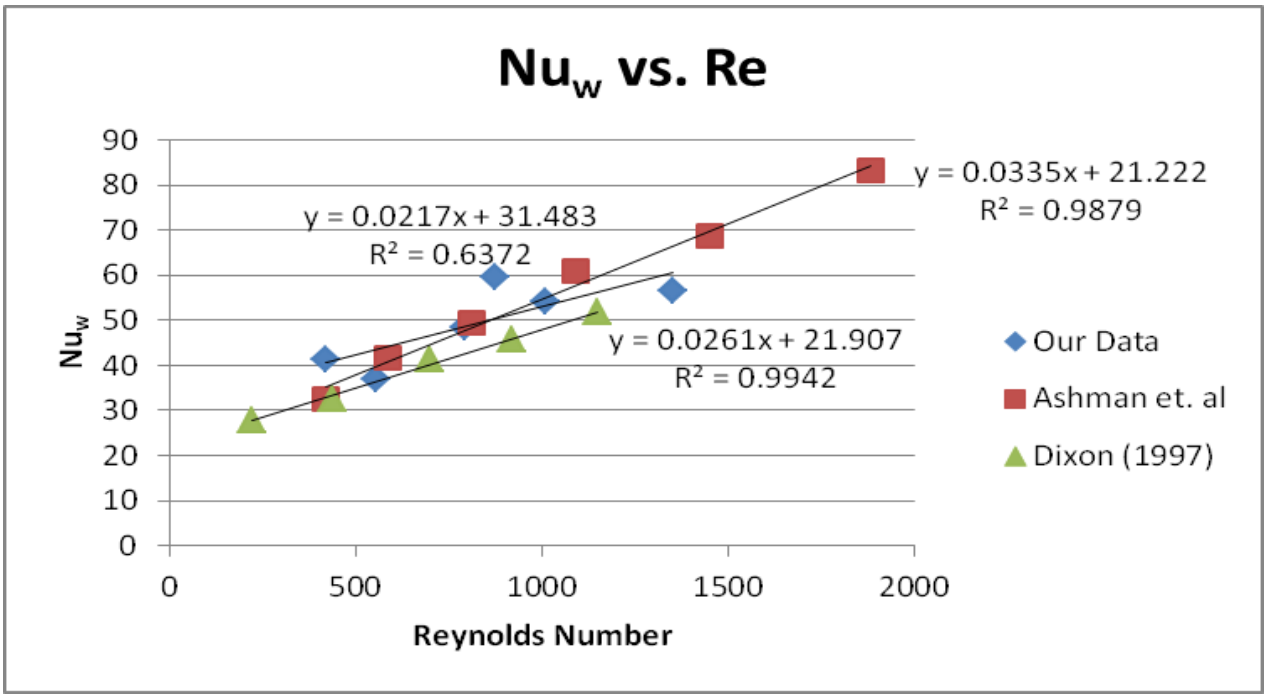
Nu_w vs. Re
90
80
70
60
50
40
30
20
10
0
Nu_w
0
500
1000
1500
2000
Reynolds Number
y = 0.0335x + 21.222
R² = 0.9879
y = 0.0217x + 31.483
R² = 0.6372
y = 0.0261x + 21.907
R² = 0.9942
Our Data
Ashman et. al
Dixon (1997)

Appendix D: Calming Section Tests (4 inch column with Raschig Rings)

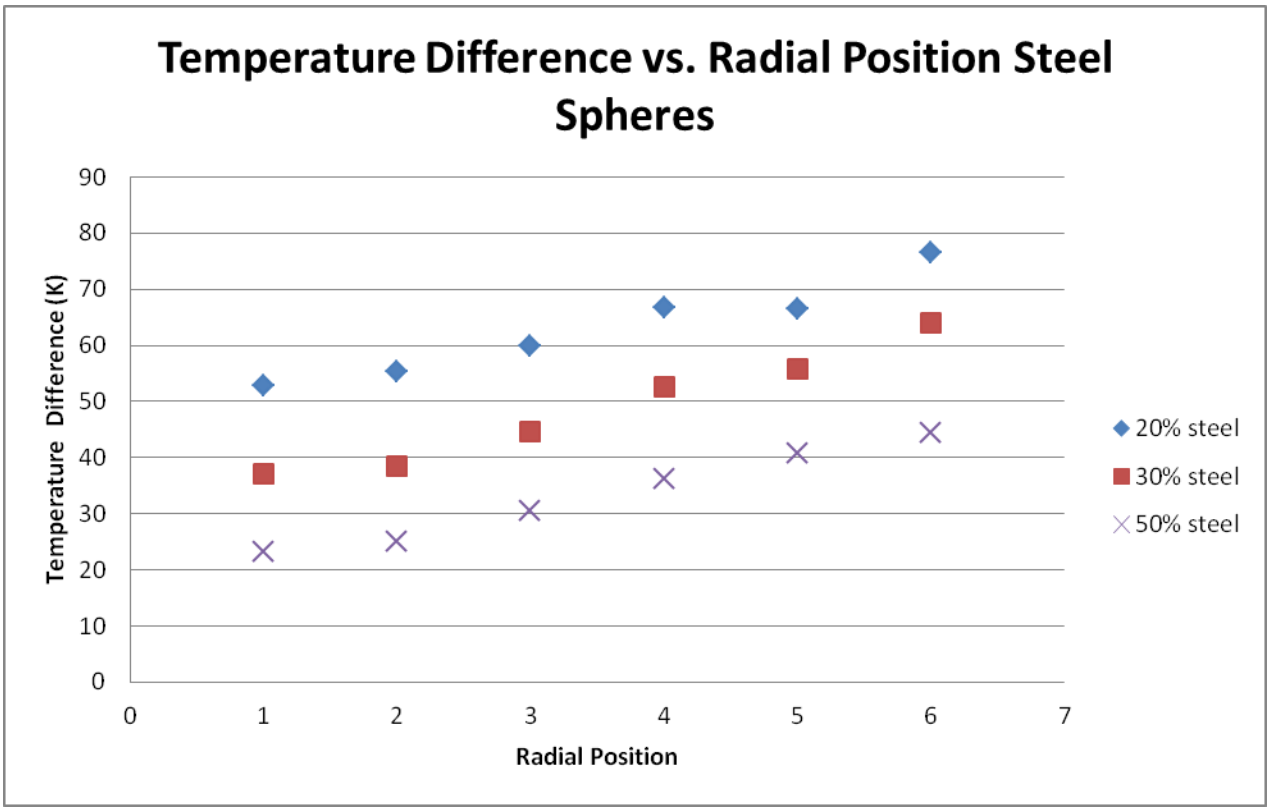

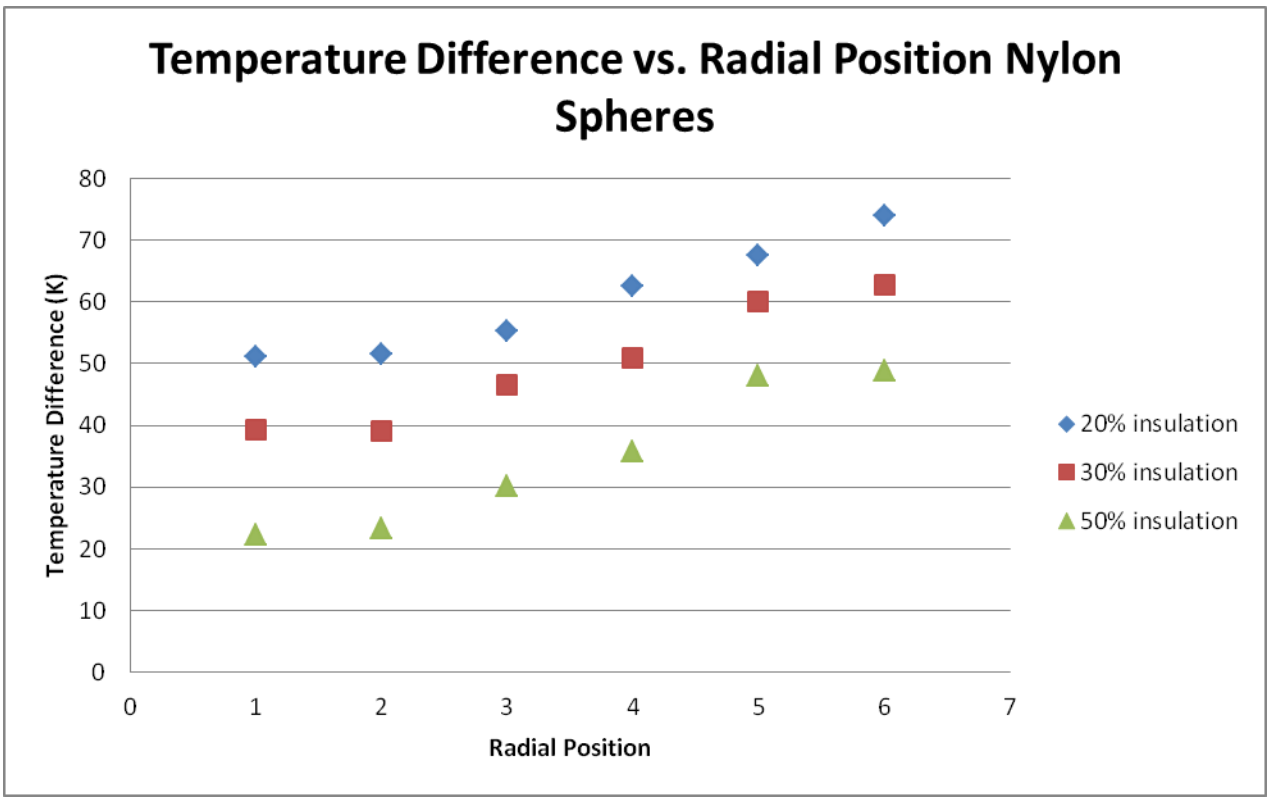
Temperature Difference vs. Radial Position Nylon Spheres
Temperature Difference (K)
80
70
60
50
40
30
20
10
0
0
1
2
3
4
5
6
7
Radial Position
20% insulation
30% insulation
50% insulation

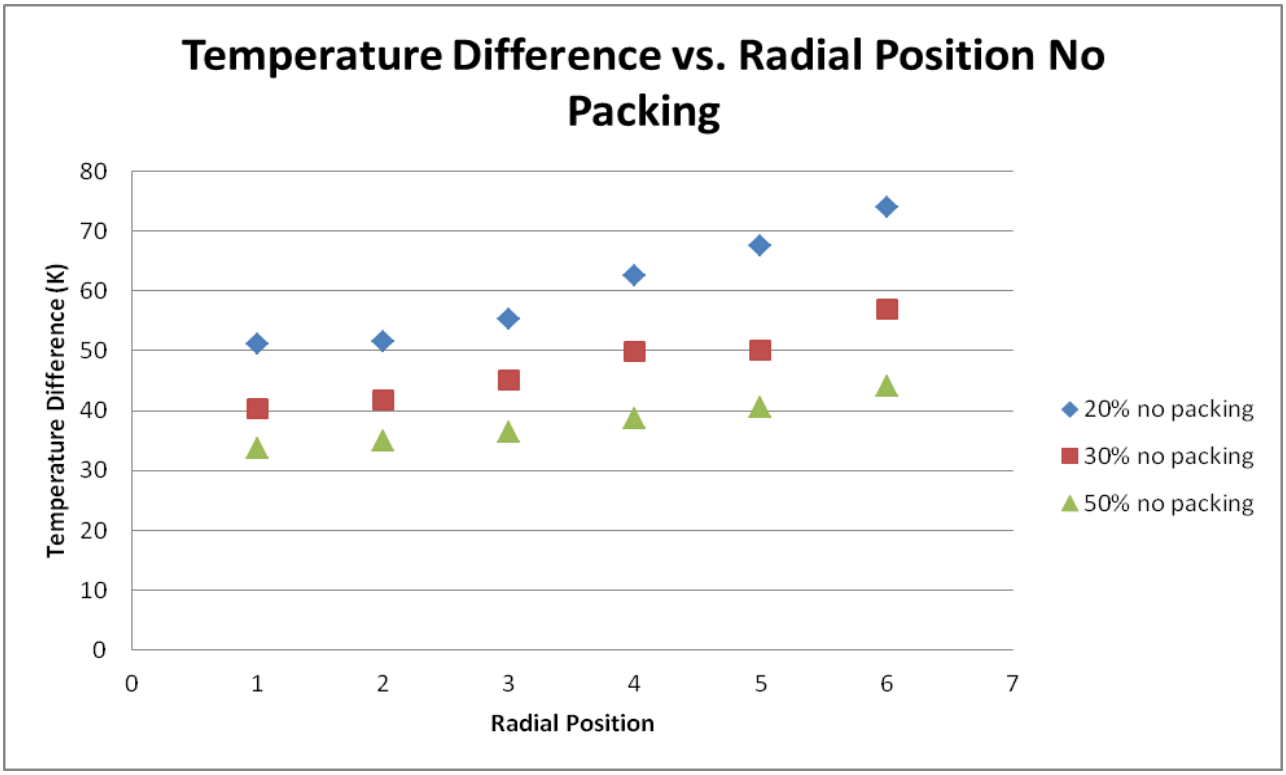
Temperature Difference vs. Radial Position No Packing
Temperature Difference (K)
80
70
60
50
40
30
20
10
0
0
1
2
3
4
5
6
7
Radial Position
20% no packing
30% no packing
50% no packing

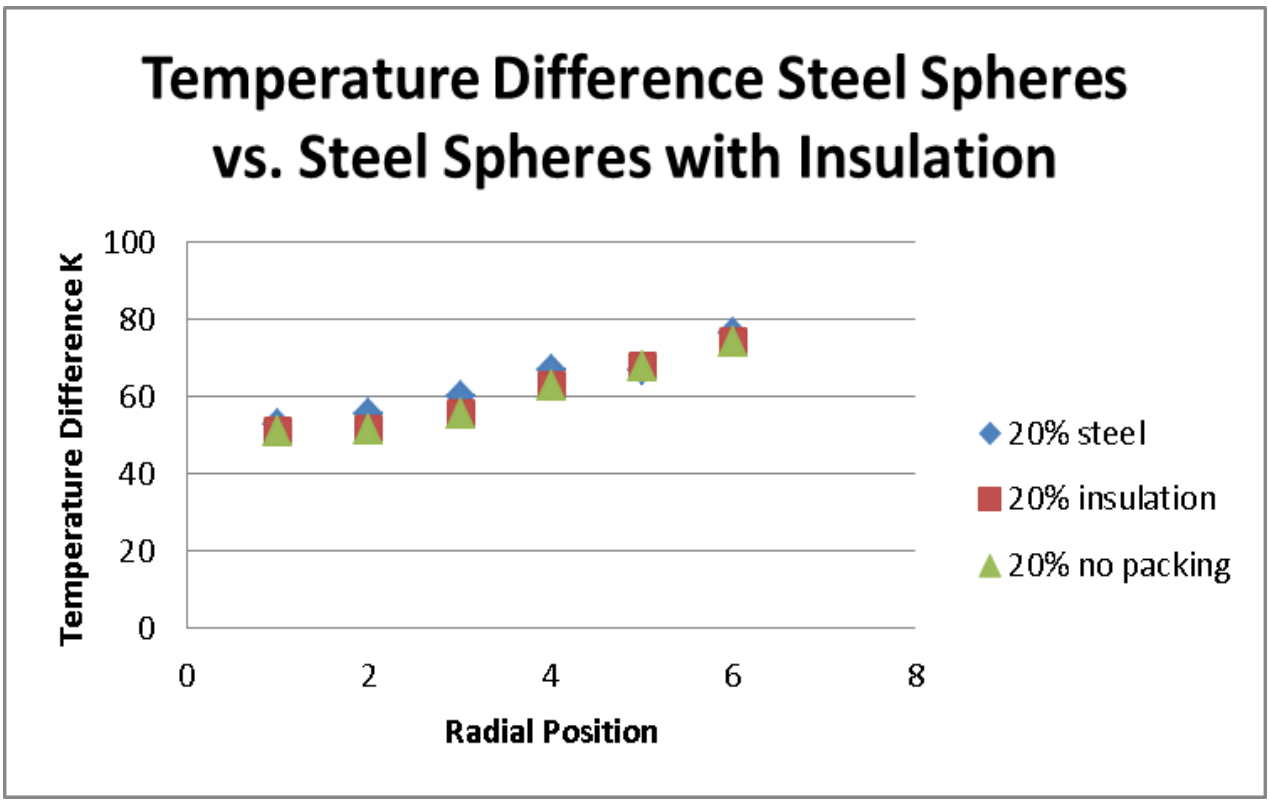
Temperature Difference Steel Spheres vs. Steel Spheres with Insulation
Temperature Difference K
100
80
60
40
20
0
0
2
4
6
8
Radial Position
20% steel
20% insulation
20% no packing

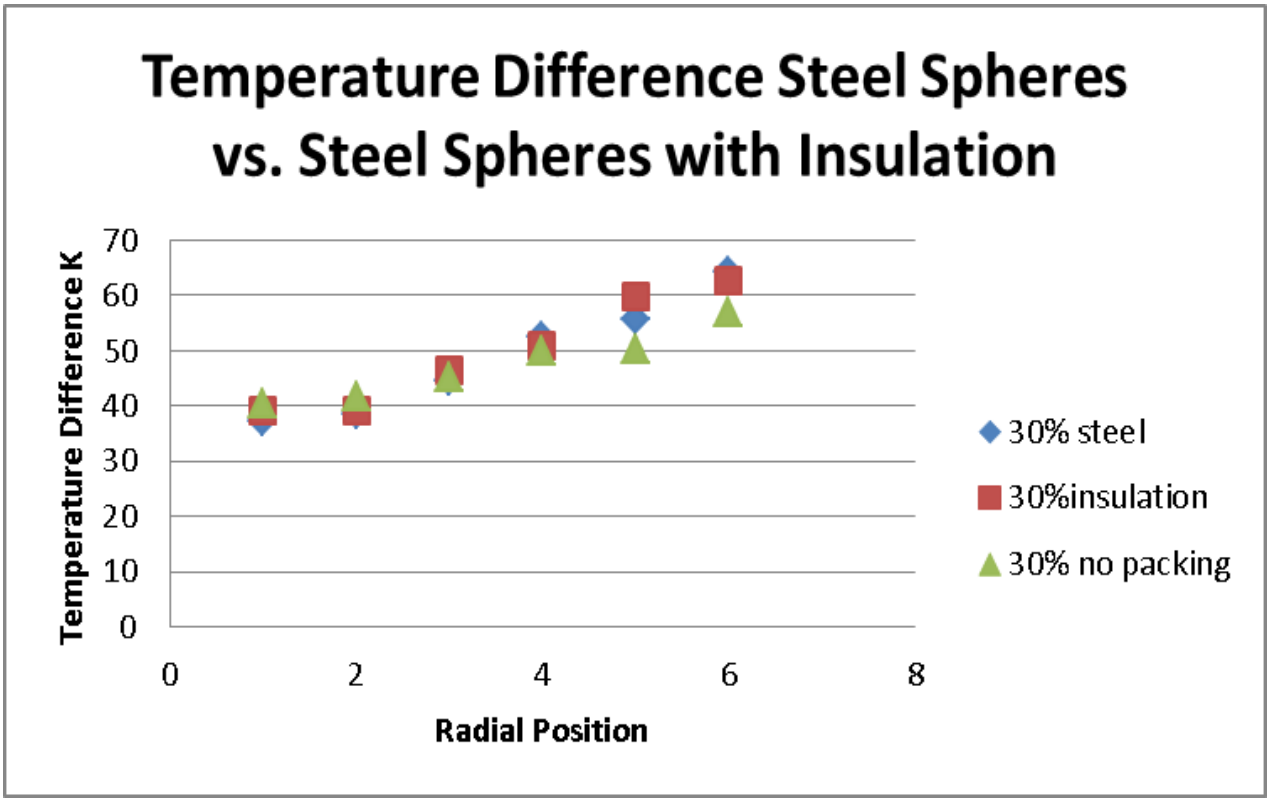
Temperature Difference Steel Spheres vs. Steel Spheres with Insulation
Temperature Difference K
70
60
50
40
30
20
10
0
0
2
4
6
8
Radial Position
30% steel
30%insulation
30% no packing

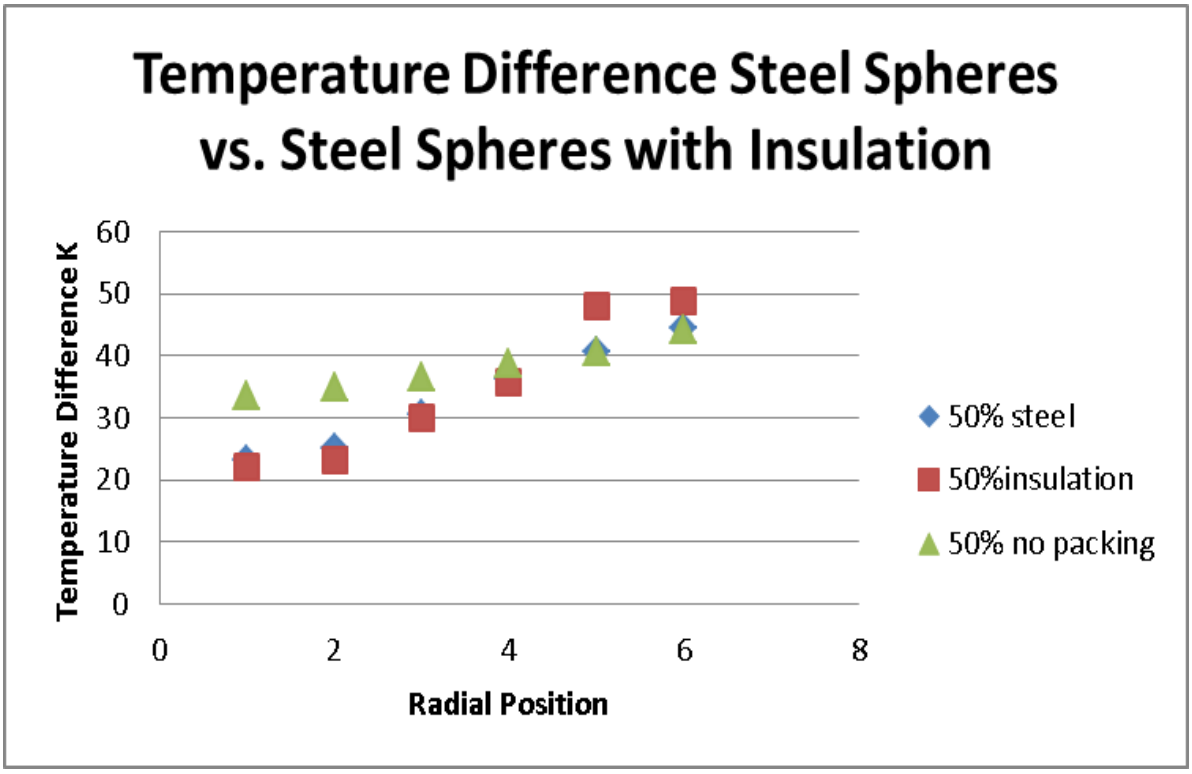
Temperature Difference Steel Spheres vs. Steel Spheres with Insulation
Temperature Difference K
60
50
40
30
20
10
0
0
2
4
6
8
Radial Position
50% steel
50%insulation
50% no packing

Wall Cooling Tests

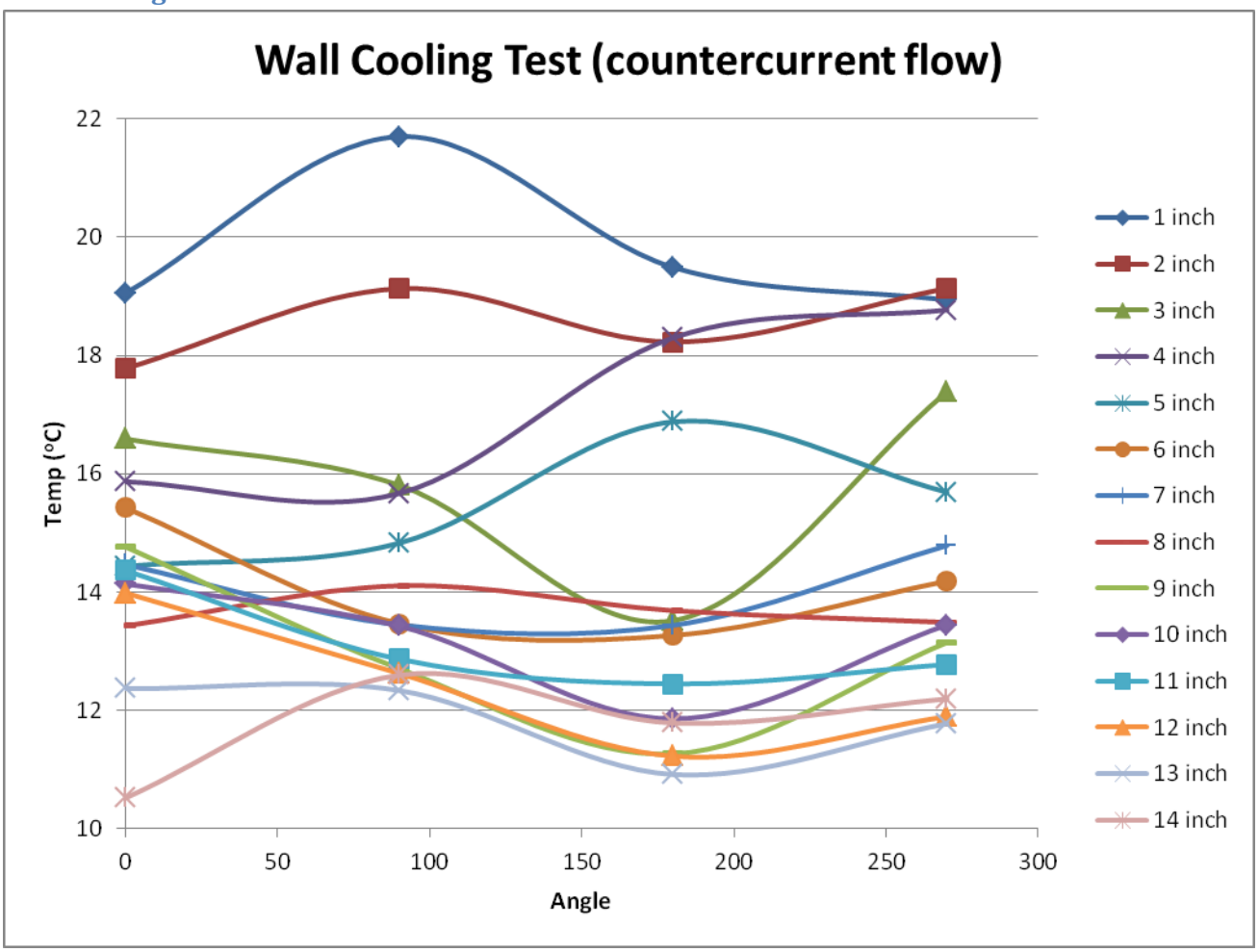

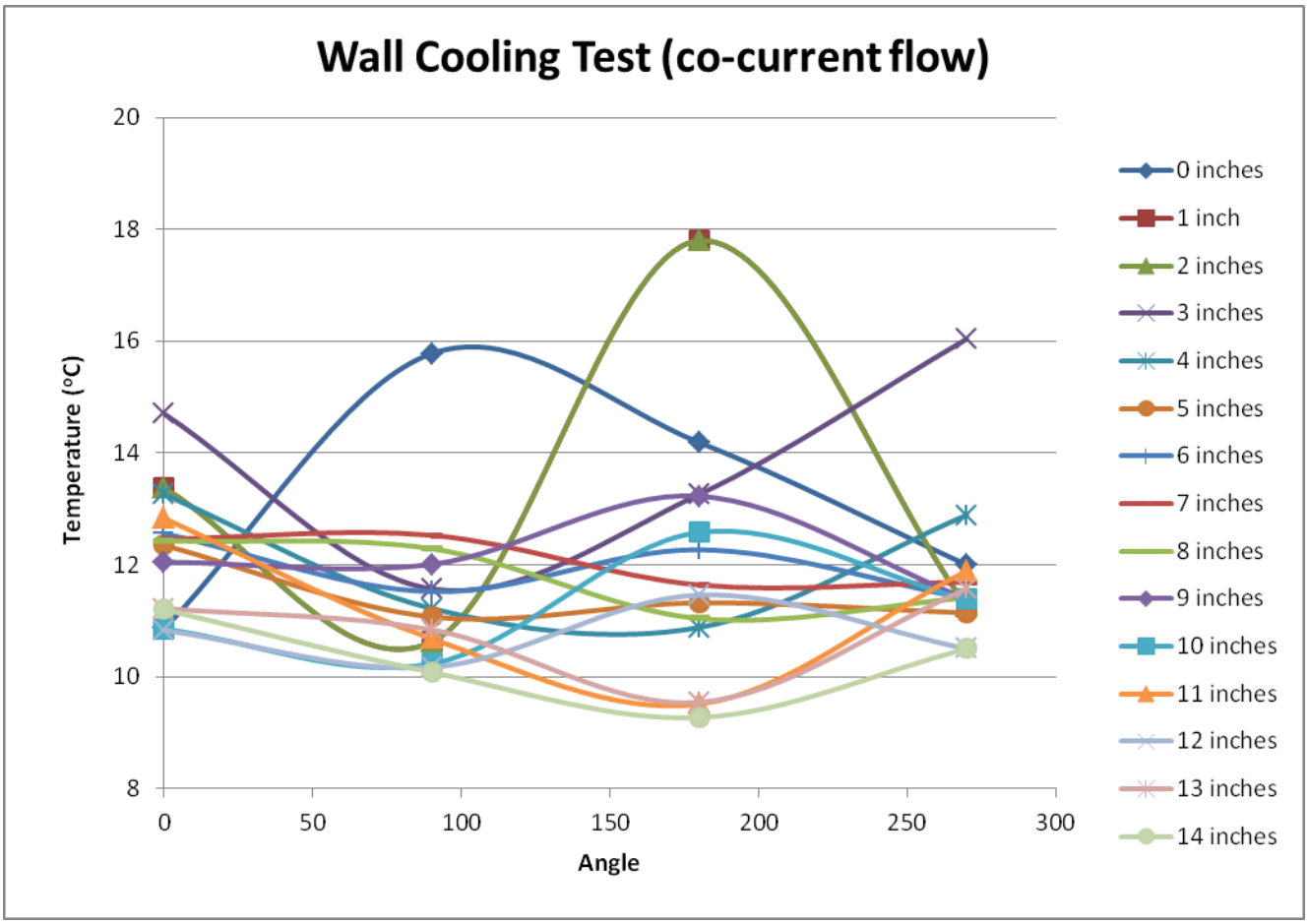
Wall Cooling Test (co-current flow)
Temperature (°C)
20
18
16
14
12
10
8
0
50
100
150
200
250
300
Angle
0 inches
1 inch
2 inches
3 inches
4 inches
5 inches
6 inches
7 inches
8 inches
9 inches
10 inches
11 inches
12 inches
13 inches
14 inches

Appendix E: Humidity Calculations

Cp of water at 32 degC: 4.179 J/(g*degC)

Cp of air at 32 degC: 1.007 J/(g*degC)

Assume the humid air is 10% water

Cp of mix: $0.1(4.179) + 0.9(1.007) = 1.3242 \frac{J}{g*degC}$

Constants for Cp calc:

Water: a*10^3= 33.46 b*10^5= 0.6880 c*10^8 =0.7604 d*10^12= -3.593

Air: a*10^3= 28.94 b*10^5= 0.4147 c*10^8= 0.3191 d*10^12= -1.965

So: ΔH=

H_2O: (0.1)(0.03346 + 0.6880*10^{-5}(26.67) + 0.7604*$10^{-8}$$(26.67)^2$ + -3.593*$10^{-12}$$(26.67)^3$)= 0.003364

Air: (0.9)(0.02894 + 0.4147*10^{-5}(26.67) + 0.3191*$10^{-8}$$(26.67)^2$+ -1.965*$10^{-12}$$(26.67)^3$)=0.02615

=0.03364+0.02615=0.05979 kJ/mol

Flow rate: SCFM: 9.34

So: if 10% water

Molar mass of mixture: 0.1(18)+(0.9)(29)= 27.9g/mol

Density of mixture: 0.1(997kg/m^3)+0.9(1.157)= 100.74 kg/m^3= **2853 g/ft^3**

$$\frac{9.34 \frac{ft^3}{min} * 2853 \frac{g}{ft^3}}{27.9 \frac{g}{mol}} = 955.09 \frac{mol}{min}$$

This gives: Qdot=nΔH= $955.09 \frac{mol}{min} * 0.0295 \frac{kJ}{mol}$ **=28.18 KJ/min**

If we have the same ΔT but only dry air:

ΔH=0.02894 + 0.4147*10^{-5}(26.67) + 0.3191*$10^{-8}$$(26.67)^2$+ -1.965*$10^{-12}$$(26.67)^3$=0.02905 kJ/mol

At: 29g/mol

Density= 1.157 kg/m^3= 32.763g/ft^3

$$\frac{9.34\frac{ft^3}{min} * 32.763\frac{g}{ft^3}}{29\frac{g}{mol}} = 10.552\ \frac{mol}{min}$$

Qdot= 0.02905*10.522= **0.3056 KJ/min**

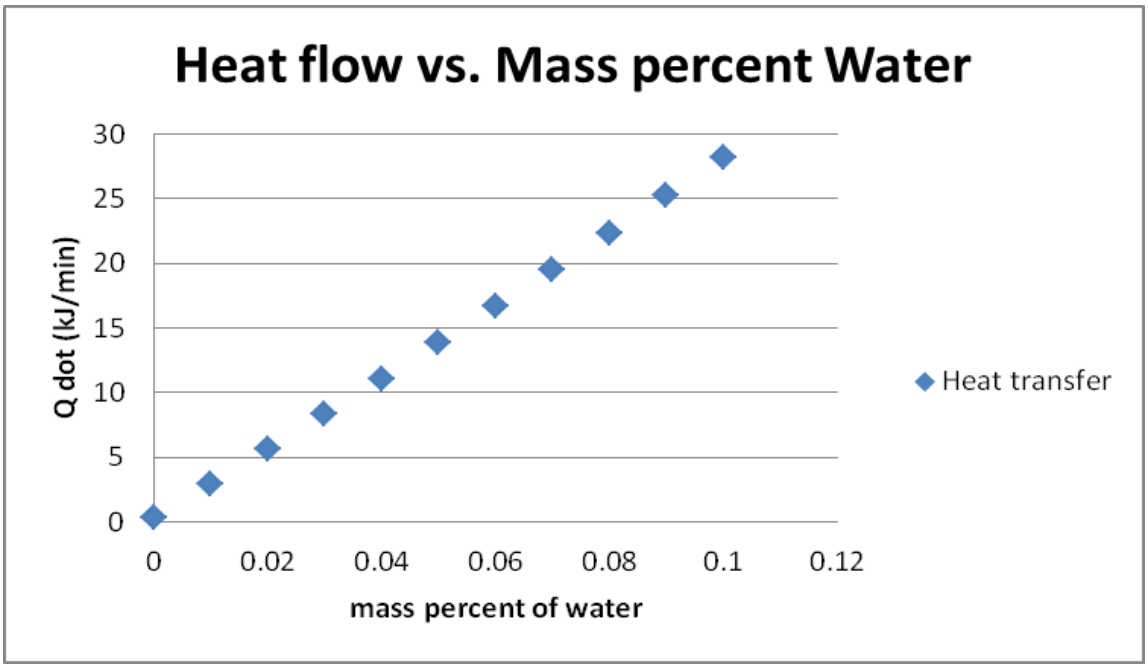

Appendix F: F-test Values

Column	Packing	Re	F/F95
4 Inch Column	Raschig Rings	90	0.299580
		180	1.690486
		235	0.610451
		270	0.636548
		370	0.487543
2 Inch Column	Raschig Rings	418	2.751992
		557	0.952127
		792	1.550117
		876	0.934997
		1008	2.102332
		1351	0.364218